January 2022

Chemical Proteomic Identification And Functional Studies Of Cardiac Protein Glutathionylation

Maheeshi Yapa Abeywardana
Wayne State University

CHEMICAL PROTEOMIC IDENTIFICATION AND FUNCTIONAL STUDIES OF CARDIAC PROTEIN GLUTATHIONYLATION

by

MAHEESHI YAPA ABEYWARDANA

DISSERTATION

Submitted to the Graduate School

of Wayne State University,

Detroit, Michigan

in partial fulfillment of the requirements

for the degree of

DOCTOR OF PHILOSOPHY

2022

MAJOR: CHEMISTRY (Biochemistry)

Approved By:

_____

Advisor   Date

_____

_____

_____

DEDICATION

This dissertation is dedicated to my loving parents, my husband

and

my doctoral research advisor Dr. Young-Hoon Ahn

TABLE OF CONTENTS

LIST OF FIGURES

LIST OF TABLES

LIST OF SCHEMES

LIST OF ABBREVIATIONS

CVD – Cardiovascular Disease

ROS – Reactive Oxygen Species

MI – Myocardial Infarction

NADPH - Nicotinamide Adenine Dinucleotide Phosphate

NOX - Nicotinamide Adenine Dinucleotide Phosphate Oxidase

XO – Xanthine Oxidase

MPO – Myeloperoxidase

H_2O_2 – Hydrogen Peroxide

NOS – Nitric Oxide Synthase

ATP - Adenosine Triphosphate

TCA – Tricarboxylic Acid/Citric Acid Cycle

ETC – Electron Transport Chain

NADH - Nicotinamide Adenine Dinucleotide Hydrate

FADH2 - Flavin Adenine Dinucleotide

CoQ – Coenzyme Q

Mn-SOD – Mitochondrial Superoxide Dismutase

VSMC – Vascular Smooth Muscle Cells

DUOX – Dual Oxidase

GPx – Glutathione Peroxidase

eNOS – endothelial Nitric Oxide Synthase

nNOS – neuronal Nitric Oxide Synthase

iNOS – inducible Nitric Oxide Synthase

BH-4 – tetrahydrobiopterin

SOD – Superoxide Dismutase

GSH – Glutathione

GSSG – Oxidized Glutathione

GR – Glutathione Reductase

PKA – Protein Kinase A

PKB - Protein Kinase B

SERCA - Sarcomeric/Endoplasmic Reticulum Calcium ATPase

NF- κB - Nuclear factor kappa-light-chain-enhancer of activated B cells

GAPDH - Glyceraldehyde 3-phosphate Dehydrogenase

GSTO – Glutathione Transferase Omega

GRx – Glutaredoxin

GCS - γ-glutamyl cysteine synthetase

GCL - γ-glutamylcysteine ligase

GS – Glutathione Synthetase

PSSG – S-glutathionylation

SQR – Succinate Ubiquinone Reductase

ETA – Electron Transfer Activity

TRx – Thioredoxin

DTT – Dithiothreitol

TCEP -Tris(2-carboxyethyl) Phosphine

BioGSH – Biotinylated Glutathione

BIOGEE – Biotinylated Glutathione Ethyl Ester

LC-MS/MS - Liquid Chromatography with tandem mass spectrometry

TMT – Tandem Mass Tagging

Iodo-TMT – Iodoacetyl Tandem Mass Tag

GS M4 – Glutathione Synthetase Mutant 4 (F152A/S151G)

N_3GSH – Azido Glutathione

L-N_3Ala/Azido-Ala – Light labeled Azido Alanine

H-N_3Ala – Heavy labeled Azido Alanine

HEK293 - Human Embryonic Kidney 293 cells

HEK293/GS M4 - Human Embryonic Kidney 293 cells overexpressing Glutathione Synthetase mutant 4

Biotin-DADPS-Alkyne - biotin-dialkoxydiphenylsilane-alkyne

I/R – Ischemic Reperfusion

PK – Pyruvate Kinase

LDH – Lactate Dehydrogenase

$R_{H/L}$ – Heavy to light Ratio

ACTN – α-actinin

DES – Desmin

FLNC – Filamin C

CV – Coefficient of Variation

TTN – Titin

MYL – Myosin Light Chain

BAG3 – Bcl2 Associated Athanogene

SILAC - Stable Isotope Labeling by/with Amino acids in Cell culture

FBS – Fetal Bovine Serum

EDTA - Ethylenediaminetetraacetic acid

PEP – Phosphoenolpyruvate

PCR – Polymerase Chain Reaction

SOC - Catabolite Repression

LB - Luria-Bertani

DMEM - Dulbecco's Modified Eagle Medium

BSA – Bovine Serum Albumin

Ad/GS M4 - Adenovirus Expressing GS M4

HEPES - 4-(2-hydroxyethyl)-1-piperazineethanesulfonic Acid

NEM - N-Ethyl Maleimide

DMSO – Dimethyl Sulfoxide

THPTA - Tris-hydroxypropyltriazolylmethylamine

SDS-PAGE – Sodium Dodecyl Sulfate Poly Acrylamide Gel Electrophoresis

TEMED - N,N,N',N'-Tetramethylethylenediamine

APS - Ammonium Persulfate

PBS – Phosphate Buffer Saline

TFA – Trifluoro Acetic Acid

ETD – Electron Transfer Dissociation

CID – Collision Induced Dissociation

GD – Glucose Deprivation

OGD - Oxygen Glucose Deprivation

OGD/O – Reoxygenation after OGD

OGD/OG – Reoxygenation with Glucose after OGD

OGD/OGF-BSA -Reoxygenation with Glucose and Fatty acid after OGD

L-N_3-GS-Spy – Cysteine Blocking Clickable Glutathione

CSRP3 - Cysteine and Glycine Rich Protein 3

CTNND1 - Catenin-Delta 1

IF – Intermediate Filament

ESI-LC/MS – Electrospray Ionization Liquid Chromatography Mass Spectrometry

MALDI – Matrix Assisted Laser Desorption Ionization

CHAPTER 1: INTRODUCTION

1.1 Cardiovascular diseases and reactive oxygen species

Cardiovascular diseases (CVDs) are the number one cause of death in the United States and account for one in every three deaths.[1-3] It is estimated that more than 80 million adults have one or more types of CVD.[2] CVDs can be classified mainly into three categories: coronary heart disease, peripheral vascular disease, and cerebrovascular disease, where the blood supply to the heart, peripheral vasculature, and the brain is compromised.[4] Atherosclerosis, which is the narrowing down of arteries by plaque formation in the arterial walls, is the common cause for these classifications. Atherosclerosis limits the delivery of oxygen and nutrient-rich blood to the tissues.[5, 6] A major concern with atherosclerotic plaque is its propensity to rupture, which gives rise to blood clots that have the ability to clog blood vessels away from the initial site of the plaque.[4] Ultimately, atherosclerosis can lead to acute phenomena, such as heart failure, stroke, and myocardial infarction (MI).[7, 8]

Oxidative stress is a major contributor to the development of atherosclerosis.[2] Important targets in oxidative stress are thiol groups in proteins, unsaturated fatty acids in membranes, and nucleic acids.[9-13] Under physiological conditions, fluctuations in reactive oxygen species (ROS) concentrations are controlled by enzymatic and non-enzymatic antioxidant systems.[5] Pathological conditions such as hypertension, diabetes, obesity, and respiratory failure induce the synthesis and activity of pro-oxidant enzymes, such as nicotinamide adenine dinucleotide phosphate (NADPH) oxidases (NOX), xanthine

oxidase (XO), and myeloperoxidase (MPO).[4, 10, 14, 15] Sustained production of pro-oxidant enzymes increases the production of pro-oxidants in the form of ROS. Oxidative stress arises when ROS production exceeds the antioxidants' capacity to scavenge excessively produced ROS, impairing cellular structure and functions leading to diseases.[5, 16, 17] Therefore, for the development of potential treatments for diseases such as CVD, it is important to identify and study proteins involved in redox signaling and oxidant defense.[18]

1.2 Reactive oxygen species and redox homeostasis

ROS are low molecular weight, short-lived, and highly reactive molecules generated as byproducts of cellular metabolism or catalytic reactions due to the partial reduction of molecular oxygen (O_2).[12, 19] They consist of radical and non-radical species such as hydrogen peroxide (H_2O_2), superoxide anion ($O_2^{\bullet-}$), hypochlorous acid (HOCl), hydroxyl radical ($^\bullet OH$), and peroxynitrite ($ONOO^-$) (Figure 1.1).[8, 10, 19-22] Under normal physiological conditions, there is a balance between the production and removal of ROS, known as redox homeostasis (Figure 1.1). Balanced production of ROS is important in two ways: 1) as a regulatory mechanism in different cellular functions such as cell signaling, cell proliferation, cell migration, tissue repair, and wound healing, and 2) as a defense mechanism against malignant cells and invading pathogens.[17, 21, 23-26] In contrast, under pathological conditions, increased concentrations of ROS can cause deleterious consequences such as apoptosis, carcinogenesis, and mitochondrial dysfunction.[27] In the presence of elevated levels of ROS, cells undergo oxidative stress by overwhelming the

inherent antioxidant defense system of the cells, damaging cellular macromolecules such as proteins, DNA, and lipids (Figure 1.1).[11, 13, 16, 27-29]
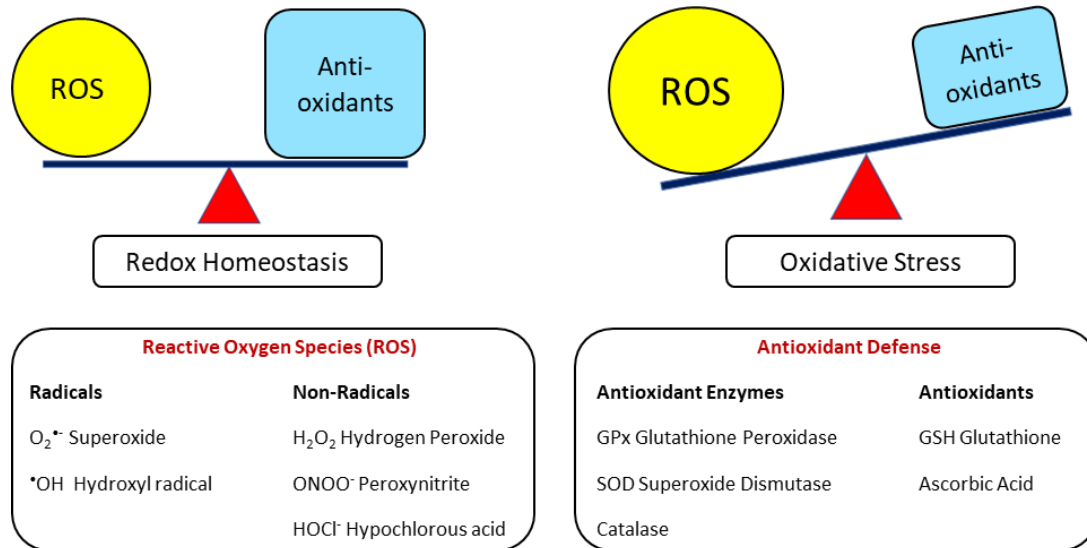
Figure 1.1 - Redox homeostasis and oxidative stress. Redox homeostasis is the balance between the generation and removal of ROS. Increased concentrations of ROS cause oxidative stress by overwhelming the antioxidant defense system.

1.3 Sources of ROS

In human tissues, the primary sources of ROS production are the mitochondrial electron transport chain, xanthine oxidase, NADPH oxidase, uncoupled nitric oxide synthase (NOS), and arachidonic acid (Figure 1.2).[17, 19, 21, 26, 29, 30]
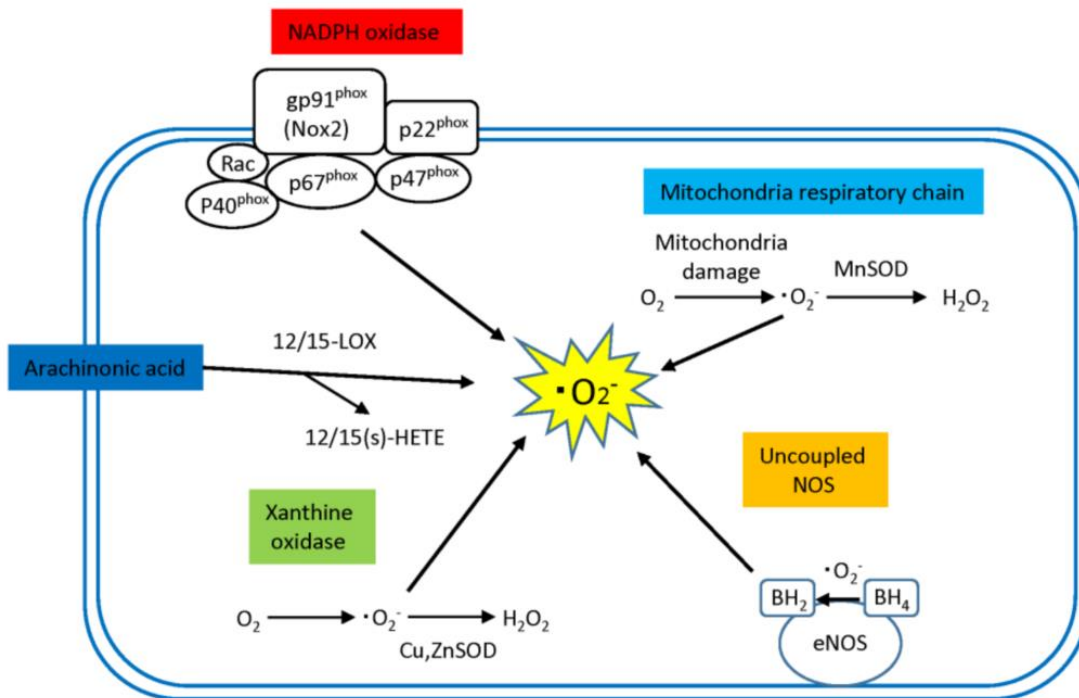
Figure 1.2 – Sources of ROS. Mitochondrial respiratory chain, uncoupled NOS, xanthine oxidase, arachidonic acid, and NADPH oxidase are the major sources of ROS that generate $O_2^{\bullet-}$. This figure adapted from Kayama *et al*. 2015 a free access article.[19]

1.3.1   Mitochondria

Mitochondria are membrane-bound organelles found in most eukaryotic cells. These organelles are essential for a number of fundamental cellular processes, including respiration and energy production, fatty acid beta-oxidation, and regulation of intracellular calcium overload.[31] Mitochondria produce the majority of the adenosine triphosphate (ATP) required for cellular functions by oxidative phosphorylation. The tricarboxylic acid/citric acid (TCA) cycle and oxidative phosphorylation are the major metabolic pathways in the mitochondria. The electron transport chain (ETC) shuttles electron carriers produced by TCA cycle, such as nicotinamide adenine dinucleotide

hydrate (NADH) and flavin adenine dinucleotide ($FADH_2$) to O_2.[32] The ETC composed of four protein complexes, named complexes I – IV. Electron transfer is initiated by the delivery of electrons from the TCA cycle to complexes I and II. These electrons are delivered to the Coenzyme Q (CoQ) pool and then passed to cytochrome c through complex III. Finally, these electrons reduce O_2 to water at complex IV. Under physiological conditions, oxidative phosphorylation converts 1-5% of all O_2 being consumed to $O_2^{\bullet -}$, an ROS.[19]

While electrons are passing through the ETC, they can escape and reduce O_2 to generate $O_2^{\bullet -}$, which is then converted to the less reactive H_2O_2 (another ROS) by the mitochondrial, manganese dependent superoxide dismutase (Mn-SOD) (Figure 1.2).[23, 31, 33, 34] Hydrogen peroxide produced by Mn-SOD can also be converted to $OH^{\bullet}$ through the Fenton reaction. The main complexes involved in mitochondrial ROS production are complexes I and III.[25, 31, 35] Superoxide radicals produced at complexes I and III, is released into the mitochondrial matrix where they can damage mitochondrial DNA. ROS generated by complex III can also be released into the intermembrane space, where they can access the cytosol.[31, 35]

1.3.2   NADPH oxidase

NADPH oxidase is primarily identified as a ROS generating enzyme in phagocytes such as neutrophils, macrophages, and monocytes, which play an important role in the host defense mechanism against infectious agents.[4, 19, 36-38] NADPH oxidase is a membrane-bound, multi-molecular enzyme that consisting cytosolic and plasma

membrane-spanning components. This enzyme complex is composed of three including regulatory subunits (p47phox, p67phox, and rac1) and three electron transfer subunits (gp91phox, nox1 or nox4).[10, 19] During a microbial invasion, NADPH oxidase is activated by translocating its cytosolic components to the plasma membrane to form an active NADPH complex that and allows the generation of $O_2^{\bullet-}$ by transferring electrons to O_2 (Figure 1.2, Scheme 1.1).[19]

$$\text{NADPH} + 2O_2 \ \rightarrow \text{NADP} + 2O_2^{\bullet-} + H^+$$

Scheme 1.1 – Production of $O_2^{\cdot-}$ by NADPH

Even though NADPH oxidase is primarily known for its role in that generates ROS in phagocytes, it has also been identified for its ROS production in atherosclerotic vascular smooth muscle cells (VSMC) and other cardiovascular cells, including cardiomyocytes, adventitial fibroblasts, and vascular endothelial cells.[19, 22]

The NOX enzyme family has seven members [NOX1-5 and dual oxidase (DUOX1-2)].[19, 38] NOX2 and NOX4 are the identified as major myocardial isoforms, where NOX2 is localized to the cell membrane, and NOX4 is localized to the intracellular organelles around the nucleus. NOX4 also has a mitochondrial localization signal and is predominantly expressed in mitochondria of cardiac muscle. Their physiological and pathological properties depend on their intracellular localization.[19]

1.3.3 Xanthine oxidase

Xanthine oxidoreductase (XO) can exist in two isoforms: xanthine oxidase (XO) and xanthine dehydrogenase (XDH). They primarily differ depending on their substrate

specificity.[19, 38] XO reacts with O_2, whereas XDH uses NAD^+ as its substrate.[8] XO catalyzes the oxidation of xanthine and hypoxanthine to uric acid using O_2, as the electron receptor, producing $O_2^{\bullet-}$ and H_2O_2 in the cytoplasm (Figure 1.2, Scheme 1.2).[8, 19, 38, 39]

$$\text{Hypoxantine} + \ O_2 \ \rightarrow \text{Xanthine} + \ O_2^{\bullet-}$$

$$\text{Xanthine} + \ O_2 + \ H_2O \ \rightarrow \text{Uric Acid} + \ H_2O_2$$
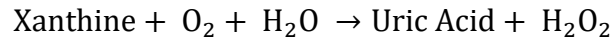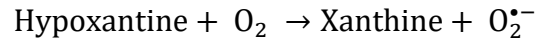
Scheme 1.2 – Production of ROS by xanthine oxidase

Antioxidants present in the cytoplasm [Cu, Zn-SOD and GPx (glutathione peroxidase)] readily eliminate the ROS produced by this reaction. However, under an ischemic/reperfusion state, hypoxanthine reacts acutely with O_2 producing a large amount of $O_2^{\bullet-}$ and H_2O_2, causing cellular damage.[19]

1.3.4 Uncoupled nitric oxide synthase

Nitric oxide synthase (NOS) is the major source of endogenous nitric oxide (NO) and can exist in three isoforms: endothelial NOS (eNOS), neuronal NOS (nNOS), and inducible NOS (iNOS). Endothelial NOS catalyzes the flavin-mediated electron transport from NADPH to a prosthetic heme group.[8, 40] For the formation of NO, eNOS requires a cofactor, tetrahydrobiopterin (BH-4) bound near the heme group to transfer electrons to the guanidino nitrogen of L-arginine. Deficiency of BH-4 or L-arginine leads to the production of $O_2^{\bullet-}$ and H_2O_2 by eNOS (Figure 1.2).[8]

1.4 ROS detoxification by antioxidants

The production of ROS is regulated by antioxidant enzymes such as glutathione peroxidase (GPx), superoxide dismutase (SOD) (Figure 1.3), and catalase or by antioxidants such as glutathione (GSH) and vitamin C (ascorbic acid).[19, 23, 41] The balance between cellular ROS production and detoxification is crucial to maintain cellular functions.
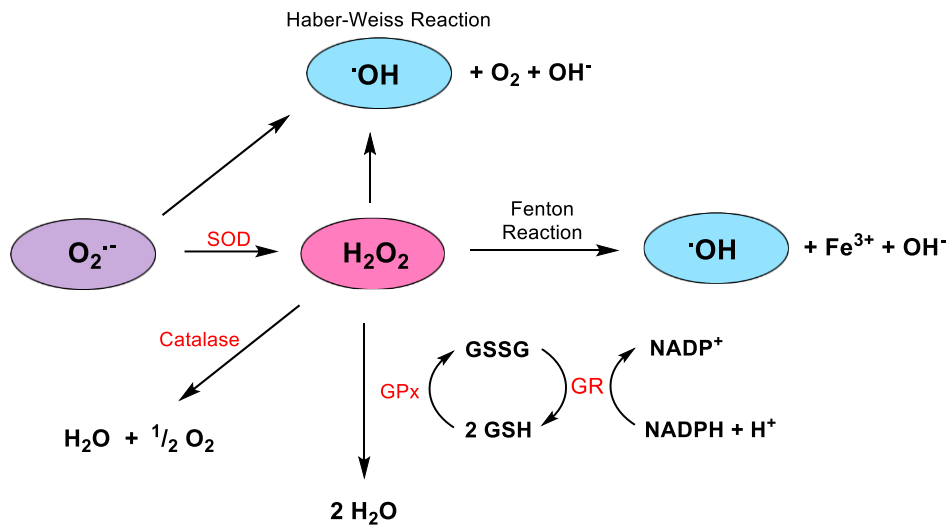
Figure 1.3 – Generation and elimination of ROS. Fenton and Haber-Weiss reactions generate ROS. SOD, catalase, and GPx are the major antioxidants that regulate the production of ROS.

1.4.1   Superoxide dismutase

Superoxide dismutase (SOD) is an antioxidant that catalyzes the dismutation of highly reactive $O_2^{\bullet-}$ to less reactive H_2O_2 and O_2 (Figure 1.3).[42] In humans, the SOD family consists of three isoforms: cytosolic SOD (Cu/Zn-SOD/ SOD1), mitochondrial SOD (Mn-SOD/ SOD2), and extracellular SOD (EC-SOD/ SOD3).[23, 42]

1.4.2 Glutathione peroxidase

Glutathione peroxidase (GPx) is an antioxidant enzyme that utilizes glutathione to scavenge H_2O_2 and lipid peroxides.[42] Glutathione peroxidase family consist of eight isoforms (GPx1-8) that belong to three groups: GPx1/GPx2, GPx3/GPx5/GPx6, and GPx4/GPx7/GPx8.[23, 42] Members of GPx family enzymes have their antioxidative function at different cellular compartments. GPx1 is in mitochondria and the cytosol; GPx2 is present in the nucleus and the cytosol; GPx3 is in plasma; GPx4 is associated with the membrane; and GPx7/GPx8 is in the endoplasmic reticulum (ER). [23, 42]

1.4.3 Catalase

Catalase is an antioxidant enzyme mainly localized in peroxisomes. The active site of catalase has an iron-bound heme group that converts H_2O_2 to water (H_2O) and O_2 (Figure 1.3).[23, 42]

1.4.4 Glutathione (GSH)

GSH is the most abundant low molecular weight thiol present in mammalian and plant cells (1-10 mM).[42-44] This high intracellular level of GSH is maintained by two factors, GSH synthesis, and NADPH-dependent reduction of GSSG by glutathione reductase (GR).[42, 44] GSH acts as a redox buffer that plays an important role in antioxidant defense, synthesizing cellular signaling molecules and removing toxins and xenobiotics.[18, 45] GPx utilizes GSH to reduce ROS. During the reaction, GSH is oxidized to GSSG.[42] Under normal physiological conditions, the ratio of GSH:GSSG is 50:1. This ratio reflects the reducing state inside the cell.

1.5   Oxidative cysteine modifications

Cysteine is the second least abundant amino acid of the 20 amino acids, with a natural abundance of 2.3% in the mammalian proteome. Protein cysteine residues are the most susceptible to ROS-induced reversible or irreversible post-translational modifications (PTMs) due to their high nucleophilicity and redox sensitivity.[26, 46, 47] Protein cysteines are important in signal transduction, maintaining redox homeostasis, structural stabilization, and enzyme catalysis.[26, 47] Due to its relatively high pK_a value (around 8.4), the cysteine sulfhydryl group remains largely protonated at physiological pH values in the cytoplasm. However, in many redox-sensitive proteins, its pK_a value of cysteines can be low as 3.5 due to electrostatic interactions or hydrogen bonding with neighboring amino acids. These deprotonated cysteine residues are more vulnerable to oxidation.[26-28, 47] In the presence of ROS, these active site cysteines can undergo reversible and irreversible oxidative events.

Cysteine can initially be oxidized to form sulfenic acid (R-SOH), which is a reversible oxidative modification. Sulfenic acid can further be oxidized to the sulfinic acid (R-SO$_2$H) and sulfonic acid (R-SO$_3$H), which are irreversible PTMs (Figure 1.4) that can cause permanent changes to the protein structure function leading to different pathological conditions.[20, 28, 48-52] Sulfenic acid can also undergo other reversible modifications such as intermolecular or intramolecular disulfide bond formation (PS-SP'), glutathionylation (PSSG), *S*-palmitoylation and S-nirtosylation (PS-NO) (Figure 1.4).[47, 48, 51,]

[53] Endogenous nitric oxide reacts with free cysteines resulting in nitrosylation, which is a key event in signal transduction.[47, 48, 51, 53]
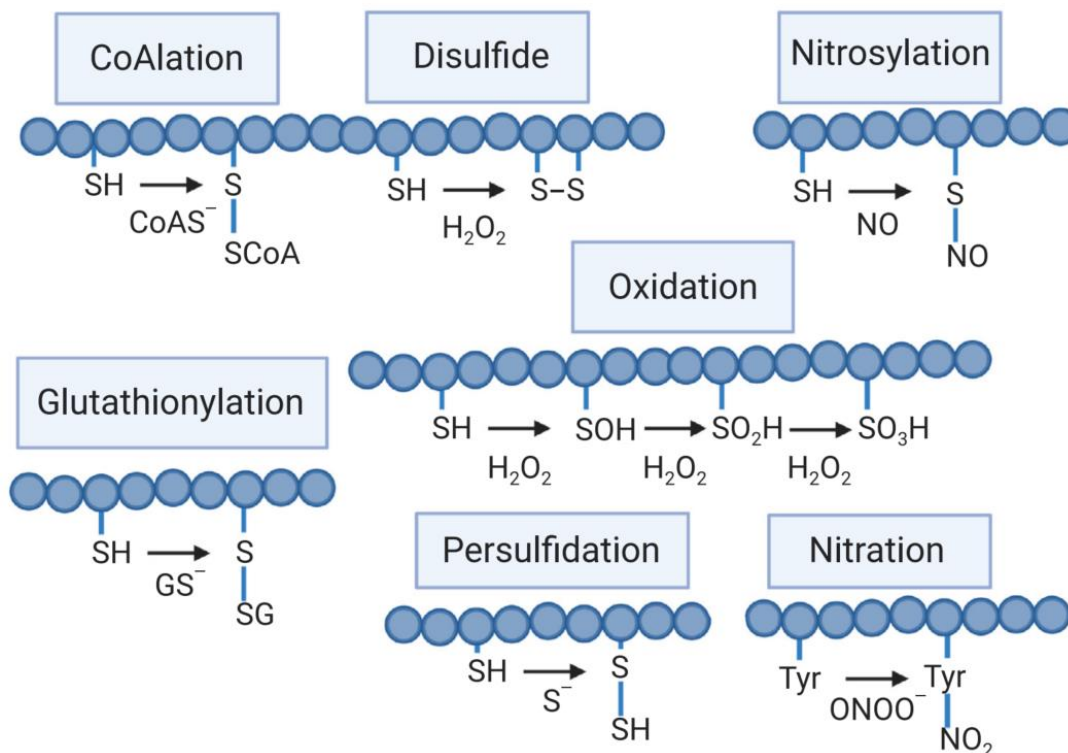
Figure 1.4 – Oxidative cysteine modifications. Cysteine can undergo reversible and irreversible modifications to form different oxo-forms such as CoAlation, disulfide formation, nitrosylation, glutathionylation, oxidation, persulfidation, and nitration. This figure was adapted from Harris *et al*. 2020, with permission from the copyrights clearance center.[54]

Glutathionylation is the formation of a disulfide bond between a protein cysteine and glutathione, and this modification is important in modulating protein activity.[47] Modifying a cysteine with the fatty acid palmitate results in S-palmitoylation which is crucial in protein trafficking and subcellular localization. Finally, disulfide bond formation is essential for regulating protein function and maintaining the tertiary structure of

proteins (Figure 1.4).[47] These reversible modifications are crucial for cellular signaling and preventing proteins from undergoing irreversible modifications.

1.6 Protein S-glutathionylation

Glutathionylation is the formation of a mixed disulfide bond between a protein cysteine and the cysteine in glutathione. Because glutathionylation is reversible, it can protect proteins from irreversible oxidative modifications, allowing recovery of protein function when the normal redox status of the cell is recovered.[28, 55, 56] Glutathionylation serves as a regulatory mechanism in redox signaling by modifying specific cysteine residues in proteins. Many proteins involved in important cellular events such as cell signaling, proliferation, migration, and apoptosis are regulated by glutathionylation.[57] Examples include signaling proteins such as protein kinases A and C (PKA/PKC), ion channel, and calcium-dependent proteins such as apoptotic death receptor protein Fas (CD95) and sarcomeric/ endoplasmic reticulum calcium ATPase (SERCA), transcription factors NF-κB and c-Jun, and enzymes containing active site cysteines such as caspase-3 and glyceraldehyde 3-phosphate dehydrogenase (GAPDH).[58-63] Since glutathionylation is transient in physiology, an increase in glutathionylation is associated with various diseases like cardiovascular diseases, cancer, and other neurodegenerative diseases causing disturbances in normal redox signaling pathways.[18, 57, 61, 64] Hence, investigation of glutathionylation and other oxidative modifications is an important area of research.

Glutathionylation is a non-enzymatic reaction that occurs in the cells in response to elevated levels of ROS. Glutathionylation can occur in two ways: 1) direct interaction

between a sulfhydryl and GSH, and 2) thiol/disulfide exchange reactions between protein cysteine and PSSG or GSSG.[28] Removal of protein glutathionylation, also known as deglutathionylation, is a reaction catalyzed by glutaredoxin (GRx) and glutathione transferase omega (GSTO) enzymes.[18, 43, 65, 66] GRx catalyzes deglutathionylation through two different mechanisms; the monothiol and the dithiol mechanisms (Figure 1.5). In the monothiol mechanism, first, the thiolate anion of GRx attacks a glutathionylated protein to release the reduced protein with its free thiol. Then, the resulting GRx enzyme intermediate is regenerated by oxidizing free glutathione, which is then reduced by glutathione reductase (GR) using NADPH. In the dithiol mechanism, GRx uses both active site cysteines to reduce the glutathionylated protein. Reduction of the GRx intermediate requires two free glutathiones to regenerate the enzyme.[67] Two mammalian GRxs have been characterized so far: GRx1 and GRx2. GRx1 is found mainly in the cytosol, and GRx2 is mostly found in mitochondria and nucleus.[63] Deglutathionylation also occurs spontaneously without enzyme catalysis due to the reductive cellular environment and high GSH concentration in some cells, but at a lower rate.[18]

A Monothiol Mechanism

B Dithiol Mechanism
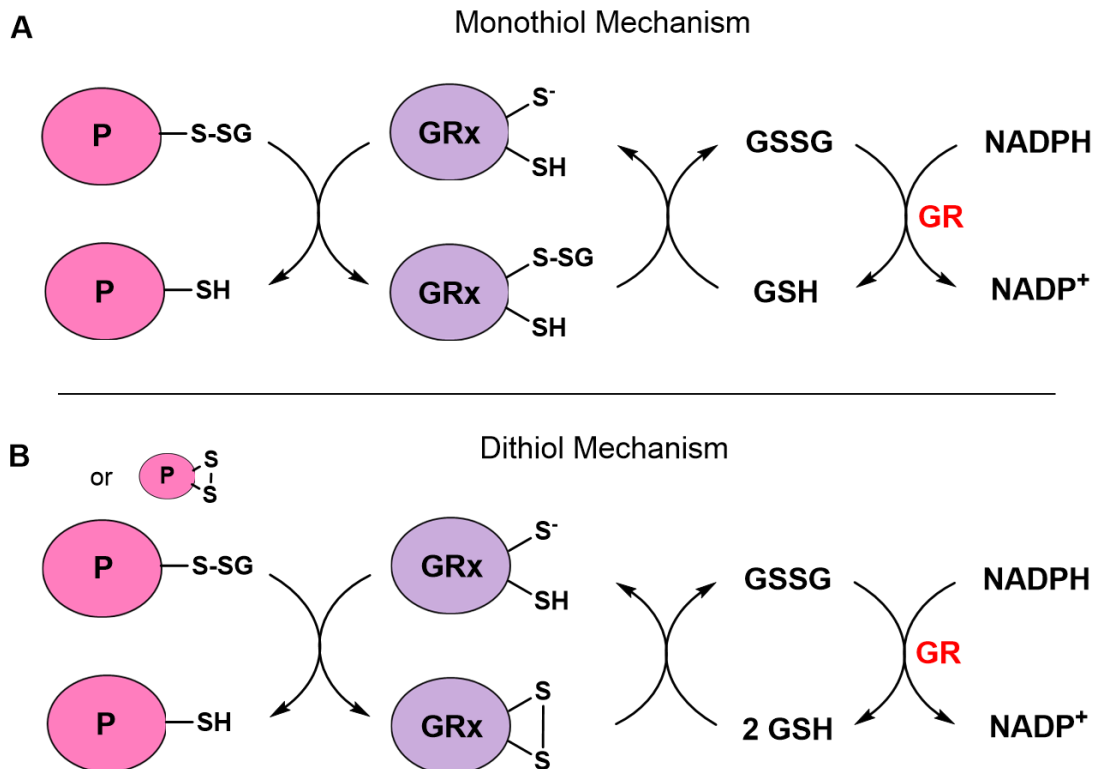
Figure 1.5 – Deglutathionylation by glutaredoxin. Deglutathionylation can be catalyzed by GRx in two different ways A) a monothiol mechanism and B) a dithiol mechanism.

Glutathione (GSH) is the most abundant low molecular weight thiol in animal cells (0.5-10 mmol/L).[64, 68-70] GSH is localized mainly in the cytosol (up to 90%) and is present in mitochondria (10%), and in the nucleus and endoplasmic reticulum in small percentages.[71, 72] GSH biosynthesis is a two-step process catalyzed by two cytosolic enzymes: γ-glutamyl cysteine synthetase (GCS), also known as γ-glutamylcysteine ligase (GCL), and glutathione synthetase (GS) (Figure 1.6).[73-75]
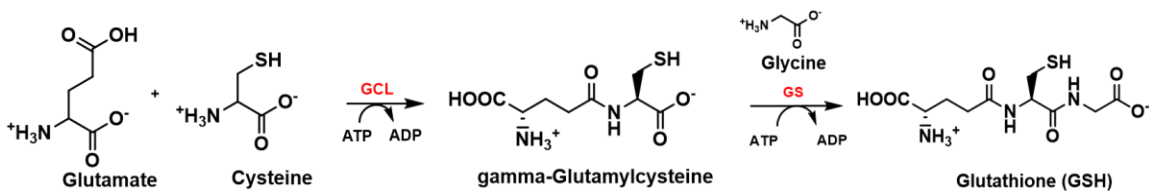
Figure 1.6 – Glutathione biosynthesis. The biosynthesis of glutathione involves two cytosolic enzymes GCL and GS.

GCS catalyzes the formation of γ -peptide linkage between the γ-carboxyl group of glutamate and amino group of cysteine to form γ-glutamyl-cysteine dipeptide. GS catalyzes the formation of the peptide linkage between γ-glutamyl-cysteine and glycine, forming the tripeptide GSH. In the biosynthesis of GSH, GCS undergoes feedback inhibition by glutathione, making it the rate-limiting enzyme.[68, 73, 76]

1.7 Significance of protein S-glutathionylation in human diseases

Proteins undergoing S-glutathionylation have been studied as possible biomarkers of oxidative stress in response to various diseases. The fluctuation in the level of glutathionylation in response to a pathophysiological condition can indicate the evolution of a disease.[27] Proteins involved in different disease conditions such as CVD, chronic renal failure, cancer, neurodegenerative diseases, and diabetes mellitus undergo glutathionylation.[18, 24, 27]

Mitochondrial complex II is the key enzyme that connects the TCA cycle to the ETC. Mitochondrial complex II is catalyzes the oxidation of succinate to fumarate in the mitochondrial matrix. Reduction of ubiquinone in the mitochondrial inner membrane is coupled with the oxidation of succinate as part of electron transport. This electron

transport from succinate to ubiquinone is mediated by succinate ubiquinone reductase (SQR). SQR has a 70 kDa FAD binding subunit (SQR-70kDa), known to be important in antioxidant defense and redox signaling. Glutathionylation of C90 of this SQR-70kDa occurs under physiological conditions. In post-ischemic myocardia, C90 is partially or completely de-glutathionylated, and the electron transfer activity (ETA) of SQR decreases significantly. This C90 deglutathionylation decreases electron leakage to O_2 and increases electron transfer efficiency to combat oxidative injury during ischemia/reperfusion.[77]

Na,K-ATPase, an enzyme found in the animal cell membrane, transports Na^+ and K^+ across plasma membrane using ATP energy to mediate transmembrane ion gradients for the active transportation of metabolic substrates and ions. During hypoxia, several cysteine sites in Na,K-ATPase undergo glutathionylation, leading to the partial or complete inhibition of this enzyme.[78] This process rescues ATP for cell survival during hypoxia.[79, 80]

Cancer is a disease caused by uncontrollable cell growth due to rapid proliferation and inhibition of apoptosis. Apoptosis is executed by a member of the cysteine protease family of enzymes known as caspases. Cancer cells have a high ROS level and exert high oxidative stress due to metabolic, genetic associated, and mitochondrial dysfunctions. They use metabolic pathways to increase antioxidant molecules such as GSH and NADPH as a response to high oxidative stress. Caspase activity in cancer cells is inhibited by the glutathionylation of caspase-3 at two cysteine sites (C145 and C45), inhibiting apoptosis. Compared to wild-type caspase-3, cysteine to serine mutants increase apoptotic ability.

Identification of glutathionylation sites of caspases such as caspase-3 that promote cancer cell survival may be important for developing novel anticancer drugs.[67]

1.8 Approaches to identify and quantify protein glutathionylation

Identification and quantification of proteins undergoing glutathionylation with their specific cysteine sites are essential to understand the relevance of protein glutathionylation in physiological and pathological processes. So far, there are a limited number of approaches available to identify and quantify protein glutathionylation.

1.8.1   Radiolabeled cysteine

One early established method to identify glutathionylated proteins uses metabolically labeled GSH with radiolabeled cysteine (S^{35}). After the induction of glutathionylation by the addition of H_2O_2 or diamide, proteins are separated on SDS-PAGE. Glutathionylated proteins can then be detected using autoradiography or phosphor imaging. This method allowed the identification of several glutathionylated proteins such as GAPDH, protein kinase C-α, thioredoxin (TRx), cyclophilin A, and pax-8.[58,81] This method is lacks sensitivity and not specific to differentiate individual glutathionylated sites in the same protein.[58]

1.8.2   Modified biotin tags

To overcome the limitations on sensitivity, new mass spectrometry-based methods to identify glutathionylated proteins have been developed. Most methods use modified biotin tags (N-ethylmaleimide-biotin tag/biotinylated glutathione tag) to label glutathionylated proteins. Biotinylated glutathione tags like biotinylated glutathione ethyl

ester (BioGEE) and biotinylated glutathione are being used for the direct identification of glutathionylation.[58, 81, 82] NEM-biotin identifies glutathionylated proteins indirectly. First, glutathionylation is induced by ROS. Next, cells are lysed in the presence of an irreversible blocking reagent to modify unreacted cysteines. Then glutathionylated sites are reduced selectively using a reducing agent [dithiothreitol (DTT), tris(2-carboxyethyl) phosphine (TCEP), or mutant GRx], and proteins are alkylated with modified biotin tag NEM-biotin]. Biotinylated proteins are enriched with streptavidin beads and analyzed by LC-MS/MS (Figure 1.7).[58, 81]
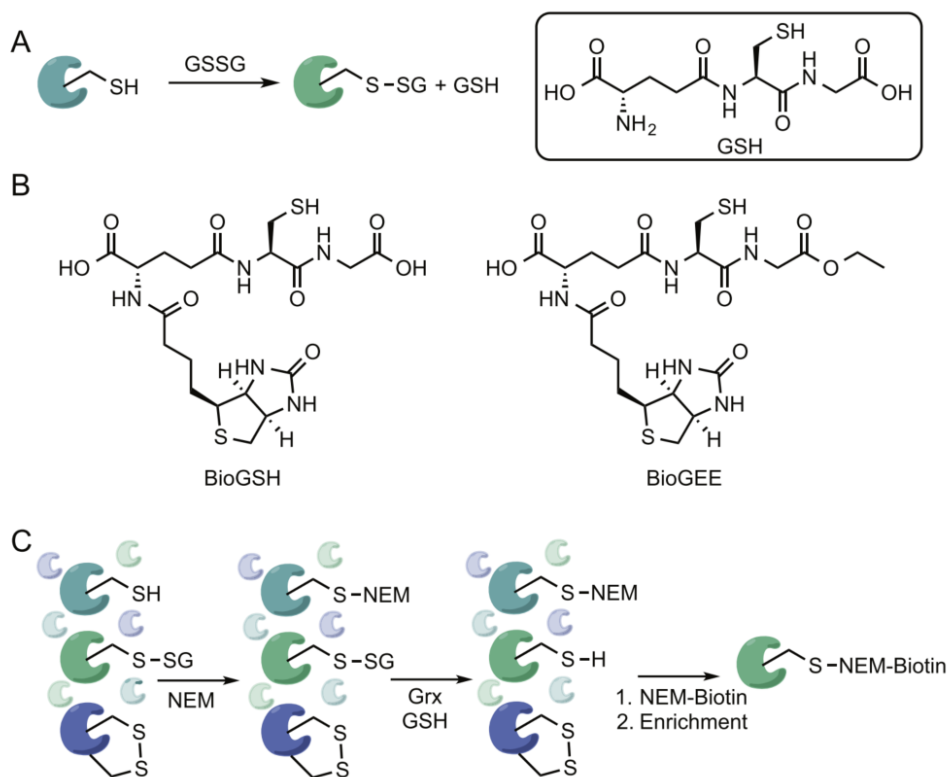
Figure 1.7 – Identification of protein glutathionylation using modified biotin tags. A) Protein glutathionylation under stress. B) Modified biotin tags BioGSH and BioGEE. C) Scheme for the identification of glutathionylation using modified biotin tags. Figure was adapted from Couvertier et al. 2014 with permission from the copyrights clearance center.[52]

1.8.3 Tandem mass tagging (TMT)

Another indirect method to identify glutathionylated proteins uses tandem mass tagging (TMT). Cells induced by ROS are lysed in the presence of an irreversible blocking reagent to modify unreacted cysteines. Then glutathionylated sites are selectively reduced using a cocktail of reducing agents (Grx, GR, GSH, and NADPH), and unmodified cysteines are labeled with iodoacetyl tandem mass tag (Iodo-TMT). Proteins are digested using trypsin, enriched with TMT antibody resin, and analyzed using LC-MS/MS.[83]
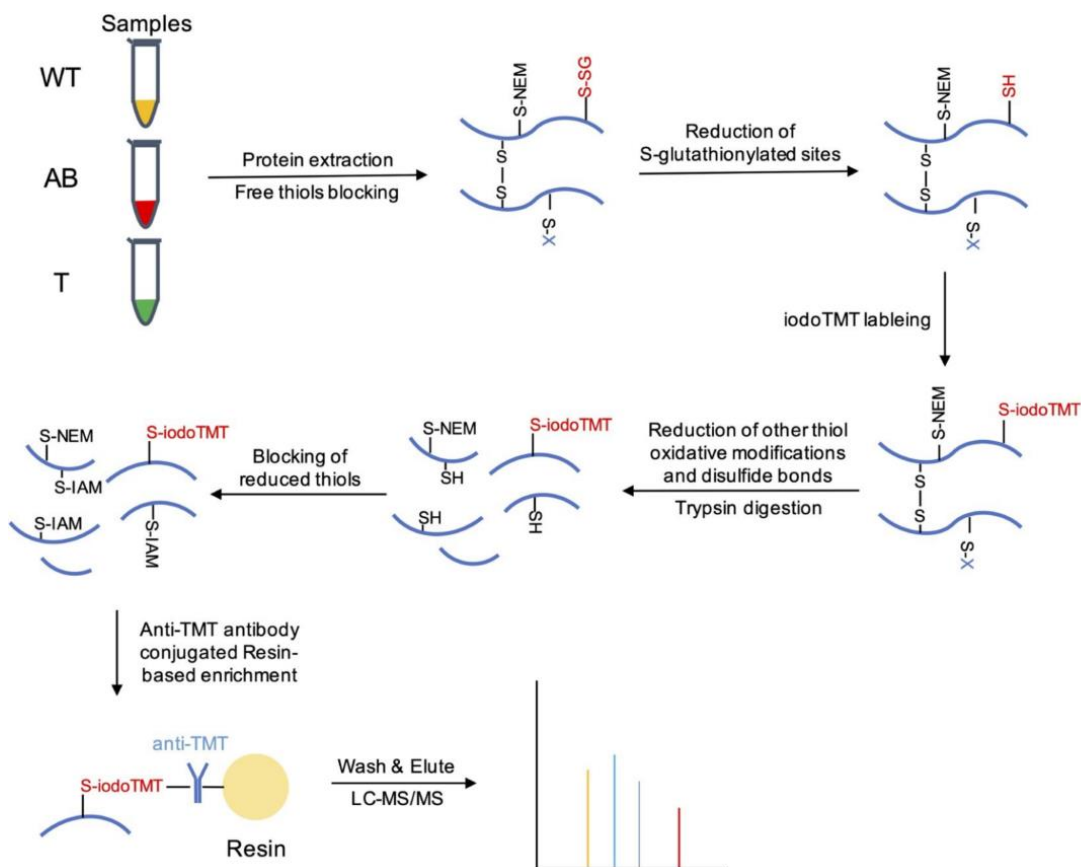
Figure 1.8 – Schematic diagram of the Iodo-TMT labeling to identify protein glutathionylation. This figure was adapted from Li *et al*. 2020, a free access article.[83]

These indirect approaches, which that use reducing agents such as Grx, DTT, or TCEP may cause the removal of reversible cysteine modifications other than glutathionylation. Therefore, it is uncertain that these methods can be used to effectively identify glutathionylation.[84] To overcome these limitations, our lab has developed a chemoproteomic method to detect protein glutathionylation, using click chemistry.

1.9 Clickable glutathione approach to detect protein glutathionylation

Previously, our lab developed a method to detect protein glutathionylation in cells by synthesizing clickable-glutathione (azido-glutathione, N_3-GSH) using a glutathione synthetase mutant (GS M4) in the presence of azido-alanine (azido-Ala). The active site of GS was engineered to incorporate an alkyne or azide-containing amino acid derivative in place of the glycine in GSH. Clickable GSH generated by the mutated GS was used to label proteins undergoing glutathionylation upon stress. The azide group of clickable glutathione can be utilized to detect glutathionylated proteins after the subsequent bio-orthogonal click reaction with biotin or a fluorophore alkyne (Figure 1.9).[85-87] This clickable glutathione approach successfully detected proteins undergoing glutathionylation at a global level in response to H_2O_2, glucose metabolism, and mitochondrial dysfunction. Our lab utilized this method for proteomic identification of glutathionylated proteins in HEK293 cells.[87]
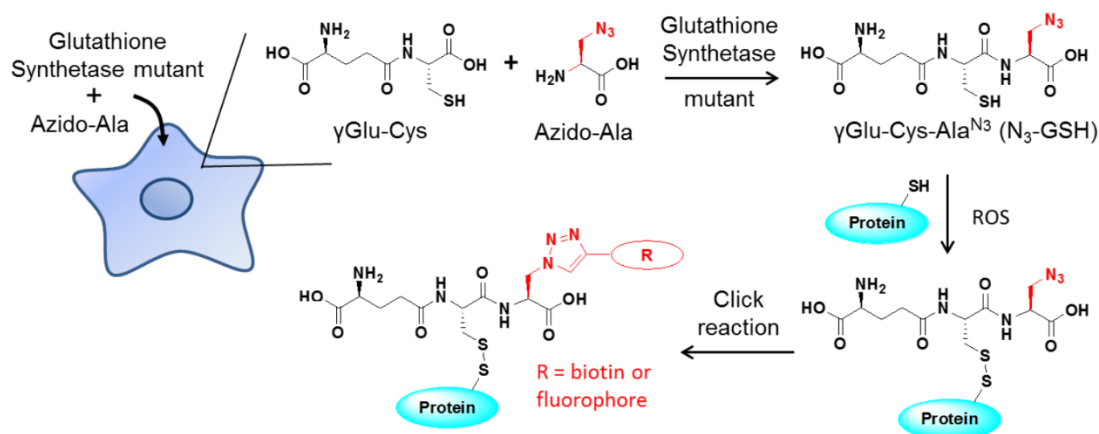
Figure 1.9 – Scheme for the clickable glutathione approach to detect protein glutathionylation. This figure was adapted from Samarasinghe *et al*. 2014 with permission from the copyrights clearance center.[85]

1.10 Proteomic identification of protein glutathionylation in cardiomyocytes

We have improved the clickable glutathione approach to detect protein glutathionylation and developed a mass spectrometry-based strategy to identify proteins undergoing glutathionylation with their specific cysteine sites in the HL-1 mouse cardiomyocyte cell line. This cell line retains differentiated cardiac morphology and an ability to contract. It is derived from AT-1 mouse atrial cardiomyocyte tumor cells.[88] This cell line maintains a gene expression profile similar to atrial cardiomyocytes, therefore it is suitable to detect cardiac protein glutathionylation.[89] Glutathionylated cysteines with clickable glutathione were subjected to click reaction with biotin-DADPS (dialkoxydiphenylsilane)-alkyne. Modified proteins were enriched with streptavidin agarose beads, and digested with trypsin/LysC to isolate modified peptides. Peptides were cleaved from the beads using acid, and samples were subjected to LC-MS/MS analysis (Figure 1.10).[89] Over 1700 glutathionylated sites were identified, and

bioinformatic analysis suggested possible biological processes affected by glutathionylation, including protein folding, metabolism, and translation. Further STRING and cluster analysis identified 125 cardiomyopathy-associated proteins undergoing glutathionylation.[89] This approach was successful in identifying proteins undergoing glutathionylation with their specific cysteine residues, but the percentage of each cysteine undergoing glutathionylation is still to be determined.
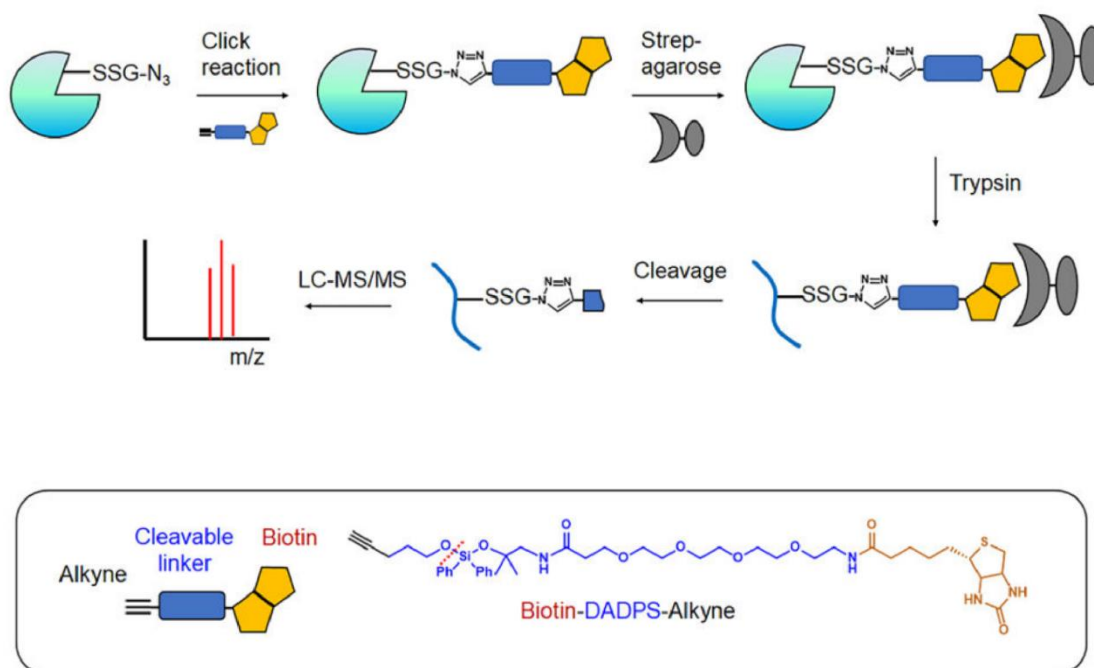
Figure 1.10 – Scheme for the clickable glutathione approach to identify glutathionylated cysteines. This figure was adapted from VanHecke *et al*. 2019 with permission from the copyrights clearance center.[89]

1.11   Current dissertation work

Elevated intracellular levels of ROS are associated with the induction of oxidative stress. Under low to moderate concentrations, ROS can act as signaling molecules to maintain cardiovascular function. However, increased levels of ROS participate in the development of CVDs by modifying proteins reversibly or irreversibly. Especially, cysteine residues in these proteins can undergo oxidative post-translational modifications, causing structural and functional modifications. One such modification is protein glutathionylation. Glutathionylation is the formation of a disulfide bond between a protein cysteine and glutathione. It is an important regulatory reversible thiol oxidation. Identification and quantification of glutathionylated proteins is important for understanding the molecular mechanisms behind the initiation and progression of many diseases. However, there are few methods to identify and quantify protein glutathionylation at specific cysteine residues. Our lab previously developed a click chemistry-based method to detect and identify glutathionylation in cells by synthesizing clickable-glutathione using a glutathione synthetase mutant (GS M4) in the presence of azido-alanine (azido-Ala).

Chapter 2 discusses our recently established mass spectrometry-based strategy for the identification and quantification of glutathionylation. Two azido-Ala derivatives with a 4 Da isotopic mass difference were used for the metabolic synthesis of isotopically labelled clickable glutathione for the identification and quantification of glutathionylated proteins. We applied this isotopically labeled clickable glutathione approach on HL-1

cardiomyocyte cells to identify and quantify over 1300 glutathionylated peptides upon the addition of H_2O_2.

Chapter 3 discusses the application of the clickable glutathione approach to detect protein glutathionylation under different ischemic stress conditions in the HL-1 mouse cardiomyocyte cell line. In addition, we have identified and relatively quantified 248 glutathionylated proteins under ischemic reperfusion (I/R) condition by applying an isotopically labeled clickable glutathione approach. From the bioinformatic analysis of the identified 248 proteins, we found 18 glutathionylated cysteine residues whose genetic modifications are known and associated with muscular disorders.

Chapter 4 will discuss our new approach for the quantification of glutathionylated cysteines compared to unmodified cysteines. We have designed and synthesized a cysteine blocking clickable glutathione reagent that mimics isotopically labeled light azido glutathione. Upon induction of glutathionylation with isotopically labeled heavy azido glutathione, this reagent can block unmodified cysteines, which enable quantification of glutathionylation. We have applied this approach on the C2C12 mouse skeletal muscle cell line and identified 1518 glutathionylated peptides upon the addition of H_2O_2.

Chapter 5 discusses the functional studies of the sarcomeric protein desmin. From our previous proteomic analysis, we have identified and confirmed that desmin undergoes glutathionylation. Desmin is a major intermediate filament protein that is important in maintaining the structural and mechanical integrity of the sarcomere. We observed that desmin loses its myofibril integrity under ischemic stress conditions. We

have used WT and mutant desmin to investigate the effect of glutathionylation on this

observation. Our data reveal that glutathionylation of desmin C332 may lead to a loss of

its myofibril integrity.

CHAPTER 2: ISOTOPICALLY LABELED CLICKABLE GLUTATHIONE TO QUANTIFY PROTEIN

S-GLUTATHIONYLATION

(The work of this chapter is adapted from VanHecke, G. C.; Yapa Abeywardana, M.; Huang, B.; Ahn, Y. H., Isotopically Labeled Clickable Glutathione to Quantify Protein S-Glutathionylation. Chembiochem 2020, 21 (6), 853-859)

2.1 Introduction

Reactive oxygen species, such as H_2O_2, have been studied extensively for their function as physiological regulators of intracellular signaling pathways.[24] However, the overproduction of ROS is associated with different diseases such as cardiovascular diseases.[90, 91] The effects of ROS can be modulated through oxidative modifications of different amino acids. Among the twenty encoded amino acids, cysteine is uniquely susceptible to oxidative modifications in the presence of oxidative stress. Cysteine can be oxidized to form different oxoforms including, sulfenylation (SOH), sulfhydration (SSH), disulfide bond formation (RS-SR'), and glutathionylation (RS-SG).[24, 61, 92] These modifications confer different functional alterations onto modified proteins because of their various sizes and chemical properties.

Glutathionylation is a reversible regulatory process that occurs in proteins as a response to changes in the redox status of cells. Glutathionylation adds a relatively bulky glutathione group to the protein through a mixed disulfide bond. The biological or functional significance of glutathionylation has been demonstrated with many examples of redox-active proteins, including titin, caspase-3, GAPDH, eNOS, SERCA, voltage-gated

calcium channels (VGCC) and ryanodine receptors (RyR).[59, 79, 93-96] Prediction of specific cysteine residues that undergo glutathionylation allows the identification of new target proteins, which can have altered functions under pathological conditions due to an impaired redox environment.[79] Therefore, many biochemical approaches, specifically mass spectrometry-based proteomic methods, have been developed to investigate protein glutathionylation,[79, 82, 83, 97] especially with the specific cysteine sites.[89, 98] The biotin switch method is a common technique for the proteomic identification of glutathionylation. In this approach, after blocking unmodified cysteines, glutathionylated cysteines are reduced by glutaredoxin and re-alkylated using biotin and enriched through streptavidin affinity isolation.[99-101] For the quantification of protein glutathionylation, this method has also been modified with isobaric tagging.[100, 102] We have also developed a mass spectrometry-based proteomic method to identify proteins undergoing glutathionylation with their specific cysteine sites and identified over 1700 glutathionylated peptides in a cardiomyocyte cell line.[89]

2.2 Approach

We have developed a mass spectrometry-based approach to quantify the relative level of glutathionylated peptides using isotopically labeled heavy and light clickable glutathione. We used heavy and light labeled azido alanine (N_3-Ala) derivatives to metabolically synthesize heavy and light azido glutathione (Figure 2.1). First, we demonstrated their ability to label clickable glutathione identically *in vitro* and *in vivo* using purified GSTO1 protein and HEK293 cells upon addition of H_2O_2. We then applied

this approach to the HL-1 mouse cardiomyocyte cell line to identify 1398 glutathionylated peptides with their relative levels of glutathionylation upon addition of H_2O_2 (Figure 2.1). Finally, we validated glutathionylation of two structural proteins in the sarcomere, desmin and α-actinin.
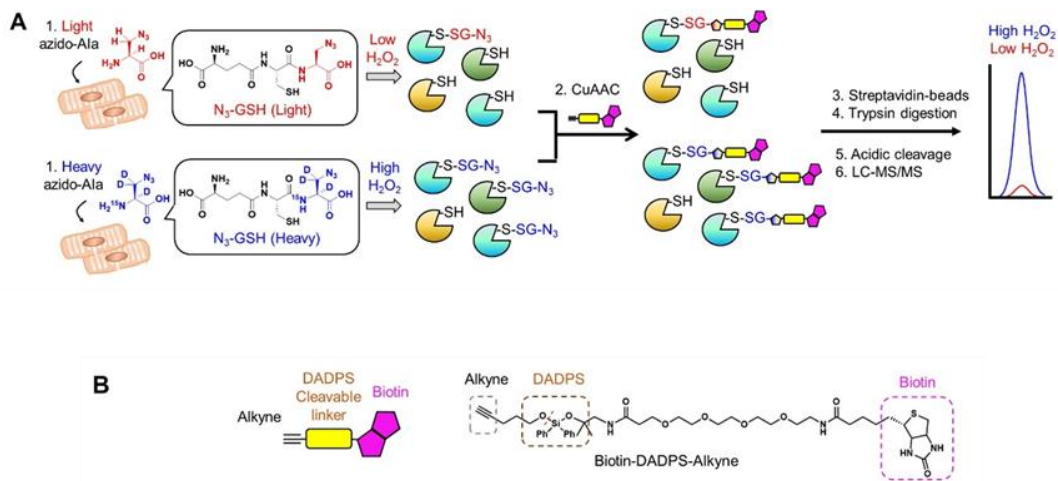
Figure 2.1 – Isotopically labeled clickable glutathione strategy to identify and quantify protein glutathionylation. A) Scheme for the quantification of glutathionylated peptides using isotopically labeled clickable glutathione. B) Structure of biotin-DADPS-alkyne.

2.3 Results

2.3.1 Examination of isotopically labeled clickable glutathione to detect S-glutathionylation - In vitro glutathione synthetase enzyme assay

Using a coupled enzyme assay, heavy and light azido alanine derivatives were compared for their efficiency to synthesize clickable glutathione by GS M4. The GS enzyme activity for two different concentrations (0.2 and 1 mM) of heavy azido alanine (H-N₃Ala, blue) or light azido alanine (L-N₃Ala, red) derivatives were determined by measuring the NADH consumption with an ATP regenerating system in the presence of pyruvate kinase (PK) and lactate dehydrogenase (LDH). The consumption of NADH was monitored by measuring UV absorbance at 340 nm. This in vitro assay demonstrated that both heavy and light N₃Ala derivatives are utilized by GS M4 as substrates with the same kinetic rates (Figure 2.2).
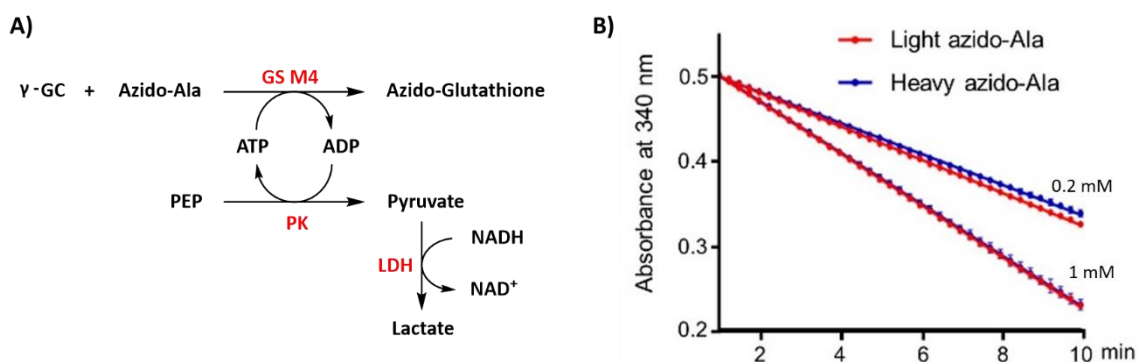
Figure 2.2 Kinetic assay for GS M4 with heavy and light N₃Ala derivatives. A) Scheme for the coupled enzyme assay. B) The GS enzyme activity for two different concentrations (0.2 and 1 mM) of heavy azido alanine (H-N₃Ala, blue) or light azido alanine (L-N₃Ala, red) derivatives were determined using the kinetic assay. H-N₃Ala and L-N₃Ala derivatives are utilized at the same kinetic rates by GS M4 in vitro

2.3.2 Isotopically labeled clickable glutathione approach on purified protein (This work was carried out by Garrett C. VanHecke)

Glutathionylation of purified GSTO1 protein was induced in the presence of equal amounts of heavy and light azido glutathione in vitro and subjected to click reaction with biotin-DADPS-alkyne. The protein was digested with trypsin/LysC, enriched using streptavidin agarose beads, eluted by incubation with acid, and analyzed by matrix-assisted laser desorption ionization (MALDI). Two peaks were identified with similar ion intensities and 4 Da apart from each other (1284.68 and 1288.71), with a median intensity ratio of heavy to light peptides 0.88 ± 0.09, n = 3. Peaks identified corresponded to the molecular weights of the peptide FC$_{32}$*PFAER after being modified with heavy or light azido glutathione. The identified cysteine residue is in the active site of GSTO1 and is known to undergo glutathionylation.[89] These in vitro results demonstrates that heavy and light azido alanine derivatives can be used for the detection of glutathionylation with a 4 Da mass difference (Figure 2.3 A).
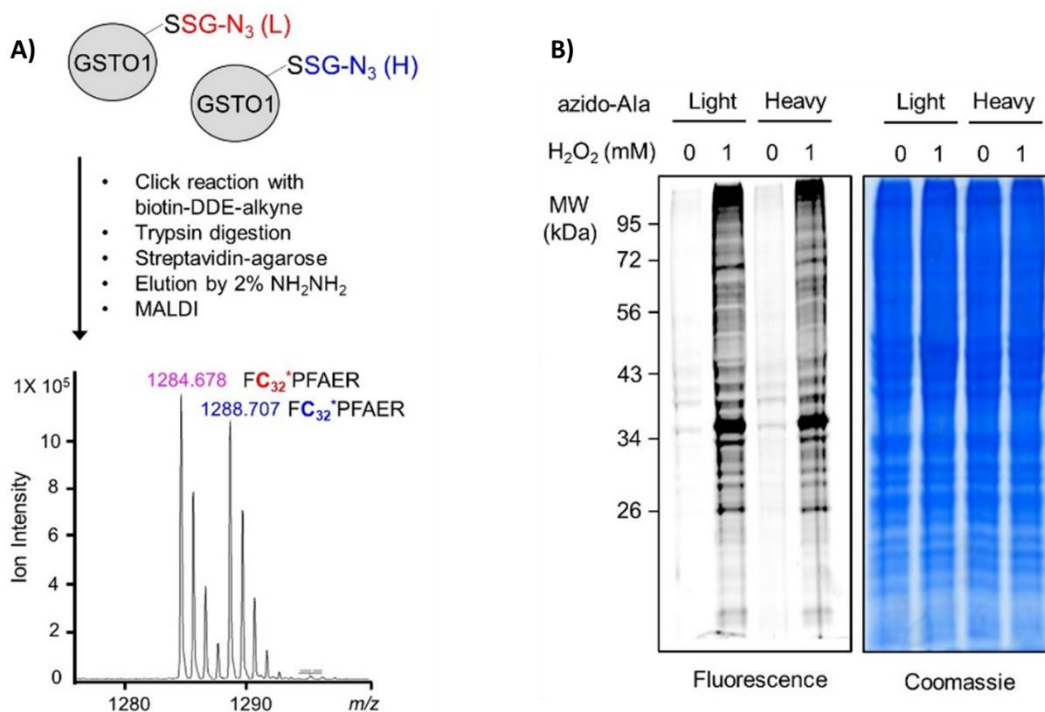
Figure 2.3 – Identification of glutathionylated peptides using heavy and light N$_3$Ala derivatives. A) Glutathionylation of purified GSTO1 protein was induced by the addition of diamide (1 mM, 30 min) in the presence of both heavy and light labeled azido glutathione derivatives (1 mM each). The glutathionylated protein was subjected to click reaction with biotin-DDE-alkyne followed by trypsin digestion, pull down, elution and MALDI analysis. These results demonstrate the ability to utilize heavy and light azido alanine derivatives for the detection of glutathionylation with a 4 Da mass difference. B) HEK293/GSM4 cells treated with heavy or light azido alanine were induced by the addition of H$_2$O$_2$ (1 mM, 15 min) and subjected to click reaction with a Cy5-alkyne. Glutathionylaation of HEK293/GS M4 cells demonstrates that heavy and light azido glutathione labels proteins identically.

2.3.3   In vivo detection of glutathionylation by heavy and light azido glutathione (This work was carried out by Garrett C. VanHecke)

Stable HEK293 cells overexpressing GS M4 (HEK293/GS M4) were incubated with heavy or light azido alanine and induced by the addition of H$_2$O$_2$. Cell lysates were subjected to a click reaction with Cy5-alkyne. Both heavy and light azido alanine treated cell lysates showed identical in-gel fluorescence patterns and intensities of global

glutathionylation (lane 2 vs lane 4). These results show that both heavy and light azido

glutathione label proteins identically (Figure 2.3 B).

2.3.4   Isotopically labeled clickable glutathione approach for proteomic analysis

The HL-1 mouse cardiomyocyte cell line was used as a model system to evaluate

heavy and light azido alanine derivatives for the proteomic identification of

glutathionylated cysteine residues. The HL-1 cell line was specifically selected due to the

importance of oxidative stress and redox signaling in cardiomyocytes.[90] HL-1 cells

overexpressing GS M4 were treated with either heavy or light azido alanine and

glutathionylation was induced with equal amounts of H_2O_2 (1 mM: E1 condition, Figure

2.4A). Lysates from the two cultures (containing equal amounts of heavy or light azido

alanine) were combined and subjected to a bio-orthogonal click reaction with biotin-

DADPS-alkyne. Modified proteins were enriched with streptavidin agarose beads,

digested on beads using trypsin/LysC, eluted by acidic cleavage of the DADPS linker, and

subjected to LC-MS/MS analysis (E1 experiment).

Individual pairs of glutathionylated peptides with +4 Da isotopic mass differences

were identified (in at least two out of three replicates). The peptides were quantified to

give a heavy to light ratio ($R_{H/L}$) using Skyline software.[103] Under these E1 conditions,

where heavy or light azido-alanine treated samples were induced with equal amounts of

H_2O_2, 1398 pairs of glutathionylated peptides were identified (Figure 2.4A) with a median

$R_{H/L}$ value of 0.94. The fact that this median value is close to 1, (92.6% of $R_{H/L}$ in range of

0.6-1.4, Figure 2.4B left), suggests that proteins/peptides undergo a nearly equal level of

glutathionylation with the heavy and light GSH analogs. Figure 2.4D shows MS1 peaks for representative individual peptides identified such as ACTN4 C352, FLNC C1067, ACTN1 C480, and DES C332 with $R_{H/L}$ values close to 1 (1.07, 0.99, 0.84, and 0.88, respectively). Also, the median coefficient of variation (CV) value (13.5%) for E1 indicates that triplicate experiments show a nearly consistent quantification (Figure 2.4B right). Many of the proteins found under E1 condition were consistent with our previous proteomic data (Figure 2.4C).[89]
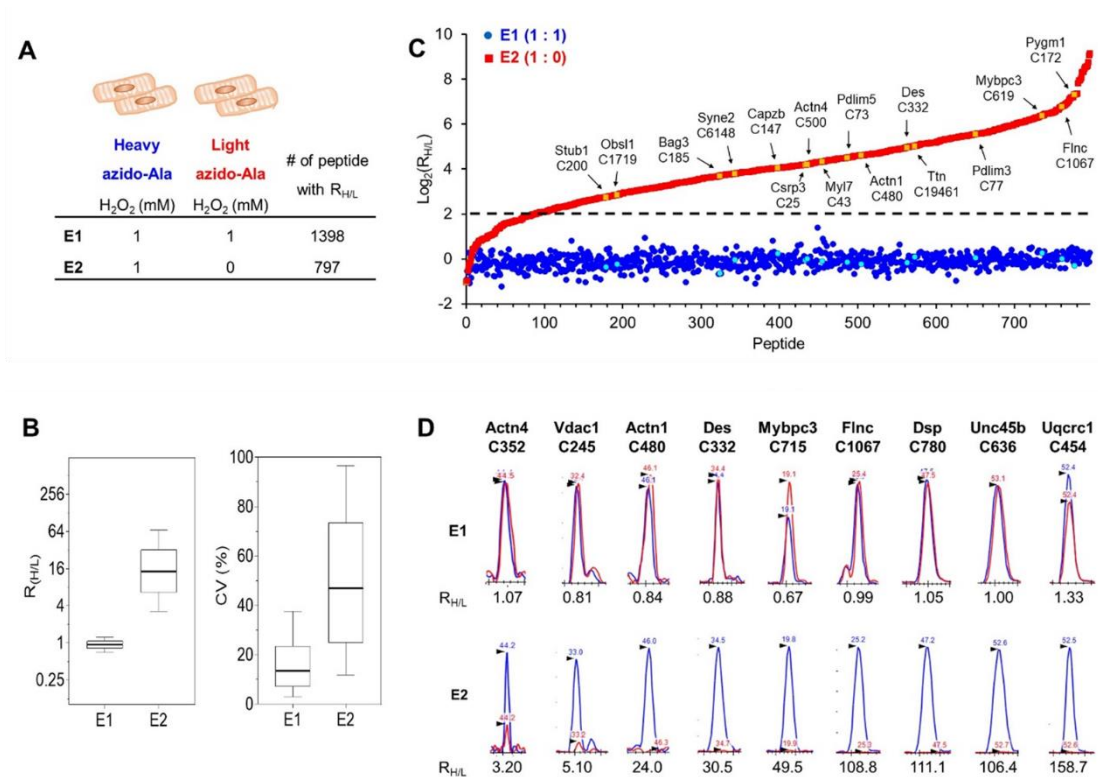
Figure 2.4 – Isotopically labeled glutathione approach for the identification and quantification of glutathionylated peptides. A) Experimental conditions and the number of glutathionylated peptides identified by isotopically labeled clickable glutathione. B) $R_{H/L}$ values and CV of glutathionylated peptides. C) $R_{H/L}$ value distribution of individual glutathionylated peptides. D) MS1 peaks showing relative quantification of heavy (blue) to light (red) azido glutathione labeled peptides.

2.3.5 Relative quantification of glutathionylated peptides

We carried out relative quantification of the levels of glutathionylation upon addition of H_2O_2. Cells treated with heavy and light azido-alanine were induced with and without the addition of H_2O_2, respectively (1 mM H_2O_2 for heavy and 0 mM H_2O_2 for light: E2 condition, Figure 2.4A). After the same sample preparation and analysis process as for E1, 797 pairs of glutathionylated peptides were identified (in at least two out of three replicates: Figure 2.4A), with a wide distribution of their $R_{H/L}$ values. The median $R_{H/L}$

value was 16.3 (80% of $R_{H/L}$ in the range of 3.7 - 0.2, Figure 2.4B left). This wide distribution of $R_{H/L}$ shows that the extent of protein glutathionylation increases upon the addition of H_2O_2. The majority of identified peptides (89%, 707 out of 798) reflected a significant increase in global glutathionylation upon the addition of H_2O_2, with $R_{H/L}$ values greater than 4. Compared to the median CV value for E1 (14.6%), the median CV value for E2 is relatively high (46.7%, Figure 2.4B right).

Using DAVID GO annotation we identified sarcomeric and muscle proteins that undergo glutathionylation under oxidative stress conditions using their $R_{H/L}$ values (Figure 2.4C-D and Table A.2.1), such as structural proteins [ACTN1 C480, ACTN4 C500, DES C332, and filamin C (FLNC) C1062 with $R_{H/L}$ values 24.0, 18.2, 30.5 and 108.7, respectively], myofilamental proteins [titin (TTN) C19461, myosin light chain 7 (MYL7) C43, and myosin binding protein C3 (MYBPC3) C619 with $R_{H/L}$ values 32.1, 19.8 and 82.0, respectively], and sarcomeric chaperone proteins [unc 45 myosin chaperone B (UNC45b) C636, BAG3 C185, and obscurin like cytoskeletal adaptor 1 (OBSL1) C1719 with $R_{H/L}$ values 106.4, 12.8, and 7.1, respectively].

2.3.6   Validation of proteomic data by pull-down analysis

We used two sarcomeric proteins, desmin (DES) and α-actinin (ACTN), to validate our data by confirming the glutathionylation of specific cysteine residues. DES is the major intermediate filament protein in muscle cells that is important in maintaining elasticity and providing mechanical strength.[104-106] DES has only one cysteine (C332), and it was found to undergo glutathionylation. ACTNs are the major actin-binding proteins in the

cytoskeleton, and they are important in regulating cell mobility, adhesion, and morphology.[107-109] Mouse ACTN1 has eleven cysteines, and three of them were found to undergo glutathionylation (C370, C480, and C690) in our mass analyses; C480 is conserved within all four isoforms of ACTN (ACTN1-4).

HL-1 cells were used to confirm DES and ACTN1 glutathionylation. Cells overexpressing GS M4 were treated with azido-alanine, and glutathionylation was induced by H_2O_2 (1 mM). After the click reaction with biotin-alkyne, glutathionylated proteins were enriched with streptavidin-agarose beads. Samples were eluted for western blot analysis. Glutathionylation was detected in both DES (lane 1 vs 2, Figure 2.5B) and ACTN1 (lane 1 vs 2, Figure 2.5A) upon the addition of H_2O_2.

To determine the glutathionylation levels at specific cysteine residues, wild type (WT) and cysteine mutants of DES (DES C332S) and ACTN1 (ACTN1 C480S) plasmids were produced and used. WT and cysteine mutants were overexpressed in HEK392/GS M4 cells, and glutathionylation was induced with and without H_2O_2. Glutathionylation was detected in both DES WT (lane 4 vs 5, Figure 2.5B) and ACTN1 WT (lane 4 vs 5, Figure 2.5A) proteins upon incubation of H_2O_2. In contrast, glutathionylation levels were completely or partially reduced in DES C332S (lane 5 vs 8, Figure 2.5B) and ACTN1 C480S (lane 5 vs 8, Figure 2.5A), respectively, upon the addition of H_2O_2. These data confirm the glutathionylation of these specific cysteines. Partial reduction of the glutathionylation signal in ACTN1 C480S (lane 8, figure 2.5A) upon incubation of H_2O_2 indicates the glutathionylation of cysteines other than C480.

ACTN2 is an important protein in skeletal and cardiac muscle, whose mutation may cause cardiomyopathy.[110] Therefore, we examined the glutathionylation of C487 in sarcomeric ACTN2, which corresponds to C480 in ACTN1. Upon addition of H_2O_2, WT ACTN2 was found to undergo glutathionylation (lane 10 vs 11, Figure 2.5A). In contrast, reduced glutathionylation levels were observed for C487S mutant ACTN2 upon incubation of H_2O_2 (lane 11 vs 14, Figure 2.5A), confirming glutathionylation at C487 in the WT protein.
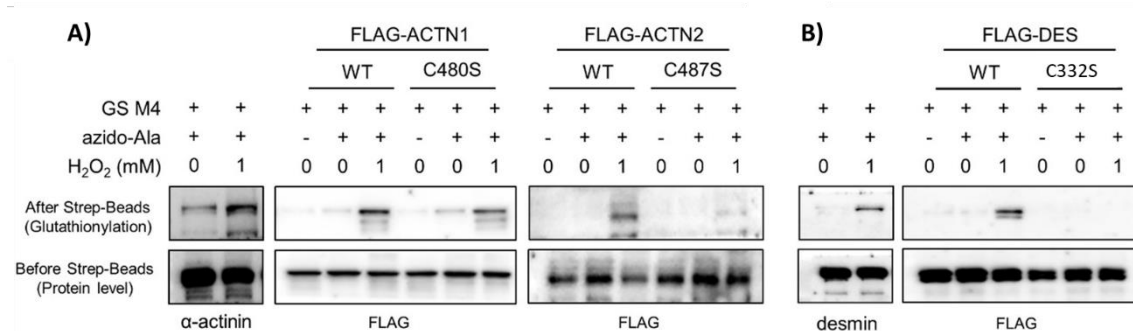
Figure 2.5 – Proteomic data validation by pull-down and western blotting in A) ACTN1, ACTN2 and B) DES. HEK293/GS M4 cells and HL-1 cells with and without overexpression of WT and mutant proteins were glutathionylated by adding H_2O_2. Cells were lysed and carried out click reaction with biotin alkyne followed by the pull-down using streptavidin agarose beads. Western blot analysis with α-actinin, desmin and flag antibodies were carried out to confirm the glutathionylation.

2.4 Discussion

Protein S-glutathionylation is an important reversible cysteine modification that regulates redox signaling and other important cellular events such as cell signaling, proliferation, and migration.[57-59] To understand the relevance of protein glutathionylation in physiological and pathological processes, identification and quantification of proteins undergoing glutathionylation with their specific cysteine cites is essential.

There are several methods available for the identification and quantification of protein glutathionylation, such as isobaric tagging, biotin labeling, and SILAC. These methods need extensive labeling of the whole proteome with isotopically labeled amino acids or labeling steps at the beginning of sample preparation.[81, 83] Even though these methods are commonly used, they suffer from major drawbacks such as inefficient selectivity of derivatization, high production costs, and limited sensitivity.[111]

Our approach utilizes a mutant of glutathione synthetase (GS M4) that was engineered to selectively modify intracellular glutathione with an azide functional group, which enables the detection or identification of glutathionylated proteins.[85, 86, 89] Here, we developed a mass spectrometry-based method to identify and quantify glutathionylated peptides with an isotopic mass difference. We feed cells with isotopically labeled heavy and light azido-alanine to metabolically synthesize heavy and light labeled clickable glutathione derivatives, which subsequently label proteins undergoing glutathionylation. We identified and quantified 797 glutathionylated peptides upon the addition of H_2O_2. Furthermore, we have validated our data using two associated sarcomere proteins: DES and ACTN, confirming glutathionylation of specific cysteine residues in each protein. This approach could be applied to profile hyper-reactive and functional cysteines in the future.

2.5 Experimental Section

2.5.1 Cell culture

T-75 dishes were coated with a gelatin-fibronectin solution and incubated at 37^0C for 1 h. The gelatin-fibronectin solution was removed by aspiration just before culturing the cells. HL-1 cells were cultured in Claycomb medium supplemented with 10% fetal bovine serum (FBS; GE healthcare), penicillin (100 U mL^{-1}), streptomycin (100 µg mL^{-1}), norepinephrine (0.1 mM), and L-glutamine (2 mM) in gelatin-fibronectin coated flasks. Cells were incubated in a humidified chamber at 37^oC and 5% CO_2.

2.5.2 Cell Splitting

At 80-100% confluency, cells were washed with warm PBS. Then, 3 mL of 0.05% warm trypsin/EDTA solution were added and incubated for 1 min at 37^oC. Trypsin/EDTA solution was removed by aspiration, and another 3 mL of fresh trypsin/EDTA solution were added and incubated for 3 min at 37^oC. After trypsinization, 3 mL of supplemented Claycomb medium were added to inactivate the trypsin. Cells were transferred to a 15 mL falcon tube and centrifuged at 500 g for 5 minutes. The supernatant was removed by aspiration, and the cells were resuspended in 6 mL of supplemented Claycomb medium. A cell suspension aliquot (2 mL) was added to each of three pre-coated T75 flasks containing 12 mL of supplemented Claycomb medium (1.5 mL of cell suspension/ 10 mL dish). Cells were maintained at 37^0C in a humidified cell culture incubator.

2.5.3 Enzyme kinetic assay

The GS M4 enzyme activity for the heavy and light azido-alanine derivatives was determined by measuring NADH consumption with an ATP regenerating system in the presence of pyruvate kinase (PK) and lactate dehydrogenase (LDH). The consumption of NADH was monitored by measuring UV absorbance at 340 nm. The reaction mixture was prepared by mixing 100 mM Tris-HCl buffer (pH 8.3, containing 150 mM NaCl and 25 mM MgCl$_2$), 2 mM γ-glutamyl cysteine, 2 mM phosphoenolpyruvate (PEP), 10 units pyruvate kinase (PK), and 15 units lactate dehydrogenase (LDH). Heavy and light azido-alanine were used as substrates with two concentrations (0.2 and 1 mM). GS M4 enzyme (0.5 µg) was added to the reaction mixture, and the reaction was started. The decrease in the absorbance at 340 nm was measured using a DU730-Beckman coulter UV/Vis spectrophotometer. The absorbance values were plotted against time.

2.5.4 Site-directed quick-change mutagenesis

Mammalian plasmids for DES, ACTN1, and ACTN2 were obtained from Origene. Cysteine to serine mutants were generated by QuikChange mutagenesis. Forward and reverse quick-change primers (Table 2.2) were incubated in two separate PCR tubes containing WT plasmid (50 ng) and pfu ultra-buffer (5 µL) each. dNTP mix (1 µL) was added, and the volume of each tube was adjusted to 49 µL. *Pfu* ultra-enzyme (1 µL, Agilent) was added to each tube. Tubes were incubated in a thermocycler and subjected to 2 thermocycles (Table 2.1). After two cycles, the two reaction mixtures were combined and incubated for another 18 cycles in the thermocycler (Table 2.1). Then, the mixture

was incubated with *Dpn*I (1 µL, 20 000 units/mL) for 1 h at 37^{0}C. *Dpn*I digested PCR

reaction (5 µL) was transformed into DH5α cells.

Table 2.1 - PCR program for quikchange mutagenesis

Cycle	Temp (^{0}C)	Time	# of cycles
Initial denaturation	95	5 min	1
Denaturation	95	45 s	
Annealing	55	45 s	2 or 18
Extension	72	20 min	
Final extension	72	10 min	1
Store	4	Hold	

Table 2.2 - Quikchange primers for desmin and ACTN

Mutation	Primer	Primer sequence 5'-3'
DES C332S	Forward	C CAG ATC CAG TCC TAC ACC TCC GAG ATT GAT GCC CTC AAG G
	Reverse	C CTT GAG GGC ATC AAT CTC GGA GGT GTA GGA CTG GAT CTG G
ACTN1 C480S	Forward	GCT CGT TGC CAA AAG ATC TCT GAC CAG TGG GAC AAT CTA GGG
	Reverse	CCC TAG ATT GTC CCA CTG GTC AGA GAT CTT TTG GCA ACG AGC
ACTN2 C487S	Forward	CGG TGC CAG GAA ATT TCC GAC CAG TGG GAT AGA TTG GG
	Reverse	CC CAA TCT ATC CCA CTG GTC GGA AAT TTC CTG GCA CCG

2.5.5 Bacterial transformation

Calcium-competent DH5α cells (50 µL) were thawed on ice and then mixed with

ice-cold plasmid DNA (50 ng) or autoclaved water (negative control) and incubated on ice

for 20 minutes. These mixtures were incubated in a heating block at 42^{0}C for 45 seconds.

Tubes were immediately removed and placed on ice for 2 minutes. Cells were mixed with

super optimal broth with catabolite repression (SOC) medium (450 µL) and incubated at

37^0C for 45 minutes Cells (100 µL) were spread evenly on agar plates containing the appropriate antibiotic. Plates were incubated for 16 h in a bacterial incubator at 37^oC.

2.5.6 Bacterial cell stock preparation

A single colony from the agar plate was inoculated in Luria-Bertani (LB) media (5 mL) with the appropriate antibiotic in a bacterial incubator at 37^0C for 16 h with shaking. The next day, an aliquot of this bacterial culture (600 µL) was mixed with 60% autoclaved glycerol (400 µL) in an Eppendorf tube, flash-frozen in liquid nitrogen, and stored at -80^{0}C.

2.5.7 Plasmid DNA isolation (Miniprep)

Plasmid isolation was carried out using a geneJET plasmid miniprep kit (Thermo Scientific) according to the instruction manual. A single colony from an agar plate or a clump of bacterial cell stock was inoculated in LB media (5 mL) containing appropriate antibiotics in a bacterial incubator at 37^0C for 16 h with shaking. This culture was centrifuged at 4500 rpm for 5 minutes at room temperature. The pellet was resuspended in resuspension solution (250 µL), and the cell suspension was transferred to an micro centrifuge tube. Lysis solution (250 µL) was added to the cell suspension and mixed thoroughly by inverting the tube 4-6 times until the solution become slightly clear and viscous. Neutralization solution (350 µL) was added, and the tube was inverted 4-6 times to thoroughly mix the contents. The solution was centrifuged at 13,000 rpm for 5 minutes to pellet chromosomal DNA and cell debris. The supernatant was transferred to the GeneJET spin column, centrifuged for 1 minute at 13,000 rpm, and the flow-through was discarded. Wash solution (500 µL) was added to the GeneJET spin column and centrifuged

at 13,000 rpm for 1 minute. The washing procedure was repeated using another 500 μL washing solution. The flow-through was discarded, and the column was centrifuged again at 13,000 rpm for 1 minute to remove residual wash solution. The spin column was transferred to a new micro centrifuge tube, and elution buffer (50 μL) was added. The solution was incubated for 2 minutes at room temperature, and centrifuged for 2 minutes at 13,000 rpm. Plasmid DNA was stored at -20^{0}C.

2.5.8 Lipofectamine transfection

At 70% - 80% confluency, HEK293/GS M4 cells were transfected with DES/ ACTN1/ ACTN2 plasmids using a lipofectamine 3000 reagent. Cell culture media was removed from the cell culture dishes (10 cm) and replaced with Opti-MEM medium (4 mL). In a sterile Eppendorf tube, the lipofectamine 3000 (24 μL) was diluted in Opti-MEM medium (250 μL). In a separate sterile Eppendorf tube, DNA (8 μg) was diluted in Opti-MEM medium (250 μL) and added P3000 reagent (16 μL). This DNA mixture was mixed with diluted lipofectamine 3000 regent and incubated for 10 minutes at room temperature. The DNA-lipid complex was then added to the cells and incubated at 37^{0}C in a mammalian cell culture incubator. After 6 h, the medium containing DNA-lipid complex was replaced with fresh complete DMEM medium (10 mL) and incubated for 18 h.

2.5.9 Bradford assay

Cell lysates were diluted 10 times using 1x PBS (2 μL lysate in 18 μL of 1x PBS). An aliquot of the diluted cell lysate (10 μL) was mixed with 1 mL of quick start 1x Bradford reagent (BioRad) in a micro centrifuge tube. A fraction (200 μL) was transferred to a clear

96 well plate, and absorbance was measured using a plate reader at 595 nm. The standard curve was generated using bovine serum albumin (BSA; BioRad) as the protein standard. BSA stock solution (1 mg/mL) was serially diluted to make 2, 4, 6, 8, 10 µg/µL solutions. Each standard solution (10 µL) was mixed with 1x Bradford reagent, and the absorbance was measured as described above.

2.5.10 Virus Transduction

At 100% confluency, HL-1 cells were infected with adenovirus expressing GS M4 (Ad/GS M4; Vector BioLabs). In HL-1 cells, the growth medium was replaced with 4 mL of 2% FBS containing DMEM medium without penicillin or streptomycin. In a sterile micro centrifuge tube, 7.5 µL of virus and 4 µL of 1 mg/mL polybrene were diluted in 500 µL of DMEM medium containing 2% FBS. The virus and polybrene mixture was incubated at room temperature for 10 minutes before adding to the cells. The virus-containing medium was replaced with supplemented Claycomb medium after 6 h of virus infection and incubated for 18 h.

Extreme safety precautions must be followed during the use of this virus in cell culture. Cell culture medium and all the contaminated media were treated with 10% bleach (final concentration) and incubated for at least 30 min. Cell culture dishes, pipets, pipet tips, and all other contaminated material were cleaned with 10% bleach solution for at least 30 min before discarding. Any contaminated media spills on a metal surface were disinfected with spore-Klenz for at least 30 minutes. Double gloving was used, and the gloves were appropriately discarded leaving the cell culture room.

2.5.11 Induction of glutathionylation and cell lysis

At 100% confluency, HL-1 cells were infected with Ad/GSM4. After 24 h, cells were incubated with heavy or light azido-alanine (0.6 mM) in supplemented Claycomb medium for 20 h. Cells were treated with or without H_2O_2 (1 mM) for 15 min. Cells were washed with cold PBS and lysed with a lysis buffer containing 100 mM 4-(2-hydroxyethyl)-1-piperazineethanesulfonic acid (HEPES, pH 7.6), 100 mM LiCl, 10% sodium dodecyl sulfate (SDS), protease inhibitor cocktail, and 50 mM N-ethyl maleimide (NEM; Sigma). The solution was incubated with rotation at 4^0C for 30 minutes and passed 10 times through a 26-gauge needle. Protein concentrations of the lysates were determined by Bradford assay.

2.5.12 Fluorescence detection of glutathionylated proteins by click reaction

Proteins in cell lysates (100 μg) were precipitated by incubating with ice-cold acetone (4x volume) for 1 h at -20^0C and centrifugation for 5 minutes at 18,000 g. The supernatant was removed, the pellet was air-dried for 5 min and resuspended in 40 μL of buffer containing 0.1% SDS, 1x PBS, 0.1% DMSO, and water. The pellet was completely resuspended by sonication. Cy5-alkyne (0.5 μL, 10 mM in DMSO) and click solution (10 μL) containing 20 mM CuBr (5 μL) in DMSO/tBuOH (3:1, v/v;5 μL) and 20 mm THPTA (5 μL) were added. The mixture was incubated in the dark for 1 h at room temperature. Proteins were separated by SDS-PAGE, and proteins in the gel were analyzed by FluorChem Q imaging system (BioRad) or Coomassie stain.

2.5.13 Sodium Dodecyl Sulfate Poly Acrylamide Gel Electrophoresis (SDS-PAGE)

Dried glass plates (1.5 mm, BioRad) were mounted on a gel preparing rack. Resolving buffer (12%) was prepared by mixing 3.4 mL of distilled water, 2.4 mL of 40% acrylamide (BioRad), 2 mL of 1.5 M Tris buffer (pH 8.8), 80 μL of 10% (w/v) SDS, 80 μL of 10% (w/v) ammonium persulfate (APS) and 8 μL of N,N,N',N'-tetramethylethylenediamine (TEMED, Sigma). The solution was poured between glass plates up to about ¾ height of the short plate. After pouring, isopropanol was added over the resolving layer, and the gel was allowed to polymerize at room temperature for 30 minutes. The stacking buffer was prepared by mixing 2.9 mL of distilled water, 750 μL of 40% acrylamide, 1.25 mL of 0.5 M Tris buffer (pH 6.8), 50 μL of 10% SDS, 50 μL of 10% APS and 5 μL TEMED. The isopropanol layer was removed, and the stacking buffer was poured over the resolving gel. A comb (10 well or 15 well) was inserted between the glass plates. The gel was allowed to polymerize.

To run the samples, the comb was removed, and the cast gel was assembled into mini-protean tetra gel apparatus (BioRad). Freshly prepared SDS running buffer (1x; 0.025M Tris, 0.05M glycine, and 0.5% SDS) was poured, and samples were loaded into the gel wells. The apparatus was closed, and the gel was electroeluted at 200V until the dye front reached the bottom of the gel. The gel was removed from the glass plates carefully and washed with distilled water, and analyzed by FluorChem Q imaging system, western blotting, or stained with Coomassie.

2.5.14 Coomassie staining

SDS-PAGE gels were washed with distilled water and incubated with a staining solution containing 0.1% Coomassie Brilliant Blue R-250 in 50% methanol, 10 % glacial acetic acid, and water for 1 h after microwaving for 30 seconds. The Coomassie stain was removed, and the gel was washed 3 times with distilled water. The gel was then de-stained overnight with a buffer containing 40% methanol, 10% glacial acetic acid and water.

2.5.15 Western botting

Western blotting was carried out to transfer proteins in SDS-PAGE to a polyvinylidene difluoride (PVDF) membrane. The stacking layer was removed, and the resolving gel was washed with distilled water and transfer buffer (24 mM Tris, 194 mM glycine, and 10% methanol). Before assembling the transfer sandwich, filter papers and sponges were soaked in transfer buffer, and the PVDF membrane was soaked in methanol. To assemble the transfer sandwich, a pre-wetted sponge was placed on the black side of the transfer cassette, followed by a filter paper and the gel. Then, the pre-wetted PVDF membrane was placed on the gel, followed by the filter paper and another sponge. The cassette was closed and locked. The cassette was placed in the transfer apparatus facing the black side of the cassette to the black side of the module. The whole setup was placed in a transfer container. An ice block was placed inside the transfer container, and the container was filled with transfer buffer. The transfer container was closed with the lid, and the whole setup was covered with ice. The transfer was carried

out for 2 h at 90 V. The cassette was removed from the transfer container, and the PVDF membrane was removed from the cassette. The PVDF membrane was washed with TBST and used immediately for the antibody probing.

2.5.16 Pull-down analysis

Proteins in cell lysates (1000 µg) were precipitated by incubating with ice-cold acetone (4x volume) at -20^{0}C for 1 h and centrifugation for 5 minutes at 18,000 g. The supernatant was removed, the pellet was air-dried for 5 min. The pellet was resuspended in 140 µL of buffer containing 0.1% SDS, 1x phosphate buffer saline (PBS), 0.1% DMSO, and water by sonication. To the mixture, 5 mM biotin-alkyne in DMSO (16 µL) and click solution (40 µL) containing 20 mM CuBr (20 µL) in DMSO/tBuOH (3:1, v/v;5 µL) and 20 mm tris-hydroxypropyltriazolylmethylamine (THPTA, 20 µL) were added. The mixture was incubated in the dark for 1 h at room temperature. Proteins were precipitated by incubation with ice-cold acetone (4x volume) for 1h at -20^{0}C, and centrifugation at 18,000g for 5 minutes. The resulting pellet was resuspended in 200 µL of PBS buffer containing 1.2% SDS by sonication. Resuspended proteins (10 µL) were saved for the gel. The remaining proteins were added to PBS buffer containing streptavidin-agarose beads (20 µL, Pierce) and incubated overnight at 4^{0}C. The next morning, beads were washed with PBS containing 0.2% SDS (3x 500 µL) and PBS (3x 500 µL). Proteins on beads were eluted by adding 50 µL of SDS-loading dye (2x) containing β-mercaptoethanol (BME, 3 µL) and heating at 95^{0}C for 10 min. Eluted proteins were resolved on SDS-PAGE and transferred to the PVDF membrane as described in section 2.5.15. This membrane was

blocked with 5% BSA in TBST (50 mM Tris-HCl, 150 mM NaCl, and 0.1% Tween-20) and incubated with primary antibody solutions [desmin (1:1000; Abcam), α-actinin (1:500; Abcam) and FLAG (1:1000; Sigma)] diluted in blocking buffer overnight at 4^0C. Appropriate horseradish peroxidase (HRP) conjugated secondary antibodies were used to visualize the proteins by chemiluminescence.

2.5.17 Proteomic sample preparation

Equal amounts of lysates prepared by incubation of heavy or light azido-alanine (5 mg proteins from each lysate) were combined. A click reaction was carried out as described earlier with biotin-DADPS-alkyne. Proteins were precipitated with ice-cold acetone (4x volume) by incubating for 1 h at -20^0C, and centrifugation at 20,800 g for 10 minutes at 4^0C. The pellet was resuspended in PBS containing 1.2% SDS (1 mL) by sonication. Resuspended proteins were added to pre-washed streptavidin-agarose beads (100 μL) containing PBS (5 mL) and incubated overnight at 4^0C. The following day, beads were washed with PBS containing 0.2% SDS (3x 1 mL) and PBS (3x 1 mL). Then, the beads were incubated with a denaturing PBS solution (500 μL) containing 6 M urea at 37^0C for 45 minutes. Proteins on beads were then digested with a PBS buffer (200 μL) containing 2 M urea, 1 mM $CaCl_2$, and trypsin/Lys-C (5 μg; Promega) overnight at 37^0C. Beads were washed with PBS containing 0.2% SDS (3x 1 mL), PBS (3x 1 mL), and water (3x 1 mL). Peptides on beads were cleaved by incubating with 10% formic acid (2x 100 μL) for 30 minutes at room temperature, followed by a wash (100 μL). Eluted fractions were combined, lyophilized, and analyzed by LC-MS/MS.

2.5.18 LC-MS/MS analysis

Lyophilized peptides were resuspended in a solution containing 0.1% formic acid, 0.005% trifluoroacetic acid (TFA), and 5% acetonitrile. Peptides were separated by UHPLC reverse phase chromatography using PepMap RSLC C18 column and an EASY-nLC system and introduced to an Orbitrap Fusion mass spectrometer (Thermo Fisher). MS1 scans were between the range of 375-1600 m/z at 240 000 orbitrap resolution. Peptides with +2 or +3 charges were fragmented by collision-induced dissociation (CID) at 32% collision energy. Peptides with charges between +3 and +7 were fragmented by electron transfer dissociation (ETD).

2.5.19 Protein identification and quantification

Raw data files were searched with MaxQuant (version 1.6.2.10) against UniProt mouse complete database (downloaded on 07.14.2017, 16 844 entries) and a contaminant database. Glutathionylation of cysteine by heavy azido glutathione (addition of $C_{16}H_{24}O_7N_6S$, exact mass = 444.14272) and light azido glutathione (addition of $C_{16}H_{21}{}^2H_3O_7N_5{}^{15}NS$, exact mass = 444.15858) were used as cysteine labels. Methionine oxidation and N-terminal acetylation were used as variable modifications. All other parameters were left as default. As determined by a reversed database search, peptide spectra matches were accepted at a 1% false discovery rate. Peptide quantifications were done using Skyline software (version 4.2.0), as previously reported.[103] Spectral libraries were prepared by importing msms.txt and modifications.XML files from MaxQuant to Skyline. Raw files were imported for peak picking. The uniprot mouse database

(downloaded on 07.14.2017) was also imported to Skyline. In MS-1 filtering, mass accuracy and the retention time window were set to 10 ppm and ±2 minutes, respectively, to find the corresponding peptide peaks in all runs that lack MS/MS identification. Peptides without S-glutathionylation were removed from the peptide list. Peptides with isotopic dot product (idotp) value less than 0.8 were removed. To have an idotp value higher than 0.8, manual integration was applied when necessary. For heavy to light labels, the peptide area ratios were calculated automatically. Out of three replicates, peptides identified at least two out of three times with an idotp value greater than 0.8 were assigned with the median $R_{H/L}$ values.

CHAPTER 3: IDENTIFICATION AND QUANTIFICATION OF GLUTATHIONYLATED

CYSTEINES UNDER ISCHEMIC STRESS

(The work of this chapter is adapted from Yapa Abeywardana, M.; Samarasinghe, K. T. G.;

Munkanatta Godage, D.; Ahn, Y. H., Identification and Quantification of Glutathionylated

Cysteines under Ischemic Stress. J Proteome Res 2021, 20 (9), 4529-4542)

3.1 Introduction

Myocardial infraction or ischemia is the restriction of blood flow to the heart

muscle. It is one of the dominant contributors to the death of millions of people

worldwide.[112, 113] During ischemia, there is a limited supply of O_2 (hypoxia) and nutrients,

which limits the production of adenosine 5'-triphosphate (ATP) that is essential for heart

muscle contraction.[114] The level of tissue damage is determined by the severity and

duration of the ischemia.[114] The damage caused by ischemia can be reversed by restoring

blood flow (reperfusion) to the ischemic heart muscle.[112] However, while restoring blood

flow is necessary, this results in significant tissue damage in the ischemic heart due to the

sudden reintroduction of O_2 and nutrients (reperfusion injury).[113, 115]

For its mechanical function, the heart needs a high amount of energy (ATP). The

heart produces ATP largely from fatty acid β-oxidation (60-90%) and from glucose

oxidation (10-40%).[112, 116-118] Therefore, ATP production processes are heavily dependent

on O_2 availability.[116, 117] During ischemia, anaerobic metabolism increases due to a lack of

O_2. The generation of lactic acid during anaerobic metabolism decreases the pH in the

cell.[114] To balance the accumulation of hydrogen ions (H^+), excess H^+ are excreted by

Na^+/H^+ exchangers. Therefore, ischemia produces a large influx of sodium ions (Na^+).[114]

Also, ATP production is slow down during ischemia, which inactivates ATPases, reducing

active calcium (Ca^{2+}) efflux. This produces a Ca^{2+} overload in the mitochondria and cells.

These cellular changes ultimately activate intracellular proteases such as calpain that

damage myofibrils and induce autophagy to reduce energy consumption.[114] Therefore,

prolonged ischemia can ultimately cause cell death. Reperfusion can reverse these

damages caused by ischemia. However, reoxygenation during reperfusion can increase

ROS production at mitochondria and other organelles.[114, 119] This sudden increase in ROS

overwhelms the detoxification capacity of the cells, inducing oxidation of proteins,

deoxyribonucleic acids, and lipids, which can cause a loss of contractility of

cardiomyocytes.[114, 120] Interestingly, during ischemia-reperfusion (I/R), the plasma levels

of fatty acids elevate, inducing fatty acid oxidation over glucose oxidation.[112, 121, 122]

Increased fatty acid oxidation is associated with reduced contractile activity and cell death

in the heart.[123, 124]

During I/R, redox homeostasis can be altered due to a burst of ROS and reduced

antioxidant production. Altered redox homeostasis can induce reversible and irreversible

modifications on proteins causing structural and functional changes in the modified

proteins.[26] Cysteines are highly susceptible to modifications including S-oxidation, S-

nitrosylation, disulfide bond formation, and glutathionylation.[26, 27, 46, 47, 125]

Glutathionylation is the mixed disulfide formation between a protein cysteine and

glutathione.[28] Glutathionylation is important in protecting proteins from irreversible

oxidative modifications and modulating protein-protein interactions.[28, 55, 56, 125] Previous reports have highlighted glutathionylation of several contractile proteins, mitochondrial, and metabolic enzymes.[77, 126, 127] However, there is a limited number of glutathionylated proteins and cysteines identified during ischemic stress in cardiomyocytes.

Our lab has previously developed a chemoselective method (clickable glutathione approach) to detect protein glutathionylation (Figure 3.1).[85, 86] This method utilizes a glutathione synthetase enzyme (GS M4) mutant to metabolically synthesize clickable glutathione (N$_3$-GSH/azido glutathione) *in situ* in cells by incorporating azido-alanine in place of glycine. A subsequent click reaction covalently connects the modified glutathione to a biotin- or fluorophore-alkyne to enable identification and detection of glutathionylated proteins (Figure 3.1).[85] Recently, we have modified this clickable glutathione approach to use a cleavable biotin-DADPS-alkyne. Combined with mass spectrometry, we can identify proteins undergoing glutathionylation with their specific cysteine sites. This approach allowed us to identify over 1700 glutathionylated peptides in the HL-1 mouse cardiomyocyte cell line upon production of H$_2$O$_2$.[89] We have further modified this method to relatively quantify protein glutathionylation using isotopically labeled heavy (+4 Da) and light (+0 Da) azido-alanine derivatives, and identified over 1300 glutathionylated cysteines with their relative levels of glutathionylation upon addition of H$_2$O$_2$.[128]
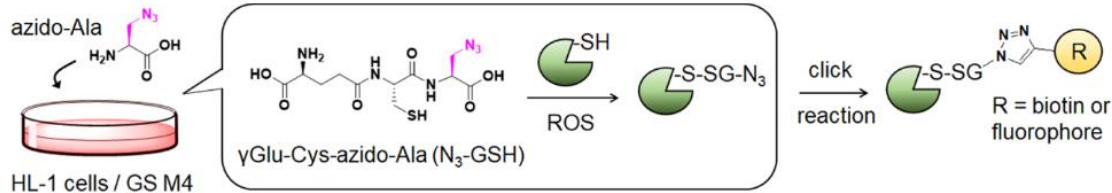
Figure 3.1 – Clickable glutathione approach for the detection and identification of protein glutathionylation.

3.2 Approach

We have applied our clickable glutathione approach to detect protein glutathionylation in HL-1 mouse cardiomyocytes under different ischemic stress conditions such as glucose deprivation (GD), hypoxia, oxygen-glucose deprivation (OGD), and OGD followed by reperfusion (OGD/R). Our data revealed that glutathionylation occurs under prolonged GD but is absent or minimal under hypoxia or OGD. Furthermore, reoxygenation after OGD (OGD/O) and fatty acid availability during OGD/R (OGD/OGF-BSA) induce a significant level of glutathionylation. However, glucose additionduring reperfusion (OGD/OG) reduces glutathionylation. By applying our quantification strategy with clickable glutathione under OGD/OGF-BSA, we have identified 248 glutathionylated proteins. Bioinformatic analyses of this data set revealed, 18 glutathionylated cysteines whose genetic variants are known to be associated with muscular disorders.

3.3 Results

3.3.1 Glucose deprivation induces glutathionylation significantly

HL-1 mouse cardiomyocyte cells were used as an *in vitro* model to reproduce I/R conditions.[88] HL-1 cells overexpressing GS M4 were treated with N_3Ala, and subjected to

various metabolic alterations that mimic GD, hypoxia, or OGD. Glucose depletion (GD) induced a global level of glutathionylation in a concentration- and time-dependent manner (Figure 3.2A). This observation suggests that glucose availability is important to maintain redox homeostasis, possibly due to NADPH production.[129] Under GD, the ratio of $NADP^+$/NADPH was significantly increased (Figure 3.2E). Also, the ratio of GSSG/GSH and the level of ROS were both increased (Figure 3.2D, F), supporting the induction of global glutathionylation levels under GD. Cell viability was not altered significantly during GD (Figure 3.2G).

3.3.2 Hypoxia or OGD does not induce glutathionylation

Then, HL-1 cells were subjected to hypoxia (1% O_2) and OGD (1% O_2 and 0 mM glucose). Under hypoxia and OGD, glutathionylation was low or rarely observed (Figure 3.2B, lane 1 vs. 3 and lane 1 vs. 4, respectively) significantly compared to glutathionylation under GD (Figure 3.2B, lane 2). Under hypoxia, ROS levels increased (Figure 3.2D), but the $NADP^+$/NADPH ratio remained unchanged (Figure 3.2E). In contrast, under OGD, the ROS levels remained unchanged (Figure 3.2D) while the $NADP^+$/NADPH ratio increased (Figure 3.2E). Consequently, the ratio of GSSG/GSH was not significantly altered by either hypoxia or OGD, consistent with the low or no glutathionylation levels observed under these dame conditions (Figure 3.2F). Furthermore, an increase in oxygen percentage (1, 5, and 21%) during GD resulted in an increased level of glutathionylation (Figure 3.2C), supporting the importance of O_2 for glutathionylation. Finally, cell viability was not altered significantly during hypoxia or OGD (Figure 3.2G).
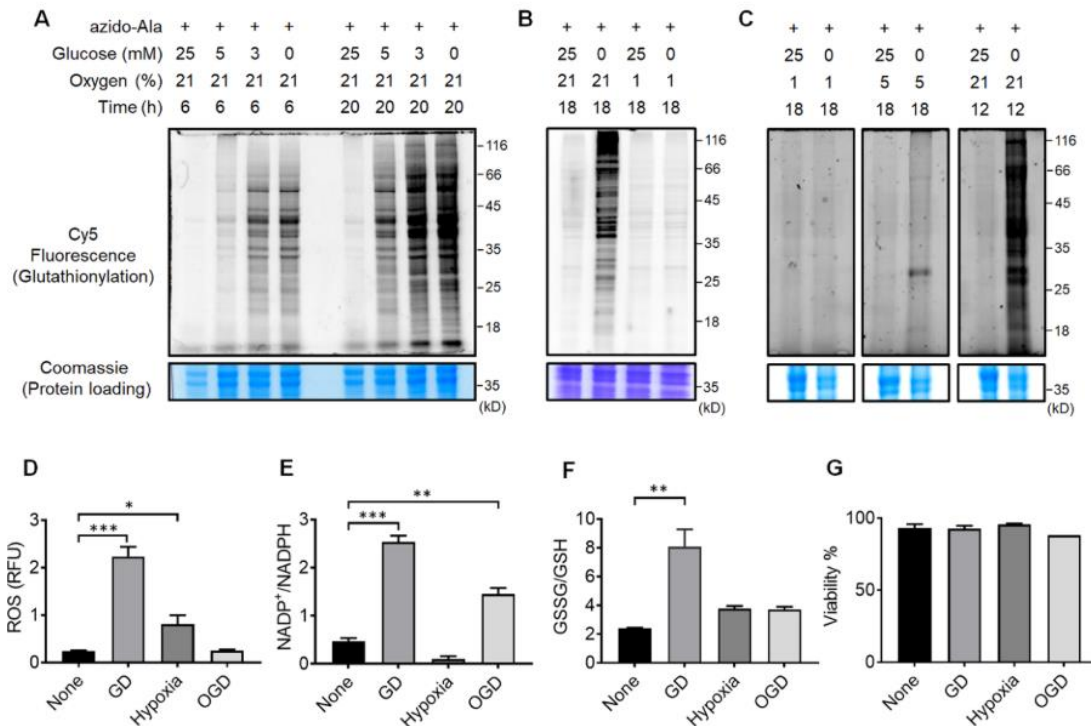
Figure 3.2 – Glutathionylation is induced significantly under GD, but only weakly under hypoxia or OGD. A-C) Global glutathionylation levels under GD, hypoxia, or OGD in HL-1 mouse cardiomyocyte cells. D-G) Analysis of ROS, $NADP^+/NADPH$ ratio, GSSG/GSH ratio, and cell viability, respectively, under GD, hypoxia, or OGD. Data representing mean ± SD, n = 3 independent experiments. Difference is significant by one-way ANOVA, followed by Tukey's post-hoc test, *p < 0.05, **p < 0.01, ***p < 0.001.

3.3.3 Oxygen and palmitate availability during OGD/R induce glutathionylation significantly

Next, we examined the impact of OGD followed by the repletion of glucose or oxygen (OGD/R) on global glutathionylation levels. HL-1 cells overexpressing GS M4 and treated with N₃Ala were reoxygenated with or without glucose after OGD. When the cells were reoxygenated without glucose (OGD/O), global glutathionylation levels were significantly increased (Figure 3.3A, lane 1 vs. 2-3 and Figure 3.3B, lane1 vs. 2). Similar to glutathionylation, the ROS level, GSSG/GSH ratio, and $NADP^+/NADPH$ ratio were

significantly elevated (Figure 3.3C-E). In contrast, the glutathionylation levels remained low when the cells were reoxygenated with glucose (OGD/OG, Figure 3.3A, lane 1 vs. 4-5 and figure 3.3B, lane 1 vs. 3). Consistent with this observation, the ROS level, GSSG/GSH ratio, $NADP^+$/NADPH ratio, and cell viability (Figure 3.3C-F) remained unchanged. These data indicate that oxygen availability is important for the induction of glutathionylation, and glucose metabolism is necessary to restore redox homeostasis.

Previous literature has shown that after ischemia, the plasma level of fatty acid elevates to high concentrations (1-3 mM). The increased fatty acid level can inhibit glucose oxidation, which was shown to elevate the I/R injury in the perfused heart.[122-124] Therefore, to explore the effect of fatty acid concentration during reperfusion, HL-1 cells were incubated with palmitate (bound to its carrier protein BSA) during reperfusion after OGD. Glutathionylation levels were significantly increased compared to repletion without palmitate (OGD/OG-BSA) (Figure 3.3B, lanes 4-5 vs. lanes 6-7). Similar to the glutathionylation levels, ROS level, $NADP^+$/NADPH ratio, and GSSG/GSH ratio (Figure 3.3C-E) were significantly higher in the presence (OGD/OGF-BSA) versus the absence (OGD/OG-BSA) of palmitate. Notably, compared to other conditions, cell viability was reduced upon the addition of palmitate (Figure 3.3F). These data demonstrate a significant increase of glutathionylation upon the addition of fatty acid during OGD/R, suggesting an adverse effect of fatty acid on the perfused heart.[123]
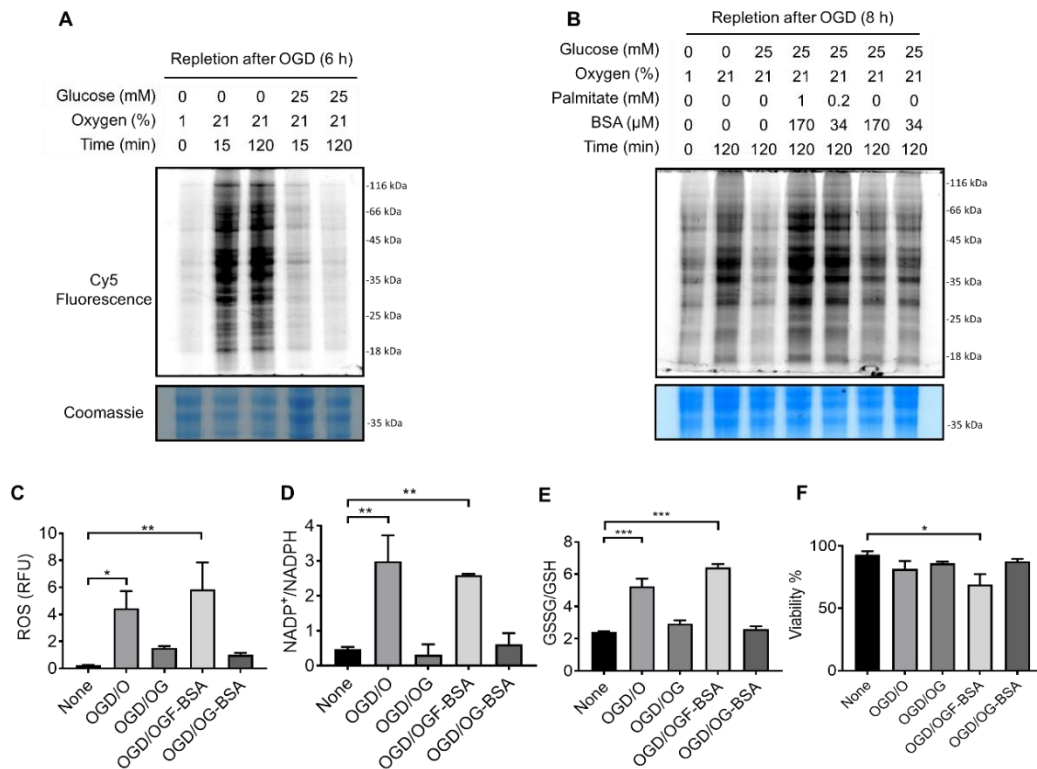
Figure 3.3 – Glutathionylation increases upon the incubation of palmitate during OGD/R. A-B) Global glutathionylation levels under OGD, OGD/O, OGD/OG, OGD/OGF-BSA, or OGD/OG-BSA in HL-1 mouse cardiomyocyte cells. C-F) Analysis of ROS, NADP$^+$/NADPH ratio, GSSG/GSH ratio, and cell viability respectively under OGD, OGD/O, OGD/OG, OGD/OGF-BSA, or OGD/OG-BSA. Data represents the mean ± SD, n = 3 independent experiments. Difference is significant by one-way ANOVA, followed by Tukey's post-hoc test, *$p < 0.05$, **$p < 0.01$, ***$p < 0.001$.

3.3.4 Identification and quantification of glutathionylated cysteines upon the addition of palmitate during OGD/R

Since palmitate availability during OGD/R induces a significant level of global glutathionylation, we applied our isotopically labeled clickable glutathione approach to identify specific cysteines undergoing glutathionylation and to quantify the extent of modification.[128] In this approach, HL-1 cells overexpressing GS M4 were incubated with isotopically labeled heavy or light N$_3$Ala to metabolically synthesize isotopically labeled

clickable glutathione with a +4 Da isotopic mass difference (Figure 3.4).[128] Cells labeled

with heavy or light N_3Ala were subjected to OGD/R with or without palmitate (Figure 3.4,

steps 1 and 2). After cell lysis, equal amounts of cell lysates were combined. Cell lysates

were subjected to a click reaction with biotin-DADPS-alkyne, and glutathionylated

proteins were enriched using streptavidin-agarose beads. After trypsin/LysC digestion on

beads, glutathionylated peptides were eluted and subjected to LC-MS/MS analysis (Figure

3.4). Individual pairs of glutathionylated peptides with +4 Da isotopic mass difference

were identified (in at least two out of three replicates), and the peptides were quantified

to give a ratio ($R_{H/L}$, Figure 3.4) using Skyline software.[103]
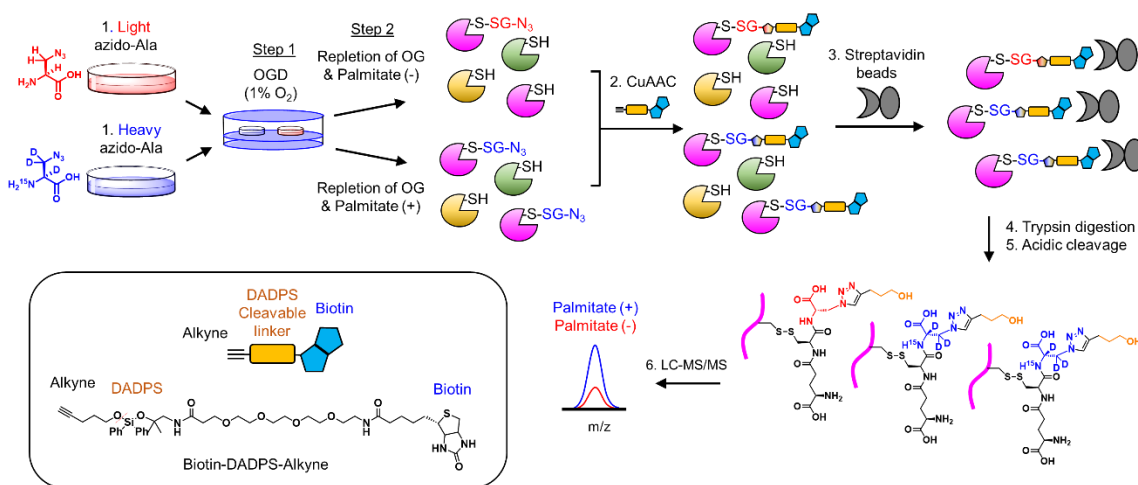
Figure 3.4 – Scheme for the identification and quantification of glutathionylated peptides upon addition of palmitate during OGD/R.

We carried out two sets of experiments, E1 and E2, to quantify the impact of

palmitate on glutathionylation of specific cysteines upon addition of palmitate during

OGD/R. Under E1 conditions, heavy and light N_3Ala treated samples were subjected to

identical stress conditions (OGD/OGF-BSA, Figure 3.5A), which is expected to give $R_{H/L}$ values close to 1 by inducing identical levels of glutathionylation. These conditions were used to validate our quantification strategy. E2 conditions were used to relatively quantify glutathionylation levels upon the addition of palmitate during OGD/R. In this case, heavy and light N_3Ala treated samples were induced with different OGD/R conditions (OGDR/OGF-BSA and OGD/OG for heavy and light samples, respectively). We identified 249 pairs of peptides under the E1 condition and 194 pairs under the E2 condition with their $R_{H/L}$ values. For the E1 experiment, the median $R_{H/L}$ value was 0.87 (90% of $R_{H/L}$ values in the range of 0.6-1.4, Figure 3.5B left). The median CV value for E1 was 14.6% (80% of CV in the range of 1 – 43%, Figure 3.5B right), supporting relatively consistent $R_{H/L}$ values between replicates. In contrast to E1, the median $R_{H/L}$ value of E2 was 5.15 (Figure 3.5 left), supporting the observation that the level of glutathionylation increases upon the addition of palmitate. Also, E2 showed a median CV value of 50.2% (80% of CV in the range of 12-88%, Figure 3.5B right). This relatively high CV value was due largely to low glutathionylation signals detected in light-labeled peptides. In the E2 experiment, individual glutathionylated peptides showed a wide distribution of $R_{H/L}$ upon addition of palmitate during OGD/R (Figure 3.5C top). Figure 3.5C (bottom) shows MS1 peaks for individual identified peptides, such as pyruvate carboxylase (PYC) C55 and aldolase (ALDOA) C338, with fairly low $R_{H/L}$ values (0.83 and 2.25, respectively) and BAG3 C184, cortactin (CTTN) C111, and CTTN C245 with significantly high $R_{H/L}$ values (9.66, 11.0 and

18.9, respectively), highlighting their differential susceptibilities for glutathionylation in response to fatty acid availability.
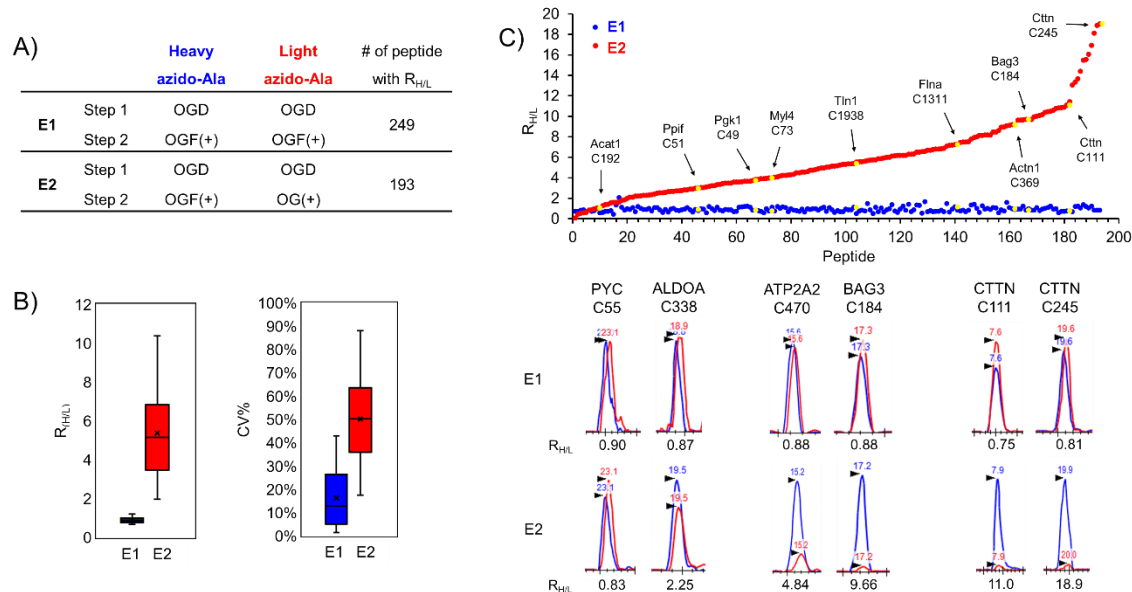
Figure 3.5 - Identification and quantification of glutathionylated peptides upon incubation of palmitate during OGD/R. A) Experimental conditions and the number of glutathionylated peptides identified under E1 and E2 conditions. B) $R_{H/L}$ values and CV of glutathionylated peptides. C) $R_{H/L}$ value distribution of individual glutathionylated peptides (top) and MS1 peaks showing relative quantification of heavy (blue) to light (red) azido glutathione labeled peptides (bottom).

3.3.5 Bioinformatic analysis of glutathionylated peptides associated with sarcomere, mitochondria, and cardiomyopathy

DAVID GO analysis was used to examine the localization of all the identified proteins (n=248) and revealed that a majority of these proteins are localized in the cytoplasm (62.5%), followed by the membrane (51.6%), nucleus (43.5%), mitochondria (22.5%) and endoplasmic reticulum (9.6%). We carried out STRING and cluster analyses to identify major protein clusters impacted by glutathionylation.[130] We identified a large cluster of proteins related to cytoskeleton organization and remodeling with a median

$R_{H/L}$ value of 6.0 (Figure 3.6, left). Proteins identified in the cluster include G protein subunits [Gnb2 C182 ($R_{H/L}$ 9.18) and Gnb1 C204 ($R_{H/L}$ 5.50)], GTPase for actin filament remodeling [Rac1 C178 ($R_{H/L}$ 5.33) and RhoA C16 ($R_{H/L}$ 5.13)], actin-binding and structural constituents [Capzb C206 ($R_{H/L}$ 7.17), Sptan1 C315 and C1622 ($R_{H/L}$ 4.96 and 5.14), Tln1 C1087, C1939 ($R_{H/L}$ 1.55, 5.36)], and myosin motor proteins [Myh9 C988 ($R_{H/L}$ 9.62) and Myl6 C2 ($R_{H/L}$ 9.05)]. These results suggest that glutathionylation of these proteins may alter the dynamics of cytoskeletal structural organization, which is important for the contractility of muscle myofibrils and sarcomere function.

Another large cluster of proteins associated with translation was identified with a median $R_{H/L}$ value of 6.0 (Figure 3.6, middle). This cluster includes proteins, such as translation initiation and elongation factor proteins [Eif3g C139 ($R_{H/L}$ 13.7) and Eef2 C693 ($R_{H/L}$ 8.44)] and ribosomal proteins. We also identified an additional cluster of proteins associated with carbohydrate metabolism with a $R_{H/L}$ of 6.0 (Figure 3.6, right). This cluster includes glycolytic proteins [LDHA C163 ($R_{H/L}$ 9.67), PGK1 C50 and C316 ($R_{H/L}$ 3.71 and 7.52), and GAPDH C245 and C22 ($R_{H/L}$ 6.14 and 7.45)].
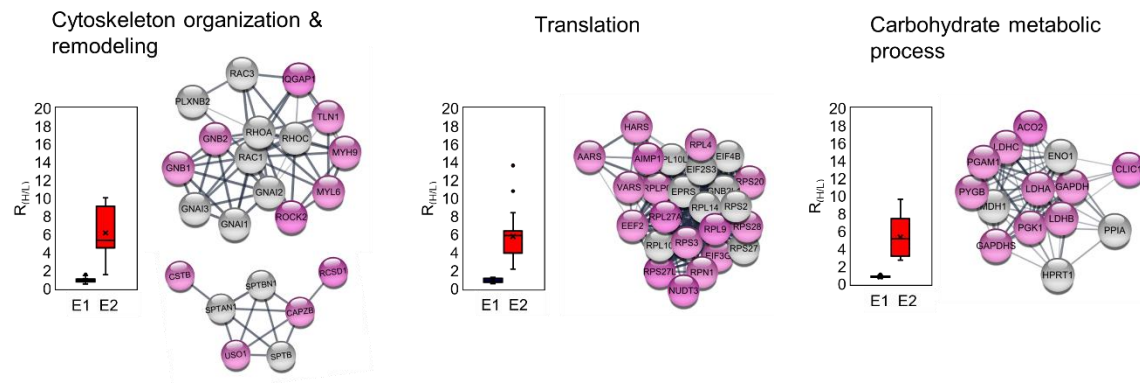
Figure 3.6 – Major biological processes associated with glutathionylated proteins identified through the DAVID GO database. Glutathioinylated proteins with low $R_{H/L}$ values (below 50%) are shown in gray spheres, and proteins with high $R_{H/L}$ values [above 50% and NL (no light labeled found)] are shown in magenta spheres.

During I/R, oxidations of sarcomeric and mitochondrial metabolic proteins impact cardiac contractility. Therefore, we analyzed sarcomeric and mitochondrial proteins undergoing glutathionylation. Using DAVID GO analysis, we identified 24 sarcomeric proteins (11% among 221 proteins with $R_{H/L}$ value > 2, Table B.3.1) with a median $R_{H/L}$ value of 6.8 (Figure 3.7, left). Major protein clusters were identified using STRING and cluster analysis. Proteins identified in the major clusters include contractile proteins (MYBPC3 C715 and MYL3 C74), chaperone and E3 ligases that regulate protein stability (BAG3 C185 and Stub1 C200), and sarcomeric structural proteins that interact with actin filaments (FLNC C1349 and C713, CAPZB C206, ACTN1 C370, and SPTAN1 C315 and 1622) (Figure 3.7, left). Glutathionylation of these sarcomeric proteins suggests they may have an impact on the structural integrity and contractility of myofibrils upon I/R.

By applying DAVID GO analysis, we also identified 44 mitochondrial proteins (20% among 221 proteins with their $R_{H/L}$ value > 2, Table B.3.2). STRING and cluster analysis of

these 44 proteins identified protein clusters in electron transport chain (ETC) subunits and ATP synthase (SDHC C107, NDUFS1 C727, and ATP5H C101), ATP transport, and ion channel (SLC25A4 C160, SLC25A5 C160, VDAC3 C65, and VDAC2 C77 and C48), and tricarboxylic acid cycle (TCA) metabolic enzyme (OGDH C395, MDH2 C275, and PCCA C107) (Figure 3.7, middle). Glutathionylation of these identified proteins may reduce ATP production and alter mitochondrial membrane permeability, leading to impaired mitochondrial function during I/R.[131]

We also compared all glutathionylated proteins (221 proteins with $R_{H/L}$ value > 2, termed the glutathionylation network) with all the proteins relevant to cardiomyopathy imported from STRING disease query (2000 proteins, termed the cardiomyopathy network). We identified 66 glutathionylated proteins associated with cardiomyopathy (30% among 221 proteins with $R_{H/L}$ value > 2, Table B.3.3). STRING and cluster analyses of these proteins identified protein clusters involved in protein stability with a chaperone and E3 ligase (BAG3 C185 and Stub1 C200), cytoskeleton remodeling and organization [Rac1 C178, RhoA C16, Myh9 C988, and Myl6 C2), and ATP production with TCA and ETC (SDHC C107, NDUFS1 C727, and ATP5H C101) (Figure 3.7, right). Glutathionylation of these proteins may be associated with cardiomyopathy.
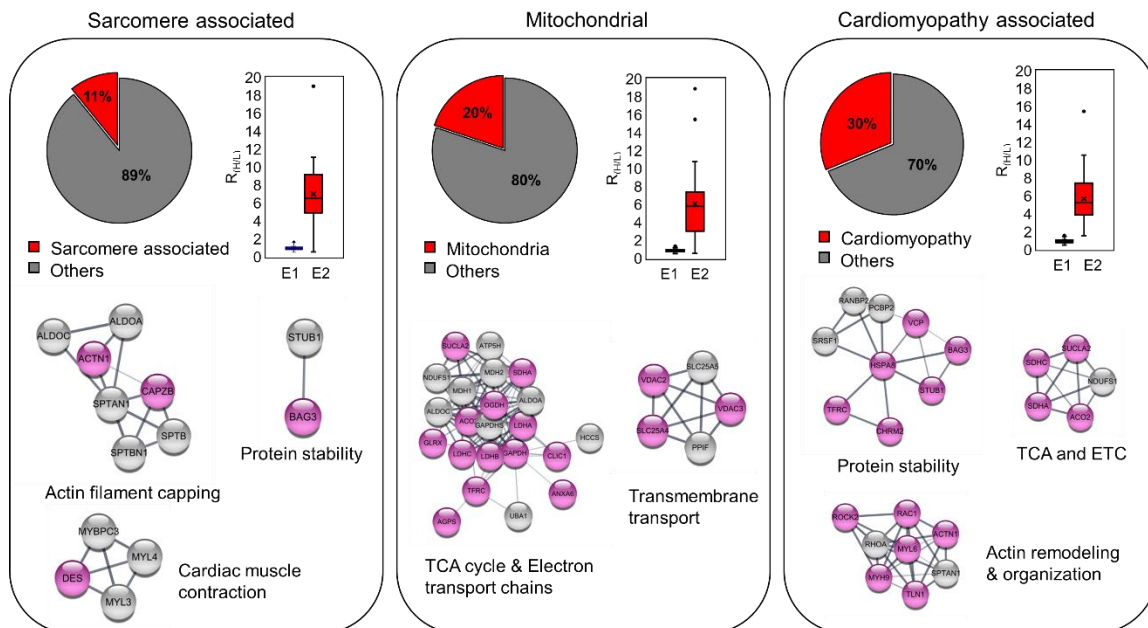
Figure 3.7 – Bioinformatic analysis of glutathionylated proteins identified upon addition of palmitate during OGD/R. Sarcomere and mitochondria-associated proteins were identified from the DAVID GO database. Cardiomyopathy-associated proteins were identified by cardiomyopathy disease query in STRING analysis. Glutathioinylated proteins with low $R_{H/L}$ values (below 50%) are shown in gray spheres, and proteins with high $R_{H/L}$ values [above 50% and NL (no light labeled found)] are shown in magenta spheres.

Finally, we examined whether glutathionylated cysteines (n = 249) or their adjacent residues (±1 position) were linked to any muscular disorders using the UniProt database.[132] In this analysis, we used the human orthologs of the identified proteins. We found that mutations of 18 cysteines or their adjacent residues were associated with muscular dystrophy or neuromuscular diseases (Table B.3.4). Interestingly, mutations at the cysteine position of seven identified proteins were associated with cardiomyopathy, suggesting that the glutathionylation at those cysteine positions may yield adverse functional effects during I/R.

3.3.6   Validation of proteomic data by pull-down analysis

We selected two proteins identified above (Desmin and BAG3) to validate their glutathionylations at specific cysteine residues in response to OGD/OGF-BSA. Desmin (DES) is the major intermediate filament protein associated with Z-disks in muscle cells, and it is important in maintaining elasticity and providing mechanical strength in the sarcomere.[104-106] Mutations in DES are linked to myofibrillar myopathy (desminopathy).[133] DES has only one cysteine (C332), and it was found to undergo glutathionylation in our analyses.[134] BAG3 is a co-chaperone protein expressed in cardiac and skeletal muscle, which is important in protein folding, cell cycle regulation, inflammation, and apoptosis.[135, 136] Different functional roles of BAG3 are associated with its functional regions, namely the Bcl2-associated athanogene (BAG) domain, isoleucine-proline-valine rich (IPV) domain, tryptophan-rich (WW) domain, and proline-rich (PXXP) domain.[135-138] Under stress, BAG3 stabilizes actin capping protein (CapzB) by shifting to the Z-disc of the sarcomere.[139] BAG3 mutations are associated with cardiomyopathy, impaired Z-disc integrity and myofibrillar myopathy.[140, 141] BAG3 (mouse) has three cysteines, C154, C185, and C378. Among them, we found glutathionylation at C185 (C179 in human BAG3).

HL-1 cells overexpressing GS M4 were treated with N_3Ala, and cells were subjected to OGD/OG and OGD/OGF-BSA. Cell lysates were subjected to a click reaction with biotin-DADPS-alkyne. Glutathionylated proteins were enriched using streptavidin-agarose beads, eluted, and analyzed by wester. We found that OGD/OG did not significantly induce the glutathionylation of DES and BAG3 (Figure 3.8A, lane 1 vs. 2 and Figure 3.8B,

lane 1 vs. 2). In contrast, the addition of palmitate during repletion (OGD/OGF-BSA) induced glutathionylation of both proteins (Figure 3.8A, lane 1 vs. 3 and Figure 3.8B, lane 1 vs. 3 respectively). To demonstrate glutathionylation at their specific cysteine sites, we overexpressed WT and cysteine mutants of mouse DES (DES WT and DES C332S) and human BAG3 (BAG3 WT and BAG3 C179S) in HEK293/GS M4 cells. Both DES WT (lane 4 and 5 vs. 6, Figure 3.8A) and BAG3 WT (lane 4 and 5 vs. 6, Figure 3.8B) showed glutathionylation under OGD/OGF-BSA. In contrast, glutathionylation levels were completely or partially reduced in DES C332S (lane 6 vs. 9, Figure 3.8A) and BAG3 C179S (lane 6 vs. 9, Figure 3.8B), respectively, in the presence of palmitate during repletion (OGD/OGF-BSA).
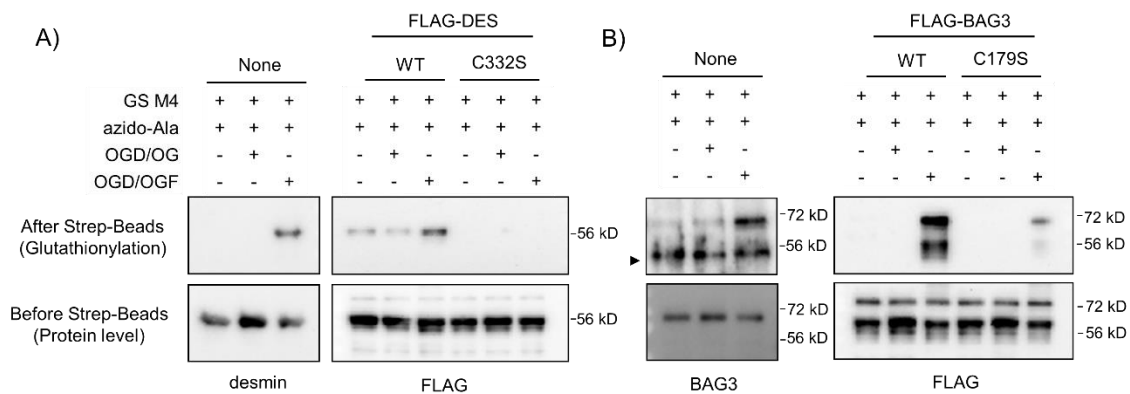
Figure 3.8– Biochemical validation of protein glutathionylation. A) DES and B) BAG3 proteins. HEK293/GS M4 cells and HL-1 cells with and without overexpression of WT and mutant proteins were subjected to stress (OGD/OG and OGD/OGF) to induce glutathionylation. Cells were lysed and used in pull-down and western blot analyses.

3.4 Discussion

During I/R, mitochondrial ROS are known to cause muscle damage via oxidative modifications of muscle proteins.[116, 142] Among different oxidative modifications, protein

S-glutathionylation is an important reversible cysteine modification that protects proteins from irreversible oxidative modifications and modulates protein-protein interactions. Many proteins undergo glutathionylation in response to external stimuli such as H_2O_2 and glucose oxidase. However, protein glutathionylation in response to metabolic alterations such as ischemia and I/R have not been studied extensively. In this chapter, we have applied our clickable glutathione approach to investigate protein glutathionylation in response to different metabolic alterations that mimic I/R.

To evaluate the global level of glutathionylation in response to ischemia and I/R, we systematically altered the concentrations of O_2 and other nutrients. Depletion of glucose under normoxia induces glutathionylation significantly compared to hypoxia. Under hypoxia and OGD, there was no significant induction of the glutathionylation. This difference may suggest that although hypoxia and OGD have adverse effects on muscles, their outcomes may not be a characteristic of glutathionylation. In contrast to OGD, reoxygenation after OGD (OGD/O) significantly increases the global level of glutathionylation. Interestingly, glutathionylation was decreased upon incubation of glucose during reoxygenation after OGD (OGD/OG). This observation supports the importance of glucose for the restoration of redox homeostasis through the production of NADPH. Next, we evaluated the addition of palmitate during reoxygenation, which has previously been used as a model for ischemia and I/R injury.[118, 143] The addition of palmitate and glucose during reoxygenation after OGD (OGD/OGF) induced a global increase in of glutathionylation. Additionally, this treatment led to a reduction in cell

viability compared to other conditions we evaluated. This observation agrees with previous literature that demonstrates that an elevated level of fatty acid increases cellular damages in the perfused heart.[122, 124, 144] Nonetheless, the limitation of our study is that these observations generated by an in vitro model using HL-1 cells may differ from an *in vivo* model.

Then using our isotopically labeled clickable glutathione approach, we identified glutathionylated cysteines with and without the addition of palmitate during reoxygenation with glucose after OGD (OGD/OGF-BSA vs. OGD/OG). We have identified 248 glutathionylated proteins with their specific cysteines. DAVID GO and cluster analyses of these proteins found a major cluster of proteins involved in cytoskeletal structure and organization, suggesting that glutathionylation of those proteins may be involved in compromising the structural integrity of the cell. Since sarcomeric proteins are important in contractile activity and their mutations are associated with muscle diseases, we analyzed glutathionylated proteins associated with sarcomere and cardiomyopathy. We identified 18 glutathionylated cysteines whose genetic variants are associated with muscular disorders, suggesting glutathionylations of these cysteines has the potential to alter their functions.

Finally, we validated our proteomic data using two proteins, DES and BAG3. Mutations of DES and BAG3 are associated with cardiomyopathy and myofibrillar myopathy. Our pull-down data validated the glutathionylation of C332 (mouse) of DES and C179 (human) of BAG3. DES has three major domains, and C332 is located at the rod

domain, which is important in the filament assembly.[134] C332 is the only cysteine in DES, and it is conserved in other intermediate filaments, such as vimentin C328. Vimentin shown to loses its filament integrity upon interaction with zinc.[145] Moreover, glutathionylation at C328 of vimentin inhibits filament elongation.[146] Therefore, glutathionylation at DES C332 is expected to result in a similar outcome. BAG3 has multiple functional regions (BAG domain, IPV domain, WW domain, and PXXP domain).[135-138] C179 is close to poly-serine residues distant from BAG and PXXP domains that are important in chaperone and autophagy activities.[147] Additional analyses of these identified glutathionylated cysteines will be necessary to understand the functional outcome and their association for the diseases.

3.5 Experimental Section

3.5.1 Cell culture and induction of glutathionylation

HL-1 cells cultured in Claycomb medium containing FBS (10%), penicillin (100 units/mL), streptomycin (100 μg/mL), norepinephrine (0.1 mM), and L-glutamine (2 mM) in fibronectin-gelatin coated flasks. Cells were maintained in a humidified incubator containing 5% CO_2 at 37°C. At 80% confluency, HL-1 cells were infected with Ad/GS-M4. After 24 h, cells were incubated in a medium containing 0.6 mM L-azido-alanine for 20 h. Cells were subjected to serum starvation for 12 h, and glutathionylation was induced using different physiological stress conditions: [glucose deprivation (GD, 0 mM glucose), hypoxia (1% O_2), oxygen-glucose deprivation (OGD, 1% O_2 and 0 mM glucose), and oxygen-glucose deprivation followed by reperfusion (OGD/R)]. For hypoxia and OGD, a

hypoxia chamber (Billups-Rothenberg, MIC 101) was used. For OGD/R, after OGD, cells were reoxygenated with or without glucose (25 mM) in the presence or absence of palmitate (1 mM conjugated with BSA, 0.17 mM). Cells were washed with cold PBS and lysed with a lysis buffer containing 1% SDS, 100 mM LiCl, 100 mM HEPES (pH 7.6), 50 mm N-ethylmaleimide (NEM), and protease inhibitor cocktail (Pierce). Cell lysates were allowed to rotate for 30 minutes at 4°C, passed through 26-gauge needles 10 times, and protein concentrations were determined using a Bradford assay.

3.5.2   Vector construction - Polymerase chain reaction (PCR)

BAG3 WT gene from the Gateway p3E vector was amplified by PCR using a forward primer with *Nhe*I restriction site (5' GTT GTT <u>GCT AGC</u> GCC ACC ATG AGC GCC GCC ACC CAC TCG CC 3') and a reverse primer with FLAG tag, a stop codon, and *Xho*I restriction site (5' GTT GTT <u>CTC GAG</u> CTA CTT GTC GTC ATC GTC TTT GTA GTC CGG TGC TGC TGG GTT ACC AGG GGT GTC 3'). Plasmid DNA (~50 ng) was incubated with 10x pfu ultra-buffer (5 µL), forward and reverse primers (1 µL from 10 µM stocks), and dNTPs (1 µL from 10 mM stock). The final volume of the reaction mixture was adjusted to 49 µL by adding autoclaved water. Pfu Ultra-Enzyme (1 µL, Agilent) was added, and the reaction mixture was mixed well. The tube was incubated for 35 cycles in a thermocycler (Table 3.1). Amplified DNA was purified using PCR purification kit (Thermo Fisher).

Table 3.1 PCR program for QuikChange mutagenesis

Cycle	Temp (^{0}C)	Time	# of cycles
Initial denaturation	95	5 min	1
Denaturation	95	45 s	
Annealing	67	45 s	35
Extension	72	1.5 min	
Final extension	72	10 min	1
Store	4	Hold	

3.5.3 PCR purification

Amplified DNA was purified using a GeneJET PCR purification kit (Thermo Scientific) according to the manufacturer's instructions. An equal volume (50 μL) of binding buffer was added to the completed PCR mixture (50 μL) and mixed thoroughly. The reaction mixture was transferred to a GeneJET purification column and centrifuged at 13,000 rpm for 1 minute. Wash buffer (700 μL) was added to the purification column and centrifuged for 1 minute at 13,000 rpm. The flow-through was discarded, and the column was centrifuged for an additional 1 minute. The purification column was transferred to a micro centrifuge tube. After addition of elution buffer (50 μL), the column was centrifuged for 1 minute at 13,000 rpm. Purified DNA was stored at -20^{0}C.

3.5.4 Restriction digestion

The BAG3 WT gene was inserted into the pcDNA 3.1 mammalian vector after restriction digestion with *Nhe*I and *Xho*I enzymes. The PCR amplified WT gene (1 μg) and the pcDNA 3.1 vector (1 μg) were seperately incubated with 10x cutsmart buffer (5 μL, NEB) and restriction enzymes (*Nhe*I and *Xho*I, 1 μL). The final volume of the reaction

mixtures was adjusted to 50 µL with autoclaved water and mixed well. The reaction

mixture was incubated at 37^{0}C for 1 h. The digested plasmid and the gene were purified

by PCR purification.

3.5.5 Ligation

Ligation between digested vector and insert was carried out using quick ligase

enzyme (NEB) according to the manufacturer's instructions. Digested BAG3 WT and

pcDNA 3.1 were mixed in a 1:3 ratio (0.02 pmol: 0.06 pmol) with 2x quick ligase buffer (10

µL) and Quick Ligase enzyme (1 µL). The reaction volume was adjusted to 20 µL with

autoclaved water and incubated at room temperature for 5 minutes. After 5 minutes, the

reaction mixture was chilled on ice, transformed into DH5α cells and plated on agar plates

containing ampicillin (50 µg/mL) according to the protocol described in Chapter 2 section

2.5.5. Single colonies were inoculated in LB media containing ampicillin (50 µg/mL)

overnight, purified using GeneJET plasmid purification kit, and the ligation was confirmed

by DNA sequencing.

3.5.6 Site-directed QuikChange mutagenesis

Cysteine to serine mutants for DES (Origene) and BAG3 (Addgene) were generated

by QuikChange mutagenesis according to the general QuikChange protocol in Chapter 2,

section 2.5.4.

Forward and reverse QuikChange primers are listed in Table 3.2.

Table 3.2 – QuikChange primers for DES and BAG3

Mutation	Primer	Primer sequence 5'-3'
DES C332S	Forward	C CAG ATC CAG TCC TAC ACC TCC GAG ATT GAT GCC CTC AAG G
	Reverse	C CTT GAG GGC ATC AAT CTC GGA GGT GTA GGA CTG GAT CTG G
BAG3 C179S	Forward	CCA GCT GCC TCT GAC TCC TCA TCC TCA TCC TCC
	Reverse	GGA GGA TGA GGA TGA GGA GTC AGA GGC AGC TGG

3.5.7 Bacterial transformation

General transformation protocol was conducted as described in Chapter 2, section 2.5.5.

3.5.8 Lipofectamine transfection

General lipofectamine transfection protocol was performed as described in Chapter 2, section 2.5.8.

3.5.9 Virus infection

General virus infection protocol was performed as shown in the Chapter 2, section 2.5.10.

3.5.10 Bradford assay

Bradford assays were performed as described in Chapter 2, section 2.5.9.

3.5.11 Click reaction for the detection of glutathionylation

Click chemistry was performed as presented in Chapter 2, section 2.5.12.

3.5.12 ROS detection by MitoSOX assay

Intracellular ROS levels were measured using MitoSOX red reagent (Sigma, M36008). HL-1 cells were induced or uninduced with different physiological stress conditions (GD, hypoxia, OGD, and OGD/R). Cells were then washed with PBS and incubated with MitoSOX red reagent (5 μM) in DMEM without phenol-red for 10 minutes in the dark. Cells were washed with PBS, and fluorescence intensities were detected with a microplate reader (BioTek) set to 510 nm excitation and 595 nm emission wavelengths.

3.5.13 NADPH quantification assay

Intracellular $NADP^+$/NADPH levels were determined using the $NADP^+$/NADPH quantification kit (Sigma, MAK038) according to the manufacturer's instructions. HL-1 cells were induced or uninduced with different physiological conditions (GD, hypoxia, OGD, and OGD/R). Cells were then lysed using $NADP^+$/NADPH extraction buffer. For the detection of total $NADP^+$, cell lysates (50 μL) were incubated with $NADP^+$ cycling enzyme mixture in an $NADP^+$ cycling buffer (100 μL) and NADPH developer (10 μL) for 1 hour at room temperature. The absorbance values were measured at 450 nm using a microplate reader (BioTek). Lysates were heated at 60°C for 30 min to decompose all $NADP^+$ for the detection of NADPH.

3.5.14 Intracellular glutathione assay

Intracellular glutathione levels [reduced (GSH) and oxidized glutathione (GSSG)] were determined using a GSH colorimetric assay kit (BioVision, K261) according to the manufacturer's instructions. HL-1 cells were induced or uninduced with different

physiological stress conditions (GD, hypoxia, OGD, and OGD/R). Cells were then lysed and incubated with glutathione reductase (20 µL), NADPH generating solution (20 µL), and glutathione reaction buffer (120 µL) for 10 min at room temperature. The absorbance values were measured at 405nm using a microplate reader (BioTek). To detect the reduced form of glutathione, glutathione reductase was replaced with glutathione reaction buffer (20 µL).

3.5.15 Cell viability assay

A trypan blue assay was used to determine cell viability. HL-1 cells were induced or uninduced with different physiological stress conditions (GD, hypoxia, OGD, and OGD/R). Cells were then detached using 0.05% trypsin and diluted with the cell culture medium. Medium containing the cells (100 µL) was mixed with trypan blue reagent (100 µl, 0.4%). The mixture (20 µL) was loaded onto the slide and analyzed by an automated cell counter (TC 20, Bio-Rad) to determine the viable cell percentage.

3.5.16 Pull-down analysis

Pull down of glutathionylated proteins was achieved as described in Chapter 2, section 2.5.15.

3.5.17 Proteomic sample preparation

Proteomic samples were prepared as in Chapter 2, section 2.5.17.

3.5.18 LC-MS/MS analysis

LC-MS/MS analyses were conducted as described in Chapter 2, section 2.5.18.

3.5.19 Proteomic data analysis

Proteomic data analysis by MaxQuant and SkyLine was performed as described in Chapter 2, section 2.5.19.

3.5.20 Bioinformatic analysis

STRING and cluster analyses were carried out using Cytoscape software. First, identified mouse proteins (proteins with $R_{H/L}$ value > 2) were converted to human equivalents and loaded into the STRING program as a "glutathionylation" network. Then a "cardiomyopathy" network was loaded from STRING disease search. To identify cardiomyopathy-relevant proteins, the glutathionylation network was merged with the cardiomyopathy network. The merged network was then clustered using MCL clustering with a granularity parameter of 4 and array source from the score. To identify sarcomere and mitochondria-associated proteins, the protein list in the glutathionylation network was loaded into the DAVID Gene Ontology (DAVID GO) program and analyzed. Then sarcomere and mitochondria-associated proteins were clustered as described above. UniProt database (feature viewer and variants) and polyphen-2 program were used to analyze disease relevance.

CHAPTER 4: PROTEOMIC APPROACH FOR QUANTIFICATION OF GLUTATHIONYLATED

AND NON-OXIDIZED CYSTEINES

4.1 Introduction

Oxidative stress can induce reversible and irreversible oxidative modifications in redox-sensitive proteins by modulating structural or functional changes.[82] Moderate stress conditions can cause reversible oxidative modifications that protect proteins from irreversible modifications. In contrast, excessive stress can trigger irreversible oxidative modifications on proteins associated with permanent damage to protein structure and function.[82, 148] Among the twenty amino acids, cysteine is the most susceptible amino acid to undergo oxidative modifications.[82, 84, 149] There are two factors that determine the susceptibility of cysteine residues to undergo modifications: 1) solvent exposure or accessibility of thiol group, and 2) reactivity of the cysteine residue. Solvent accessibility is determined by the relative ease of a cysteine side chain to be exposed to the solvent, depending on the secondary or tertiary structure of the protein.[82] Cysteine residue reactivity is determined by the neighboring amino acids. Cysteine residues remain largely protonated under physiological pH conditions because of their pK_a value of ~8.3. However, neighboring basic amino acids in redox-sensitive proteins can depress this pK_a value, making them more nucleophilic and susceptible to oxidative modifications.[82, 150]

Among different oxidative protein modifications, S-glutathionylation is an important reversible post-translational modification that regulates many fundamental biological processes.[84, 151-153] Glutathionylation is the formation of a mixed disulfide bond

between protein cysteine and glutathione.[81, 84, 154, 155] Glutathionylation can occur under both physiological and pathological conditions, highlighting its role in cellular signaling events, regulating protein functions, and protecting proteins from over oxidation.[82-84, 156, 157] Protein sulfhydryls show differential susceptibility to glutathionylation even within the same protein.[82, 84] Only a small portion of cysteinescan undergo glutathionylation depending on their chemical and physical properties.[82] Identification and quantification of specific cysteines undergoing glutathionylation in living cells is important for identifying molecular targets involved in regulating cellular functions.[154, 158]

Over the years, a number of methods have been developed to characterize protein glutathionylation. Some methods include radioactive (^{35}S) labeling of the glutathione and visualization with an anti-glutathione antibody.[52, 81, 84, 154] However, the specific site of modification cannot directly be identified using these methods.[84] Therefore, mass spectrometry techniques methods conjugated with chemical derivatives have been developed for the mapping and relative quantification of glutathionylated cysteines. These are indirect approaches that use modified biotin tags (N-ethylmaleimide-biotin tag, or biotinylated glutathione tag) and iodoacetyl- tandem mass tagging (TMT).[58, 81, 84, 159, 160] However, the reduction of glutathionylation in these indirect approaches may involve the removal of reversible modifications other than glutathionylation on cysteines, making these methods nonspecific for the identification of glutathionylated sites only.[84] Our lab previously developed a proteomic approach to identify and relatively quantify glutathionylated proteins directly with their specific cysteine residues.[87, 89, 128] We have

identified and relatively quantified over 1300 glutathionylated cysteines that emerge upon addition of H_2O_2 in HL-1 mouse cardiomyocyte cell line. In our quantification strategy, the approach analyzes how much glutathionylation is increased on each cysteine before and after oxidative stress, i.e., a fold increase of glutathionylation. However, current approaches do not analyze the level (or percentage) of glutathionylation on each cysteine, i.e., a relative portion of glutathionylation versus non-glutathionylation on each cysteine, which is important information to predict and understand the biological significance of glutathionylation on the identified cysteines.

4.2 Approach

In this Chapter, we have devised a strategy with clickable glutathione that enables us to compare the levels of glutathionylation versus non-glutathionylation (unmodified or reduced form) on each cysteine using mass spectrometry. We have designed and synthesized a cysteine-reactive or electrophilic clickable glutathione derivative (L-N_3-GS-SPy) that can react with the reduced cysteine to form the same structure as in glutathionylation (Figure 4.1). We envisioned that heavy-labeled clickable glutathione could be used to form glutathionylation on individual cysteines after oxidative stress while the remaining unmodified portion of the cysteines could be detected after reacting or blocking with electrophilic N_3-GS-Spy. This approach would yield the same structure as glutathionylation, only with 4 Da mass difference that can be analyzed by mass spectrometry. First, using purified proteins, we have demonstrated that upon glutathionylation of cysteines with heavy azido-glutathione, the electrophilic or blocking

GSH derivative can react with unmodified cysteines effectively and enables the quantification of glutathionylation compared to unmodified glutathionylated cysteines. In addition, we have evaluated the electrophilic clickable glutathione in two different cell lines. Finally, we have applied this quantification approach on the C2C12 mouse skeletal muscle cell line and identified 1,518 glutathionylated cysteines with their $R_{H/L}$ values upon the addition of H_2O_2. We have identified additional 1174 cysteines that reacted only with our electrophilic clickable glutathione.

L-Azido Alanine

Cysteine blocking clickable glutathione
L-N₃-GS-SPy
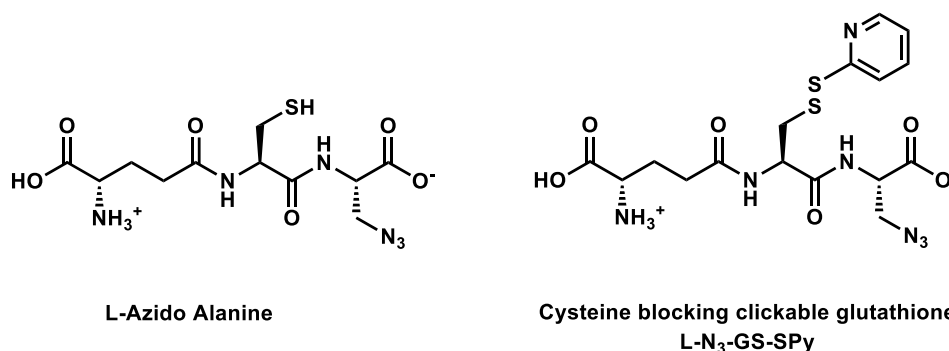
Figure 4.1 – L-Azido-glutathione and cysteine blocking clickable glutathione (L-N₃-GS-SPy)

4.3 Results

4.3.1 Design and synthesis of the electrophilic clickable glutathione (L-N₃-GS-SPy)

We previously developed a mass spectrometry-based method to identify and relatively quantify the glutathionylation in HL-1 cardiomyocyte cell line using isotopically labeled heavy and light azido-alanine.[128, 161] We envisioned that after proteins were glutathionylated with heavy azido-glutathione (Figure 4.2 A) and unmodified cysteines were blocked with our electrophilic clickable glutathione that mimics the structure of light azido-glutathione (Figure 4.2 B), we will be able to quantify glutathionylated

cysteines compared to the unmodified cysteines with an isotopic mass difference. Therefore, we have designed a cysteine-reactive electrophilic clickable glutathione (N_3-GS-SPy) that contains a light azido-glutathione bound to a 2-thiopyridine by a disulfide linkage (Figure 4.1). Light azido-glutathione was synthesized by an enzymatic reaction using light azido-alanine and γ-glutamyl cysteine in the presence of GS M4. Light azido-glutathione was reacted with 2,2-dithiodipyridine for the chemical synthesis of L-N_3-GS-Spy.

A)

Cysteine blocling clickable glutathione
L-N_3-GS-SPy

Disulfide formation

Pyridine
2-thione

B)

H-Azido glutathione

Glutathionylation
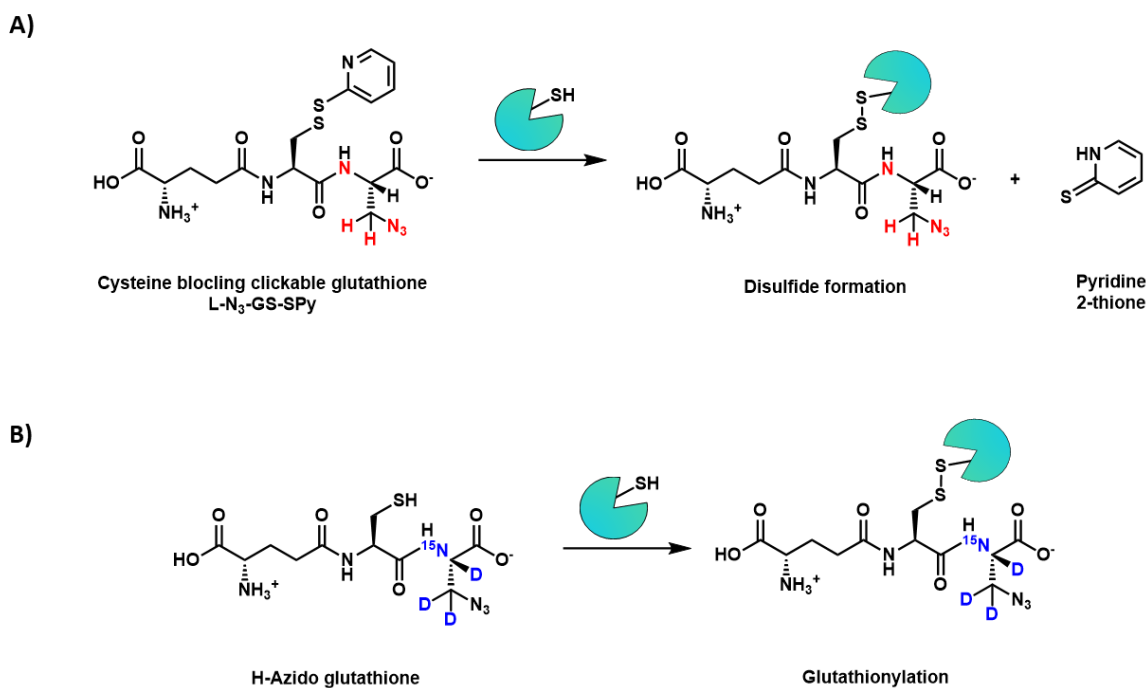
Figure 4.2 – Reactions of cysteine blocking clickable glutathione and glutathione with proteins. A) Reaction of cysteine blocking clickable glutathione forms a mixed disulfide bond between protein and L-azido glutathione. B) Reaction of H-azido glutathione with protein forms a mixed disulfide bond between protein and H-azido glutathione (glutathionylation).

4.3.2   Evaluation of L-N$_3$-GS-Spy to block unmodified cysteines with purified proteins

N$_3$-GS-Spy was evaluated for its ability to block unreacted cysteines using two purified proteins, GSTO1 and CSRP3. Glutathionylation was induced in purified GSTO1 protein in the presence of heavy azido-glutathione in vitro using different H$_2$O$_2$ concentrations. Subsequently, the GSTO1 protein were treatedwith L-N$_3$-GS-Spy to react with or block any remaining unmodified (reduced) cysteines. The protein was then subjected to click reaction with biotin-DADPS-alkyne. Protein was digested with trypsin/LysC, enriched using streptavidin-agarose beads, eluted by incubation with acid, and analyzed by MALDI. Two peaks were identified with a 4 Da mass difference (1284.83 and 1288.87) that correspond to GSTO1 peptides (FC$_{32}$*PFAER) conjugated with heavy or light azido-glutathione (Figure 4.3A). Importantly, the signal intensity of heavy-labeled peptide was increased with the increased concentration of H$_2$O$_2$ (Figure 4.3A) versus light-labeled peptide, which estimate the relative portion of glutathionylation on the given cysteine over the increasing amount of H$_2$O$_2$. Identified cysteine residue is an active site cysteine known to undergo glutathionylation.

A similar approach was applied to purified CSRP3 protein. Two peaks were identified (1964.12 and 1968.12) with a 4 Da mass difference that correspond to peptides (TVYHAEEIQC$_{25}$*NGR) conjugated with heavy or light azido-glutathione (Figure 4.3B). Similar to GSTO1, the signal intensity of heavy-labeled peptide of CSRP3 versus light-labeled one was also increased with the increased concentration of H$_2$O$_2$ (Figure 4.3B). These data suggest that our blocking reagent (L-N$_3$-GS-Spy) can effectively be used for the

quantification of glutathionylated cysteines compared to the unmodified portion with an isotopic mass difference of 4 Da.

A) GSTO1

0 mM H_2O_2 0.2 mM H_2O_2 0.5 mM H_2O_2

B) CSRP3

0.2 mM H_2O_2 0.5 mM H_2O_2
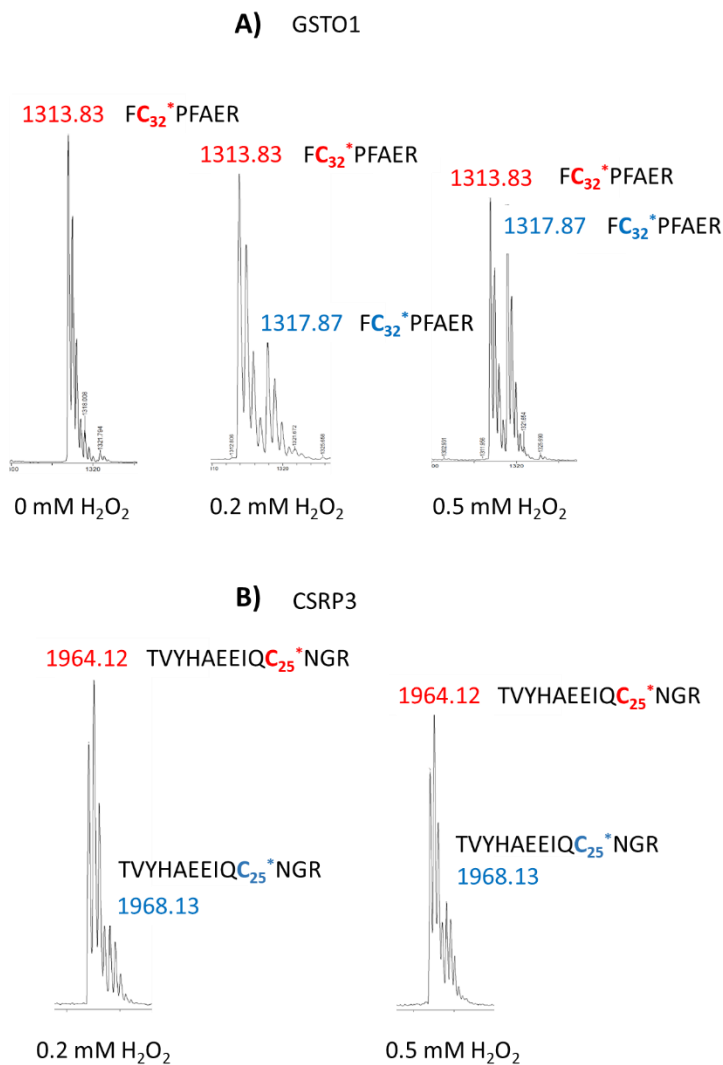
Figure 4.3 – Evaluation of blocking reagent with purified proteins. A-B) Glutathionylations of GSTO1 C32 and CSRP3 C25 increase with increasing H_2O_2 concentration.

4.3.3 Evaluation of L-N₃-GS-Spy with cell lines

The reactivity of L-N₃-GS-Spy was evaluated with two cell lines, HEK293/GS M4 and C2C12 mouse skeletal muscle cell line[162]. Cells were lysed using a lysis buffer

containing NEM or L-N₃-GS-Spy and subjected to click reaction with Cy5-alkyne. Compared to the sample lysed in the presence of NEM, an intense fluorescence signal was detected in the sample lysed with the buffer containing L-N₃-GS-Spy (Figure 4.4A, lanes 1 vs. 2 and 4 vs. 5). Increased concentration of L-N₃-GS-Spy (10 and 20 mM) did not change the fluorescence signal significantly (Figure 4.4A, lanes 2 vs. 3 and 5 vs. 6).
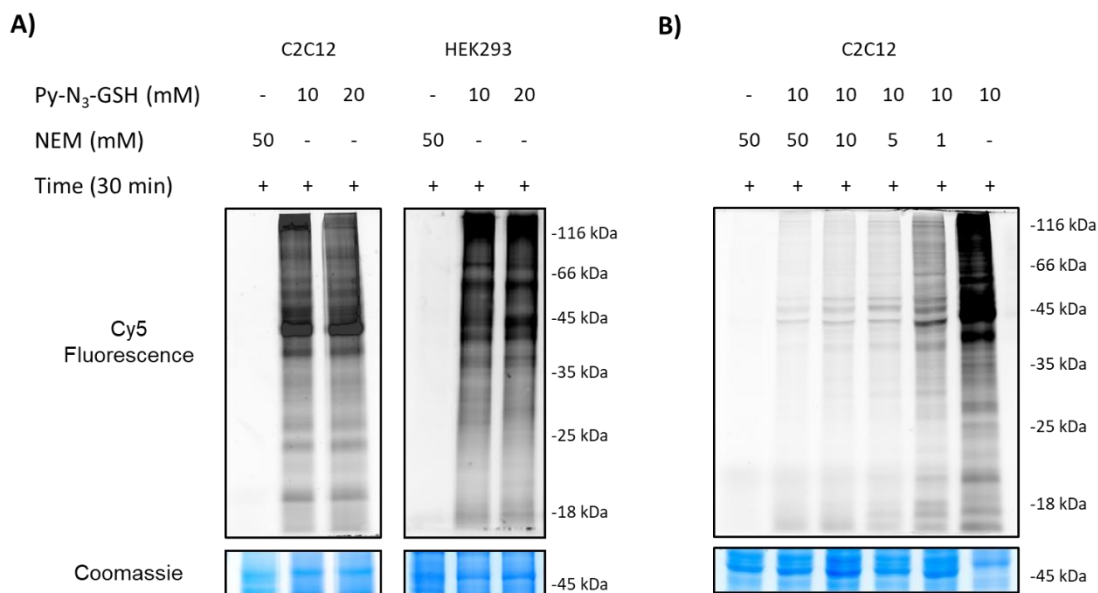
Figure 4.4 – Evaluation of electrophilic clickable glutathione (L-N₃-GS-Spy). A) cysteine blocking by L-N₃-GS-Spy in HEK293/GS M4 and C2C12 cell lines. B) Competition of L-N₃-GS-Spy with NEM to block cysteines.

Then we carried out a competition assay to confirm the blocking of cysteines by L-N₃-GS-Spy in the presence of NEM. C2C12 cells were lysed with a lysis buffer containing different concentrations of NEM and a fixed concentration of L-N₃-GS-Spy. When the concentration of NEM decreased, the fluorescence signal gradually increased (Figure 4.4B). This confirms the reactivity of L-N₃-GS-Spy on the cysteines. These data

demonstrate that L-N$_3$-GS-Spy can be used to label unmodified reduced forms of cysteines in cell lysates.

4.3.4 Identification and quantification of protein glutathionylation using an isotope-labeled clickable glutathione with L-N$_3$-GS-Spy

After confirming that L-N$_3$-GS-Spy can block cysteines in a global level, we applied our mass spectrometry-based clickable glutathione approach to identify and quantify proteins undergoing glutathionylation. In this approach, after differentiation for five days, C2C12 cells overexpressing GS M4 were treated with heavy azido-alanine. GS M4 utilizes heavy azido-alanine for the synthesis of heavy azido-glutathione. Then the glutathionylation was induced by the addition of H$_2$O$_2$. Subsequently, cells were lysed with a lysis buffer containing L-N$_3$-GS-Spy, and the lysates were subjected to click reaction with biotin-DADPS-alkyne. Biotinylated glutathionylated proteins were enriched using streptavidin-agarose beads and carried out trypsin digestion. Finally, the glutathionylated peptides were eluted by acid cleavage of the DADPS linker, and samples were analyzed by LC-MS/MS (Figure 4.5A). Heavy and light azido-glutathione modified peptide pairs were identified with a 4 Da mass difference (found at least two times in triplicate experiments). MS1 peak intensities of identified peptides were calculated using SkyLine software to determine their R$_{H/L}$ values. These R$_{H/L}$ values represent the level of glutathionylation of individual peptides compared to their unmodified or reduced portion. We have identified 1518 peptides labeled with both heavy and light azido-glutathione (i.e., glutathionylated peptides) with their R$_{H/L}$ values (Figure 4.5B). The

median $R_{H/L}$ value for the glutathionylated peptides is 0.116 (90% in the range of 0.04-0.32, Figure 4.5C left). Interestingly, we have identified additional 1174 peptides labeled with light azido glutathione only (i.e., unmodified cysteines blocked by the electrophilic clickable glutathione reagent Figure 4.5B). The median coefficient of variation (CV) for the data set was 19.8% (80% of CV in the range of 9-40%). These CV values demonstrate the relative consistency of $R_{H/L}$ values between triplicate experiments. The distribution of $R_{H/L}$ values and MS1 peaks of individual glutathionylated peptides show different levels of glutathionylation upon the addition of H_2O_2 (Figure 4.5D, E). For example, FLNC C1181, CTTND1 C692, and ME1 C164 show relatively high $R_{H/L}$ values (3.67, 2.51, and 1.63, respectively), representing a relatively high level of glutathionylation upon addition of H_2O_2 (Figure 4.5D, E). The data suggest that these cysteines are more reactive or sensitive to undergo glutathionylation upon stress. FLNC C1062, VIM C328, and DES C332 show relatively low $R_{H/L}$ values (0.04, 0.07, and 0.09, respectively, Figure 4.5D, E), suggesting their relatively low level of glutathionylation and low reactivity or sensitivity to undergo glutathionylation.
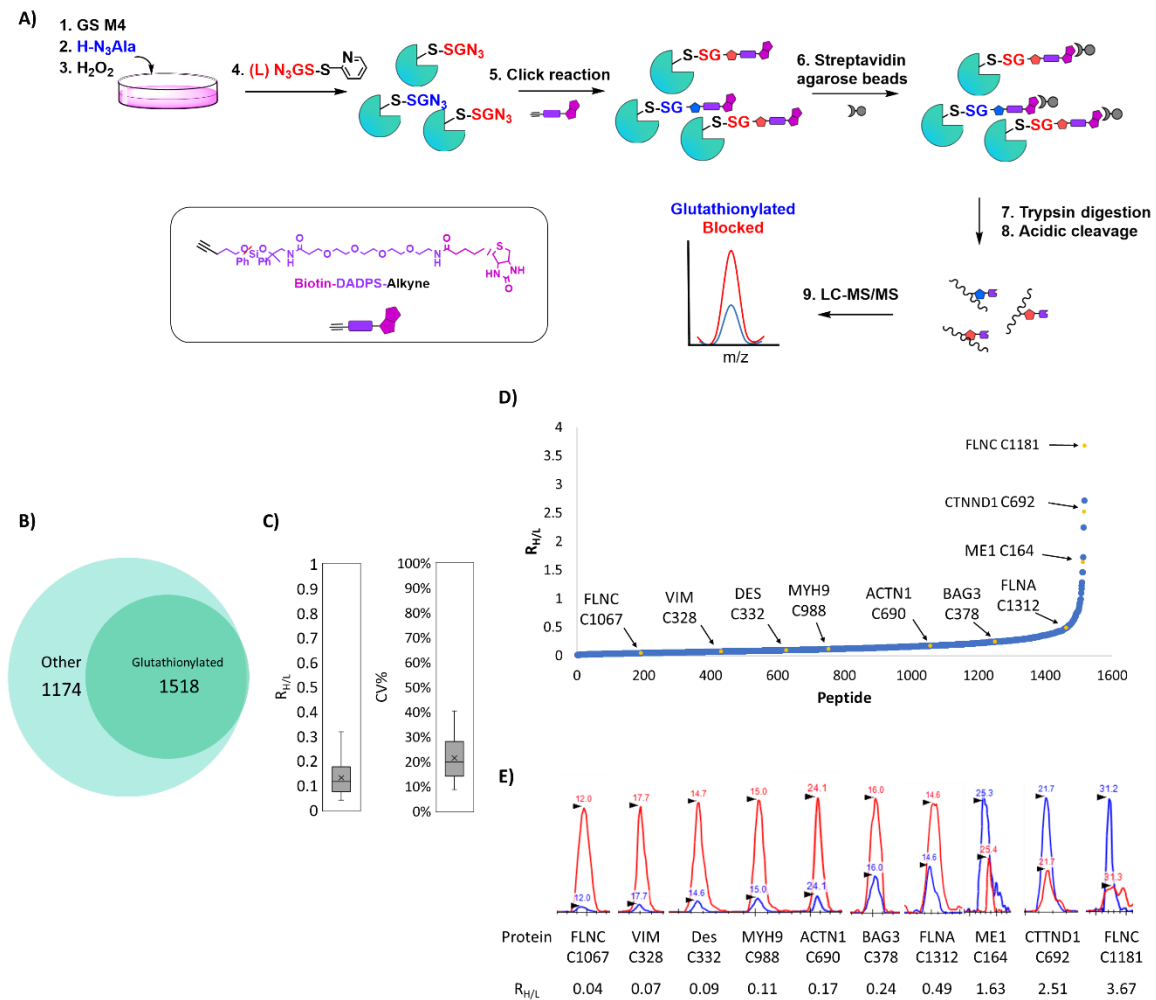
Figure 4.5 – Identification and quantification of glutathionylated proteins in the C2C12 cell line. A) Scheme for the quantification of glutathionylated peptides compared to unmodified cysteines. B) Number of glutathionylated (1,518) and nonmodified (1,174) peptides. C) Plots of $R_{H/L}$ values and CV of glutathionylated peptides. D) Distribution of $R_{H/L}$ values of glutathionylated peptides. E) MS1 peaks showing relative quantification of glutathionylated peptides (heavy/blue) over unmodified peptides (light/red).

4.3.5 Validation of data by pull-down and western blot analysis

We used catenin-delta 1 (CTNND1) to validate our proteomic data. CTNND1 is a member of the catenin superfamily, armadillo repeat protein. It is important in signal transduction and cell-cell adhesion.[163-165] In humans, CTNND1 is mainly expressed in mesenchymal cells and epithelial cells.[164] The major function of CTNND1 is the

stabilization of cadherin, the main cell-cell adhesion molecule.[163, 166] CTNND1 has a dual role as a tumor inhibitor and a metastasis promoter depending on its subcellular localization and stabilization of cadherin.[166-168] Armadillo domain mediates the cell-cell interactions of CTNND1 and C692 is located in one of the armadillo domains.[169] From our data, we found that C692 of CTNND1 undergoes glutathionylation. Based on its $R_{H/L}$ ratio (2.61), C692 was selected as one of reactive and sensitive cysteine for glutathionylation. We also identified two additional cysteines (C394 and C450) that only reacted with our electrophilic clickable glutathione reagent, L-N$_3$-GS-Spy, i.e., their $R_{H/L}$ values are zero in mass analyses. To validate the glutathionylation of C692 and its sensitivity to glutathionylation, we produced and used WT and cysteine mutants of CTNND1 (C394S, C450S, and C692S). WT and cysteine mutant plasmids were overexpressed in HEK392/GS M4 cells, and glutathionylation was induced with different concentrations of H_2O_2 (0, 0.2, 0.5, and 1 mM). Glutathionylation signal was gradually increased in WT, C394S, and C450 mutant proteins with the increasing concentration of H_2O_2 (Figure 4.6 lanes 1-4 and 4-8). The glutathionylation signal of WT protein at low H_2O_2 concentrations suggests the relatively high reactivity of CTNND1 for glutathionylation. In contrast, glutathionylation was significantly reduced in CTNND1 C692S upon H_2O_2 incubation (Figure 4.6 lanes 9-12). The reduced signal in C692S mutant confirms the higher tendency to glutathionylation at C692 residue.

	FLAG-CTNND1															
		WT				C394S				C692S				C450S		
GS M4	+	+	+	+	+	+	+	+	+	+	+	+	+	+	+	+
azido-Ala	+	+	+	+	+	+	+	+	+	+	+	+	+	+	+	+
H_2O_2	-	0.2	0.5	1	-	0.2	0.5	1	-	0.2	0.5	1	-	0.2	0.5	1

After Strep-Beads (Glutathionylation) — -130 kD / -95 kD

Before Strep-Beads (Protein level) — -130 kD / -95 kD

FLAG
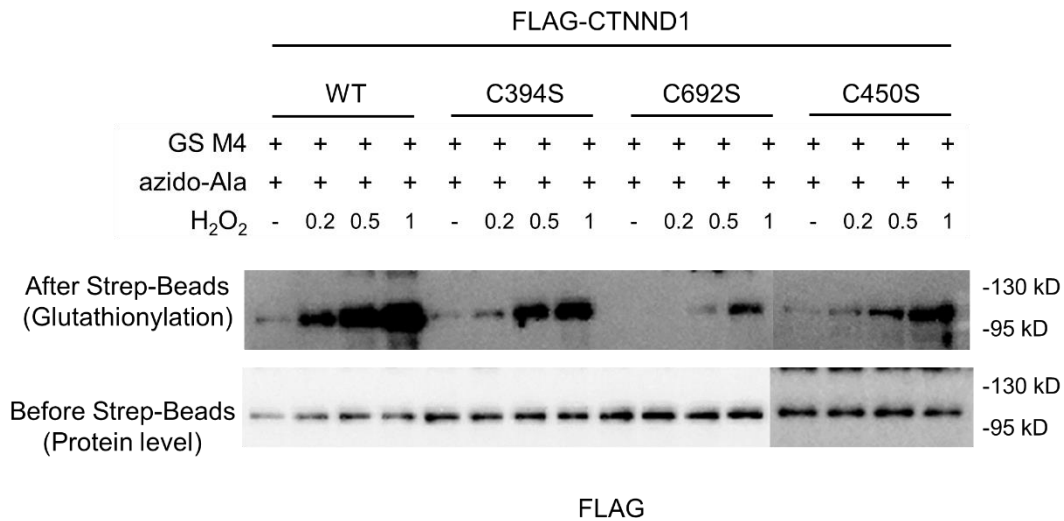
Figure 4.6 Glutathionylation of CTTND1. HEK293/GS M4 cells overexpressing CTNND1 WT and mutants were treated with azido-Ala (0.6 mM, 20 h) and glutathionylation was induced by adding different concentrations of H_2O_2 (0-1 mM). Cells were lysed, carried out click reaction with biotin alkyne, enriched using streptavidin agarose beads, subjected to western blot analysis and detected with flag antibody.

4.4 Discussion

Protein S-glutathionylation is an important reversible -post-translational modification that regulates many fundamental biological processes. During the past years, many methods have been developed to identify protein glutathionylation. But methods for the quantification of glutathionylation have been limited. While a biotin-tag method and iodoacetyl-TMT labeling method use two sets of samples for the relative quantification of glutathionylation, our approach needs only one set of samples for the quantification of glutathionylated cysteines compared to the unmodified cysteines. Therefore, our approach enables the identification of potentially more reactive cysteines toward glutathionylation . We have used GSTO1 and CSRP3 proteins to demonstrate that L-N₃-GS-Spy can be used to quantify protein glutathionylation with an isotopic mass

difference of 4 Da. We used C2C12 mouse skeletal muscle cells for the quantification of glutathionylation upon the addition of H_2O_2. We specifically selected the C2C12 cell line because it has been widely used to study the skeletal muscle biology as a model cell line due to its ability to develop into myotubes expressing contractile proteins after differentiation.[162, 170] We have identified 1518 glutathionylated proteins upon the addition of H_2O_2 (1 mM). We have identified additional 1174 cysteines that are not glutathionylated even after the addition of H_2O_2. Finally, we validated the glutathionylation and reactivity of one protein CTNND1 identified from our proteomic data.

4.5   Experimental Section

4.3.2   Synthesis of cysteine blocking clickable glutathione (L-N₃-GS-SPy)

4.3.2.1 Enzymatic synthesis of light azido glutathione (N₃GSH)

Light azido-glutathione (N₃-GSH) was synthesized enzymatically using the GS M4 enzyme. L-azido-alanine (4 mM), γ-glutamyl-cysteine (4 mM), ATP (10 mM) in Tris buffer [200 mM tris (pH 7.4), 50 mM $MgCl_2$, and 300 mM NaCl) were mixted with GS M4 (100 ng) to a final volume of 10 mL in a falcon tube and incubated for three days at 37°C with rotation. After three days, the reaction mixture was acidified using trichloroacetic acid (10%), centrifuged at 4,500 rpm to precipitate the enzyme and purified using HPLC. After lyophilization of the positive fractions, oxidized azido-glutathione (N₃GS-SGN₃) was obtained as a white solid. Oxidized azido glutathione was reduced using dithiothreitol (DTT, 2 equivalents) in PBS (100 mM, pH 7.4) at room temperature for 1 h. The sample

was purified using HPLC and lyophilized to obtain the reduced azido-glutathione as a white solid.

4.3.2.2 Chemical synthesis of L-N$_3$-GS-Spy

L-N$_3$-GS-Spy was synthesized chemically using 2,2'-dithiodipyrdine. Azido-glutathione (0.28 mmol, 1 equivalent) was dissolved in water (3 mL) and methanol (3 mL) by stirring. After azido-glutathione was completely dissolved, 2,2'-dithiodipyridine (0.56 mmol, 2 equivalents) was added. The mixture was stirred at room temperature for 16 h. After the reaction was completed, methanol was removed by rotary evaporation. The remaining aqueous layer was extracted several times with dichloromethane to remove excess 2,2'-dithiodipyrdine, and the aqueous layer was lyophilized to obtain a white solid.[171, 172] Mass was confirmed by ESI-LC/MS (Figure 4.6).
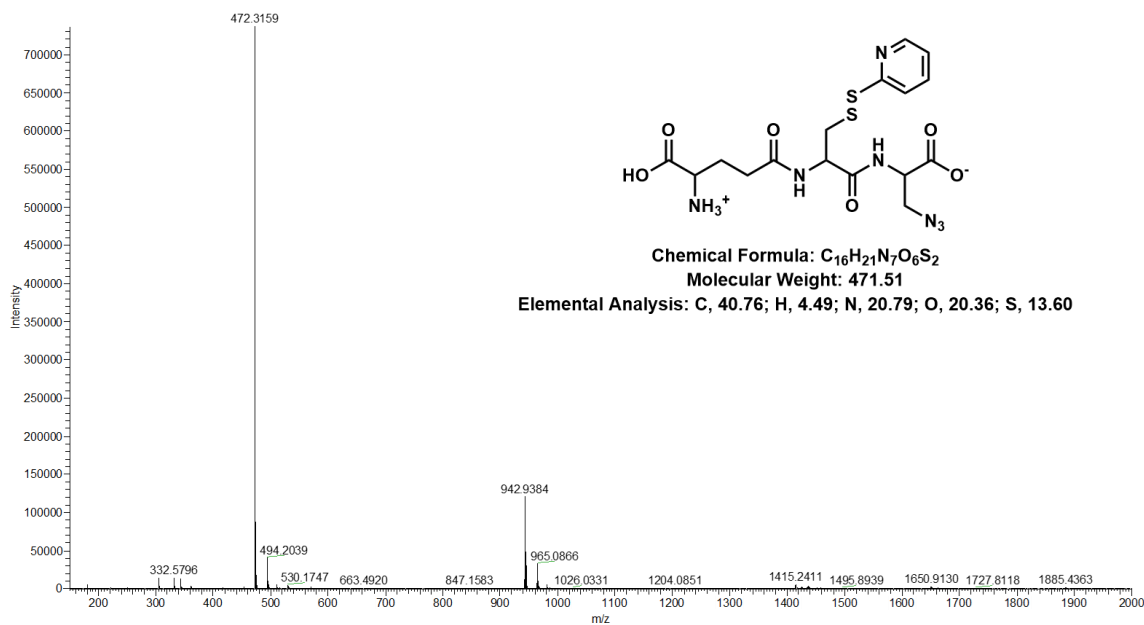
Figure 4.7 – ESI mass spectrum of L-N$_3$-GS-Spy.

4.5.2 Evaluation of L-N$_3$-GS-Spy with purified proteins

Reactivity of L-N$_3$-GS-Spy was evaluated with two purified proteins, GSTO1 and CSRP3. The purified protein (100 μg) was incubated with heavy azido-glutathione (1 mM) in PBS (1x, pH 7.4) for 30 minutes at room temperature to induce glutathionylation. Protein was incubated with L-N$_3$-GS-Spy (5 mM) and SDS (1%) for 30 minutes at 37°C to react with unmodified cysteines. Then, proteins were precipitated by adding ice-cold acetone (4x volume) and incubated at -20°C for 30 minutes. After centrifugation at 13,000 rpm for 3 minutes, the supernatant was removed, and proteins were resuspended in resuspension buffer (40 μL) containing 10x PBS (pH 7.4, 5 μL), 10x SDS (1 μL), and water. Pellet was completely dissolved by sonication. To the solution was added 5 mM biotin-DADPS-alkyne (4 μL) and click solution (10 μL) [pre prepared by mixing 20 mM THPTA (5 μL) and 20 mM Cu(I)Br dissolved in DMSO/tBuOH (3:1, v/v; 5 μL)]. The mixture was incubated for 1 h at room temperature. Proteins were precipitated by adding ice-cold acetone (4x volume) and incubated at -20°C for 30 minutes. The mixture was centrifuged, and the supernatant was removed. The pellet was resuspended in a buffer (100 μL) containing 1.2% SDS in PBS (1x, pH 7.4) by sonication. The resuspended solution was added to pre-washed streptavidin-agarose beads (20 μL) and incubated overnight at 4°C. The next day, beads were washed with 0.2% SDS in PBS (1x, pH 7.4) and PBS (1x, pH 7.4) three times each. Then the beads were incubated with denaturation buffer (200 μL) containing 6 M urea and PBS for 45 minutes at 37°C. After removing the buffer, beads were incubated with digestion buffer (50 μL) containing 2 M urea in PBS, 1 mM CaCl$_2$, and

trypsin/LysC (1 μg) overnight at 37°C. Beads were washed three times with 0.2% SDS in PBS, PBS, and water. Peptides were eluted by incubating beads with 10% formic acid (50 μL x 2) for 30 minutes and a final wash with another 50 μL of 10% formic acid. Three eluates were combined, lyophilized, and analyzed by MALDI.

4.5.3 Cell culture with L-N$_3$-GS-Spy

C2C12 cells (Sigma) were cultured in DMEM supplemented with FBS (10%), penicillin (100 U/mL), and streptomycin (100 μg/mL) and incubated in a humidified chamber with 5% CO$_2$, at 37°C. Upon 100% confluency, cells were differentiated for 7 days using differentiation media [DMEM supplemented with horse serum (2%, Sigma), penicillin (100 U/mL), and streptomycin (100 μg/mL)]. Cells were lysed using a lysis buffer containing 1% SDS, 100 mM LiCl, 100 mM HEPES (pH 7.4), L-N$_3$-GS-Spy (0-30 mM), and protease inhibitor cocktail. The lysates were allowed to rotate at 4°C for 45 minutes and passed through a needle (26-gauge) 10 times. Protein concentrations of the lysates were determined by Bradford assay as shown in Chapter 2, section 2.5.9.

4.5.4 Click reaction for the detection of fluorescence for blocked proteins

General click chemistry procedure was performed as shown in Chapter 2, section 2.5.12

4.5.5 Site-directed QuikChange mutagenesis

Cysteine to serine mutants for CTNND1 (Origene) was generated by QuikChange mutagenesis. Forward and reverse QuikChange primers are listed in Table 4.1. General Quikchange protocol is shown in chapter 2, section 2.5.4

Table 4.1 – Quikchange primers for CTNND1

Mutation	Primer	Primer sequence 5'-3'
CTNND1 C394S	Forward	C CTG CAA CAC TTA TCC TAC CGC AAT GAC AAG G
	Reverse	C CTT GTC ATT GCG GTA GGA TAA GTG TTG CAG G
CTNND1 C450S	Forward	GCC ATA AAA AAC TCT GAT GGT GTG CCT GCC C
	Reverse	G GGC AGG CAC ACC ATC AGA GTT TTT TAT GGC
CTNND1 C692S	Forward	GCT ATC AGA AAC TTG TCT GCT GGG CGC TGG ACG
	Reverse	CGT CCA GCG CCC AGC AGA CAA GTT CTG GAT AGC

4.5.6 Bacterial transformation

General transformation protocol is shown in Chapter 2, section 2.5.5

4.5.7 Virus infection

General virus transfection procedure is shown in Chapter 2, section 2.5.10

4.5.8 Proteomic sample preparation

After differentiation for five days, C2C12 cells were infected with Ad/GS M4. After 24 h, cells were incubated with heavy azido-alanine (0.6 mM) in differentiation media for 20 h. After 20 h, cells were treated with H_2O_2 (1 mM) for 15 minutes and lysed with a lysis buffer containing 1% SDS, 100 mM LiCl, 100 mM HEPES (pH 7.4), 10 mM L-N_3-GS-Spy, and protease inhibitor cocktail. The lysates were allowed to rotate at 4°C for 45 minutes and passed through a needle (26-gauge) 10 times. Protein concentrations of the lysates were determined by Bradford assay as explained in Chapter 2, section 2.5.9. Then the proteomic samples were prepared as shown in Chapter 2, section 2.5.17

4.5.9 LC-MS/MS analysis

LC-MS/MS analysis protocol is shown in Chapter 2, section 2.5.18

4.5.10 Protein identification and quantification

Proteomic data analysis by MaxQuant and SkyLine was performed as shown in Chapter 2, section 2.5.19

CHAPTER 5: FUNCTIONAL STUDIES OF CARDIAC PROTEIN GLUTATHIONYLATION

UNDER ISCHEMIC STRESS

5.1 Introduction

All vertebrates, including humans, have three major muscle types: cardiac, skeletal, and smooth muscle. The basic functional and structural unit of the cardiac muscle is a sarcomere. The sarcomere is mainly composed of thick and thin filaments that are arranged between Z-lines.[173] Z-line is mainly composed of α-actinin that anchors thin filaments from neighboring sarcomeres. Thick and thin filaments are made up of myosin and actin proteins, which provide the striated pattern to the cardiac muscle cells.[173] The three-dimensional structure of thick and thin filaments is maintained by intermediate filaments (IFs) that are attached to the periphery of the sarcomere. IF proteins are encoded by about 70 genes, including vimentin, desmin, synemin, nestin, and plectin.[133, 173-175] IF proteins are important in providing structural and functional support to the cells.[174]

Desmin is the major component in IFs.[105, 106, 174-178] Depending on the mode of assembly, structural homology, and intracellular and tissue distribution, IF proteins are divided into six subclasses. Desmin belongs to type III, which also contains vimentin.[134, 174, 175, 179-181] Desmin anchors many different cell structures like mitochondria, and nuclear membrane, desmosomes and connect the sarcomeric Z-lines to the cytoskeleton.[134, 182-187] As the integrator of these cell structures, desmin facilitates the mechanochemical

signaling and crosstalk between the organelles.[182, 188] Desmin also plays a critical role in maintaining the structural and mechanical integrity of sarcomere.[177]

All IF proteins have a common tripartite structure composed of a conserved central helical rod domain, an N-terminus head domain, and a C-terminus tail domain.[134, 174, 179, 186] Rod domain contains four α-helical domains: 1A, 1B, 2A, and 2B that are separated by three non-helical linkers: L1, L12, and L2.[104, 174] Rod domain is essential for the polymerization of desmin monomers. The tail domain is important for the construction of the assembled filamentous network.[174] Desmin filament assembly is a stepwise process. Rod domains of two desmin monomers form a coiled-coil dimer. Two dimers antiparallelly anneal to form tetramers. Eight tetramers laterally anneal to form unit-length filaments (ULFs). Unit-length filaments are the building blocks of the long desmin filaments. The ULFs fuse longitudinally to form mature desmin filaments (Figure 5.1).[134, 174] Desmin filaments are extremely dynamic, that they are very responsive to extracellular and intracellular stimuli such as PTMs.[174]
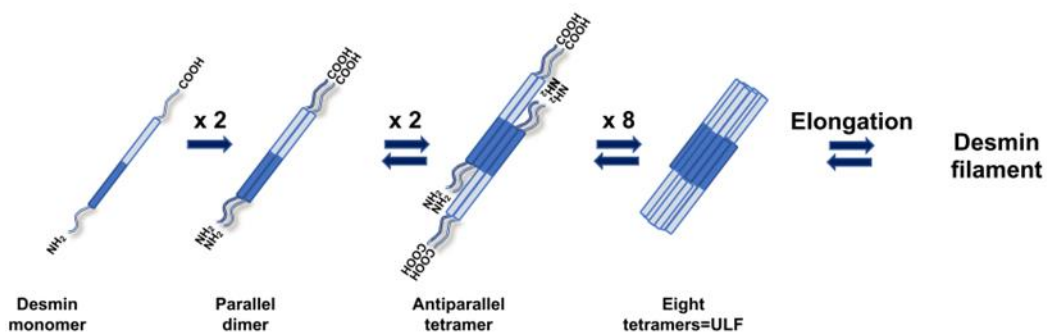
Figure 5.1 –Desmin filament assembles in a stepwise process. Figure adapted from Agnetti *et al*. 2021 with permission from the copyrights clearance center.[174]

Mutations in desmin gene or PTMs of desmin protein are associated with skeletal and cardiac myopathies (desminopathy).[179, 181-183, 185, 186, 189, 190] About 70 mutations have been reported so far that have been associated with desminopathy.[179, 182, 191] Majority of these mutations are localized in the rod domain, which is important for the filament assembly.[179] In addition to those mutations, it has been found that phosphorylation and ubiquitination of desmin also regulate cellular homeostasis and heart disease.[174] However, other PTMs such as glutathionylation and their effect on desmin function have not been studied so far.

Desmin has only one cysteine residue (C332; mouse), and it is conserved with the type III IFs including vimentin (C328; mouse), the most extensively studied type III IF (Figure 5.2).[179, 191, 192] Glutathionylation and nitrosylation of C328 of vimentin has been studied previously. Glutathionylation has been shown to inhibit the filament elongation of vimentin.[146] Therefore, we hypothesized that glutathionylation of C332 may have a similar effect on filament assembly and elongation on desmin.


```
sp|P31001|DESM_MOUSE   SKVSDLTQAANKNNDALRQAKQEMMEYRHQIQSYTCEIDALKGTNDSLMRQMRELEDRFA   356
sp|P20152|VIME_MOUSE   SKFADLSEAANRNNDALRQAKQESNEYRRQVQSLTCEVDALKGTNESLERQMREMEENFA   352
                       **.:**:.:***.**********   ***.*.** *:*.*******:** *****.:..**
```

Figure 5.2 - Sequence alignment around desmin C332 with vimentin. C332 of desmin is conserved with vimentin (C328).

5.2 Approach

From our previous proteomic analyses, we have identified that desmin is undergoing glutathionylation.[128, 161] To investigate the effect of glutathionylation on desmin under ischemic stress, we have used HL-1 mouse cardiomyocyte cell line, adult

rat cardiomyocytes, and neonatal rat cardiomyocytes. With or without overexpression of desmin WT and desmin C332S mutant, glutathionylation was induced by ischemic stress conditions such as GD, OGD, or OGD/R. Cells were then immunostained and observed under a confocal microscope.

5.3 Results

5.3.1   Pull down and western blot analysis for desmin glutathionylation

HL-1 cells overexpressing GS M4 were treated with N_3Ala, and cells were subjected to OGD/OG and OGD/OGF. After lysis, cell lysates were subjected to click reaction with biotin -alkyne. Glutathionylated proteins were enriched using streptavidin-agarose beads, and western blot analysis was carried out. We found that the addition of palmitate during repletion (OGD/OGF) induced glutathionylation of desmin compared to OGD/OG (Figure 5.3, lane 1 vs. 3). This confirms the glutathionylation of desmin under OGD/OGF. To confirm the glutathionylation at the specific cysteine site, we overexpressed WT and cysteine mutant of desmin (desmin WT and desmin C332S) in HEK293/GS M4 cells. Desmin WT (Figure 5.3, lane 4 and 5 vs. 6) showed glutathionylation under OGD/OGF. In contrast, glutathionylation levels were completely or partially reduced in desmin C332S (Figure 5.3, lane 6 vs. 9) in the presence of palmitate during repletion (OGD/OGF).[161] This confirms the glutathionylation at C332 of desmin.
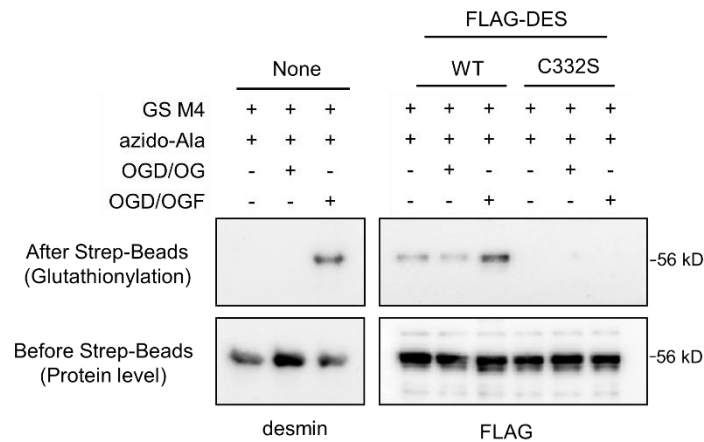
Figure 5.3 – Glutathionylation of desmin C332 in response to OGD/OGF. HEK293/GS M4 cells and HL-1 cells with and without overexpression of desmin WT and mutant were subjected to stress (OGD/OG and OGD/OGF). Cells were lysed and carried out pull-down and western blot analysis.

5.3.2 Sarcomeric proteins lose myofibril stability upon oxidative stress in adult rat cardiomyocytes

First, adult rat cardiomyocytes isolated from adult rats were subjected to stress, glucose depletion (GD) for 20 h, oxygen-glucose depletion (OGD) for 4 h, or OGD for 4 h followed by repletion of fatty acid (OGD/OGF) for 12 h. The cells were immunostained with three different antibodies, titin, α-actinin, and desmin, and observed under a confocal microscope. Under control conditions, where no stress was applied, all three proteins displayed a parallel striated myofibril structure (Figure 5.4, A-C). When the cells were subjected to OGD for 4 h, all three proteins could still maintain the myofibril integrity (Figure 5.4, D-F). In contrast, upon GD or OGD/OGF, all three proteins showed a misaligned and disoriented myofibril structure (Figure 5.4, G-I and K-M). This suggests that all three proteins lost their myofibril integrity upon the ischemic stress.
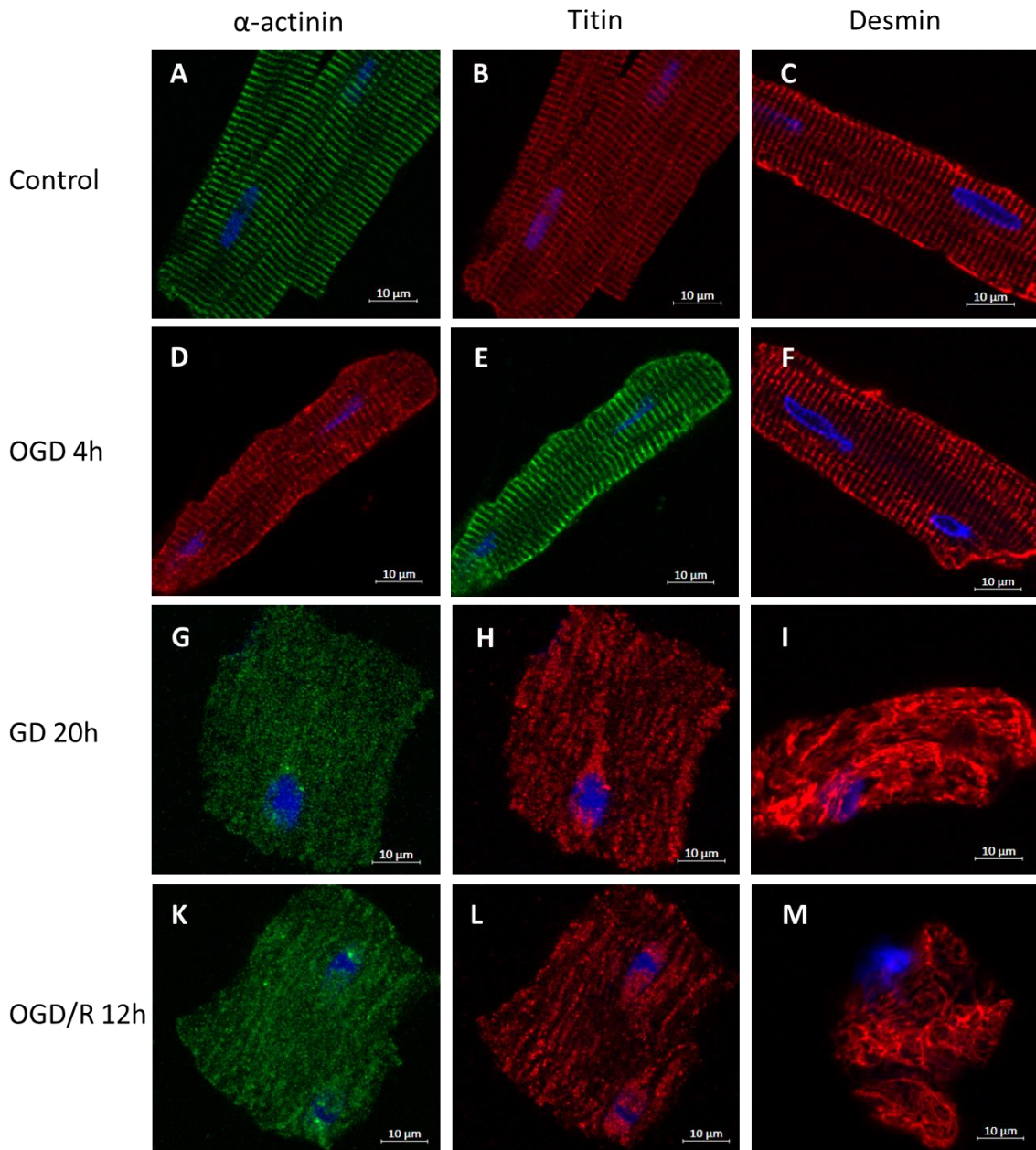
Figure 5.4 – Visualization of α-actinin, titin, and desmin in adult rat cardiomyocytes by fluorescence imaging. Cells were subjected to A-C) no stress, D-F) OGD, G-I) GD, and K-M) OGD/R. Cells were fixed and immunostained with the appropriate antibody.

5.3.3 Desmin C332S recovers myofibril integrity upon oxidative stress in HL-1 mouse cardiomyocyte cells

Desmin WT and C332S mutant were expressed in the HL-1 mouse cardiomyocyte cell line. Cells were then subjected to stress, GD or OGD/OGF. Cells were then immunostained with FLAG antibody and imaged using a confocal microscope. In control samples, both WT and C332S mutant overexpressed cells have shown an intermediate filament network spanning from the nucleus to the periphery of the cells (Figure 5.5, A and B). However, under stress, desmin WT has shown the degeneration of the cell structure and localization of desmin intermediate filaments to the nucleus (Figure 5.5, C and E). Interestingly, upon the stress, the desmin C332S mutant was still able to maintain its intermediate filament network spanning from the nucleus to the cell periphery (Figure 5.5, D and F). This data suggests that glutathionylation at C332 may interfere with the filament elongation of desmin.
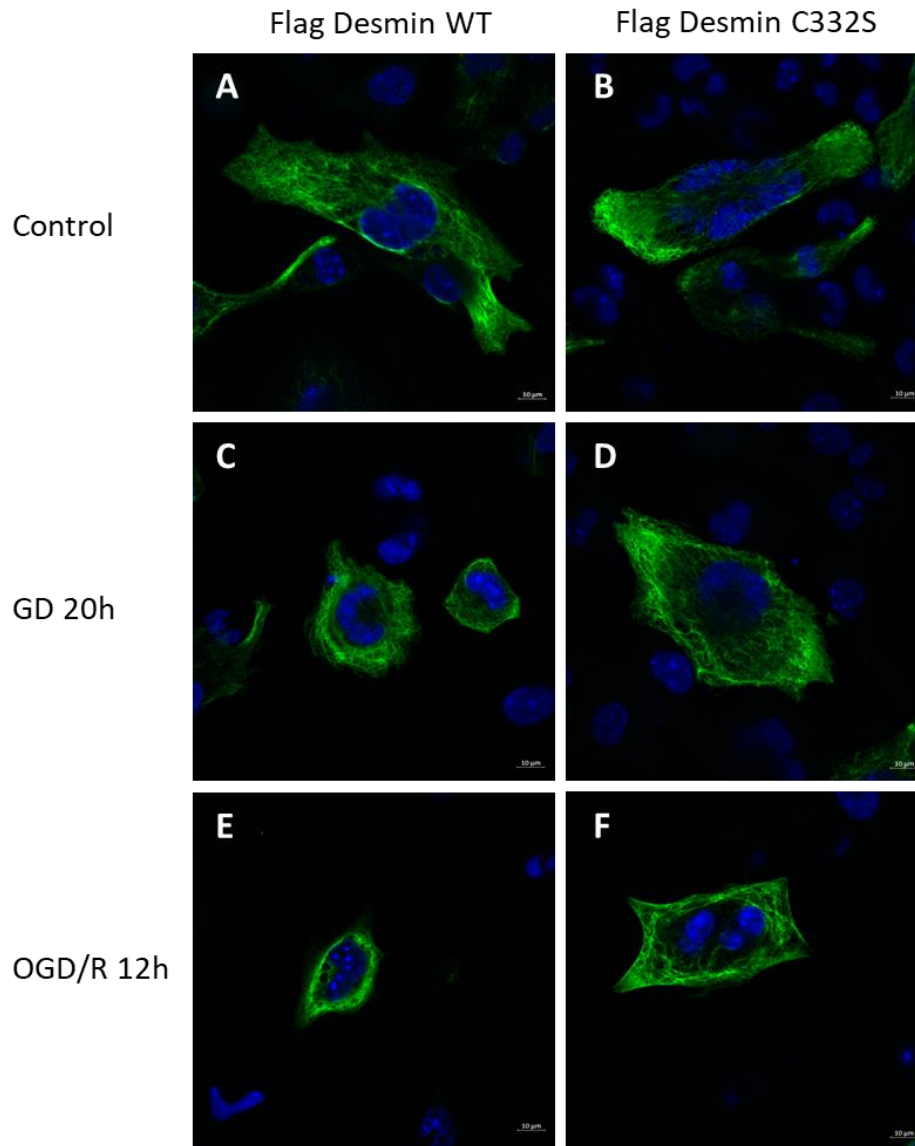
Figure 5.5 - Visualization of desmin WT and C332S mutant in HL-1 cells by fluorescence imaging. Cells overexpressing desmin WT and C332S mutant were subjected to A-B) no stress, C-D) GD, and E-F) OGD/R. Cells were fixed and immunostained with FLAG antibody.

5.3.4 Desmin C332S recovers myofibril integrity upon oxidative stress in rat neonatal cardiomyocytes

Desmin WT and C332S mutant were expressed using mRNA in rat neonatal cardiomyocytes. Cells were subjected to stress or GD for 20 h. Then the cells were immunostained with FLAG antibody and imaged using a confocal microscope. Under the control condition, where no stress was applied, both WT and C332S mutant of desmin have shown a parallel and striated myofibril structure (Figure 5.6, A and B). In contrast, upon the induction of stress by GD, WT desmin has shown a disoriented and misaligned myofibril structure. This suggests that desmin lose its myofibril integrity upon subjecting to stress. (Figure 5.6, C). Importantly, the desmin mutant was still able to maintain its parallel and striated myofibril structure under both stress conditions (Figure 5.6, D). This data further validates our hypothesis that bulky glutathione modification at C332 may interfere with the desmin filament formation and elongation.

Flag Desmin WT   Flag Desmin C332S
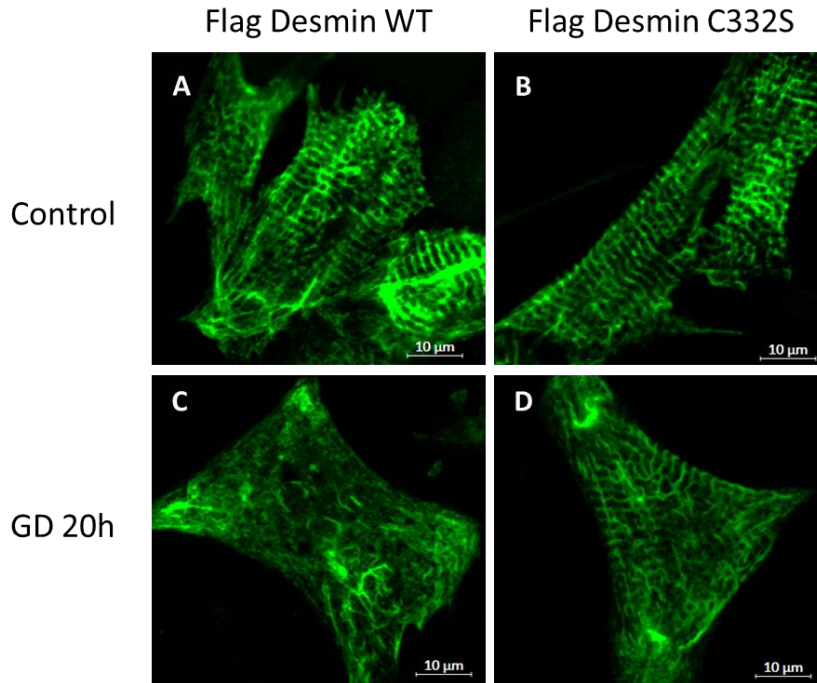
Figure 5.6 - Visualization of desmin WT and C332S mutant in rat neonatal cardiomyocytes by fluorescence imaging. Cells overexpressing desmin WT and C332S mutant were subjected to A-B) no stress, and C-D) GD for 20 h. Cells were fixed and immunostained with FLAG antibody.

5.4 Discussion

Desmin is a type III IF, which is important in maintaining the structural and mechanical integrity of the sarcomere. Desmin is mainly localized in the periphery of the Z-line, but it also spans to other cellular organelles such as mitochondria and nucleus. Mutations and PTMs in desmin are well known to cause desminopathy. From our previous proteomic data, we found that desmin undergoes glutathionylation under stress. Similar to type III Ifs, desmin has only one cysteine, C332. Desmin protein has three major domains: N-terminus head domain, rod domain, and C-terminus tail domain. The Rod

domain is involved in the desmin filament assembly, and C332 is located in the rod domain. C332 of desmin is conserved with type III IFs such as vimentin (C328).

Previous studies have shown that glutathionylation of C328 inhibits the filament elongation of vimentin. Therefore, glutathionylation at C332 of desmin is expected to result in a similar outcome. We hypothesize that a bulky glutathionylation modification at the rod domain may interfere with the desmin filament formation andinhibit the filament elongation as seen in vimentin. Therefore, using adult and neonatal rat cardiomyocytes and HL-1 mouse cardiomyocytes, we investigated how desmin responds to different ischemic stress conditions. We have observed that endogenous and overexpressed WT desmin loses its myofibril integrity upon stress induction by GD and OGD/OGF. Interestingly C332S mutant of desmin maintained its parallel and striated myofibril organization under GD and OGD/OGF, supporting our hypothesis that glutathionylation at C332 may interfere with the desmin filament assembly and elongation.

5.5 Methods

5.5.1   Adult rat cardiomyocyte isolation

Adult and neonatal rat cardiomyocytes were isolated according to a method described previously.[193] Rats and neonates (1-day old, Sprague Dawley) were used under the guidelines of protocols approved by the Wayne State University Animal Care and Use Committee. The heart was isolated after euthanasia and rinsed with ice-cold PBS. The heart was digested in collagenase buffer [3 mL; 130 mM NaCl, 5 mM KCl, 0.5 mM

NaH$_2$PO$_4$, 10 mM HEPES, 10 mM glucose, 10 mM 2,3-butanedione monoxime (BDM), 10 mM Taurine, 1 mM MgCl$_2$, 0.5 mg/mL collagenase 2, 0.5 mg/mL collagenase 4, and 0.05 mg/mL protease XIV] by teasing apart and triturating using a 1 mL pipette with wide-bore tip. Then the stop buffer (5 mL; 130 mM NaCl, 1 mM MgCl2, 0.5 mM NaH2PO4, 5 mM KCl, 10 mM BDM, 10 mM HEPES, 10 mM Taurine, 10 mM glucose, and 5% FBS) was added to the tissue suspension to inhibit enzymatic digestion and pipetted for another 2 minutes. Then the cell suspension was transferred to a 50 mL falcon tube, and the tube was stored on its side to prevent cells from clumping. After 2 h, the cell suspension was passed through a strainer (100 μM pore size) to remove undigested tissue debris. The strainer was washed with stop buffer (5 mL), and cells were allowed to settle by gravity for 20 minutes. Cells were then resuspended sequentially in three calcium reintroduction buffers (0.34, 0.68 and 1.02 mM Ca^{2+}) before plating. The final myocyte pellet was resuspended in culture medium [2 mL; M199 (Sigma), BSA 0.1%, BDM 10 mM, and penicillin/streptomycin 1x]. Cells were counted using a hemocytometer. Cells (~50,000 cells/ well of 6 well plate) were plated in 6 well plates pre-coated with laminin (5 μg/mL laminin in PBS) containing plating media (2 mL; M199, FBS 5%, BDM 10 mM, and penicillin/streptomycin 1x). After 1 h, cells were washed with culture medium and incubated with culture medium.

5.5.2   HL-1 cell culture and induction of glutathionylation

The general procedure is shown in Chapter 3, section 3.5.1

5.5.3 Lipofectamine transfection

The general lipofectamine transfection procedure is shown in Chapter 2, section 2.5.8.

5.5.4 Desmin WT and desmin C332S mutant mRNA synthesis

5.5.4.1 Polymerase Chain Reaction (PCR)

PCR template for the mRNA synthesis was generated by amplifying desmin WT and desmin C332S genes from pCMV6-entry vector. 5'- GCT CGT TTA GTG AAC CGT CAG AA -3' and 5'- G TTC AGG AAA CAG CTA TGA CCG C -3' were used as forward and reverse primers, respectively. General PCR procedure from Chapter 3 section 3.5.2 was used for the amplification.

5.5.4.2 mRNA synthesis

mRNA synthesis was carried out using the mMESSAGE mMACHINE T7 ULTRA Transcription Kit (Invitrogen, AM1345) according to the manufacturer's instructions. First, a capped transcription reaction was assembled at room temperature by mixing 2x NTP (10 µL; a buffer solution containing ATP 15 mM, CTP 15 mM, UTP 15 mM, and GTP 15 mM), 10x T7 reaction buffer (2 µL), template DNA (0.2 µg) and T7 enzyme mix (2 µL). The reaction volume was adjusted to 20 µL by adding nuclease-free water and incubated for 2 h at 37°C.

Poly A tailing reaction was then assembled by mixing the capped transcription reaction (20 µL), nuclease-free water (36 µL), 5x E. coli Poly(A) Polymerase I (E-PAP) buffer

(20 µL), 25 mM MnCl$_2$ (10 µL), and ATP solution (10 µL). The reaction volume was adjusted to 100 µL by adding E-PAP (4 µL) and incubated at 37°C for 45 minutes.

Finally, mRNA was recovered by phenol/chloroform extraction. The tailing reaction was stopped by adding ammonium acetate stop solution (10 µL). The reaction mixture was extracted first with an equal volume of phenol/chloroform and then with an equal volume of chloroform. The aqueous phase was recovered and transferred to a new tube. mRNA was precipitated by adding isopropanol (1x volume) and incubating at -20°C for 15 minutes. mRNA was pelleted by centrifuging at 4°C for 15 minutes. The supernatant was removed, and mRNA was resuspended in nuclease-free water.

5.5.5   mRNA transfection

Neonatal rat cardiomyocytes were transfected with desmin WT and C332S mutant mRNA using lipofectamine MessengerMAX reagent (Invitrogen, LMRNA001) at 24 h after plating. Cell culture media was removed and replaced with Opti-MEM medium (2 mL/well). In a sterile Eppendorf tube, lipofectamine MessengerMAX (3.75 µL/well) was diluted in Opti-MEM medium (125 µL) and incubated for 10 minutes at room temperature. In a separate sterile Eppendorf tube, mRNA (2.5 µg/well) was diluted in Opti-MEM medium (125 µL). Diluted mRNA mixture was added to the diluted lipofectamine MessengerMAX reagent and incubated for 5 minutes at room temperature. After 5 minutes, the diluted mRNA-lipofectamine mixture was added to the cells and incubated at 37°C in the incubator. After 6 h, the medium containing mRNA and

lipofectamine was replaced by a fresh complete DMEM medium (3 mL) and incubated for 18 h.

5.5.6 Induction of stress

In adult and neonatal rat cardiomyocytes, stress was induced by applying GD and OGD/OGF. After plating the cells, cells were subjected to serum starvation for 1 h. For GD, cells were maintained in media without glucose for 20 h at 37°C in a humidified chamber. After 20 h, the cells were used for immunostaining. For OGD/OGF, cells were maintained in media without glucose for 4 h in a hypoxia chamber containing 1% O_2 at 37°C. Cells were then reoxygenated with glucose (25 mM) and palmitate (1 mM) for another 12 h at 37°C in a humidified chamber. After 12 h, cells were used for immunostaining.

5.5.7 Immunostaining and Imaging

After inducing stress, cells were washed with PBS and fixed with 4% paraformaldehyde at room temperature for 10 minutes. Cells were washed with PBS (3x with 5 minutes incubation) and incubated with permeabilization buffer (0.1% Triton x-100 in 1x PBS) for 15 minutes at room temperature. Cells were then washed with PBS (3x with 5 minutes incubation) and blocked for 30 minutes at room temperature using a blocking buffer [3% BSA in PBST, (0.1% Tween-20 in 1x PBS)]. After blocking, cells were incubated with the primary antibody in blocking buffer overnight at 4°C. Primary antibodies include mouse α-actinin antibody (1:500; Abcam), rabbit titin antibody (Novus biologicals, Cat# NBP 1-8807), rabbit desmin antibody (1:1000; Abcam) and mouse FLAG antibody (1:1000; Sigma). Cells were washed with PBS (3x with 5 minutes incubation), incubated with

secondary antibodies [anti-mouse Alexa fluor 488 (Invitrogen, A11001) or anti-rabbit Alexa fluor 555 (Invitrogen, A27039)] for 1 h at room temperature and analyzed using the confocal microscope (Zeiss LSM 780).

CHAPTER 6: SUMMARY

Cardiovascular diseases are the number one cause of death in the United States. A constant supply of oxygen and nutrient is essential for the survival of the heart. However, atherosclerosis can limit the blood flow to the heart tissue causing oxidative stress. Under oxidative stress, proteins can undergo different reversible and irreversible post translational modifications. Especially, the cysteine residues can undergo oxidative post-translational modifications such as glutathionylation. Glutathionylation is an important regulatory reversible thiol oxidation. Identification and quantification of glutathionylated proteins is important for the understanding of the molecular mechanisms behind initiation and progression of many diseases. Our lab previously developed a click chemistry-based method to detect and identify glutathionylation in cells by synthesizing clickable-glutathione.

We have established a mass spectrometry-based strategy coupled with the clickable glutathione approach in which two azido-Ala derivatives with isotopic mass difference were used to metabolically synthesize isotopically labelled clickable glutathione for the identification and quantification of glutathionylated proteins. We applied this isotopically labeled clickable glutathione approach on HL-1 cardiomyocyte cells to identify and quantify 1398 glutathionylated peptides upon the addition of H_2O_2. Then we validated the glutathionylation of two identified proteins: desmin and α-actinin with their specific cysteine residues. Since this mass spectrometry based clickable glutathione approach enables the identification and quantification of glutathionylated

cysteines, this approach can be applied for the profiling of hyper reactive or functional cysteines in the proteins.

Ischemia or ischemic reperfusion is well-known to contribute to heart diseases. During ischemia and reperfusion, a flux of nutrients and oxygen to cardiomyocytes is altered, which causes a burst of ROS from mitochondria and other enzymes. Elevated levels of ROS can cause oxidative modifications of cardiac proteins such as protein glutathionylation. Despite previous extensive studies, proteomic identification of glutathionylated proteins in cardiomyocytes under altered levels of nutrients and oxygen has been relatively limited. We have applied our clickable glutathione to a HL-1 cardiomyocyte cell line under metabolic alterations of glucose, oxygen, and fatty acids. We found that glucose is important for maintaining a redox homeostasis, while fatty acid oxidation is one of major factors that induce a high level of glutathionylation during reoxygenation. We have applied our isotopic clickable glutathione approach on HL-1 cells upon addition of fatty acids during reoxygenation, identifying and quantifying 248 proteins undergoing glutathionylation. We carried out DAVID GO and cluster analysis on these proteins and identified major clusters of proteins are sarcomere and mitochondria associated proteins. This suggests that glutathionylation on these proteins may be associated with the altered cardiac muscle integrity and impaired mitochondrial activity during ischemia reperfusion. We also validated the glutathionylation of two identified proteins: BAG3 and desmin with their specific cysteine residues under OGD/OGF condition. Finally, we identified 18 glutathionylated cysteines whose genetic variants are

associated with muscular disorders, suggesting glutathionylations of these cysteines have the potential to alter their functions. We can further investigate the functional significance of the glutathionylation of identified proteins for their association with diseases such as cardiomyopathy and mitochondrial dysfunction.

Over the years, several methods have been developed to characterize protein glutathionylation. Despite the significant advances in the field for developing these methods to identify and relatively quantify glutathionylation, methods for the direct quantification of glutathionylation compared to the unmodified cysteines have been limited. We developed a proteomic approach for the direct quantification of glutathionylated cysteines compared to the unmodified cysteines by designing and synthesizing an electrophilic clickable glutathione reagent (L-N$_3$-GS-SPy) that can react with unmodified cysteine to form the same structure as glutathionylation. Using purified proteins, we validated that the L-N$_3$-GS-Spy can be used to block unreacted cysteines. We have applied this quantification approach on C2C12 mouse skeletal muscle cell line and identified 1518 glutathionylated cysteines upon the addition of H$_2$O$_2$. We identified additional 1174 cysteines that were blocked by L-N$_3$-GS-Spy. Finally, we validated the glutathionylation and sensitivity to undergo glutathionylation of one of the identified proteins from our proteomic data (CTNND1). Since this is a direct approach for the quantification of the glutathionylated cysteines compared to their unmodified portion, this approach can be used for the profiling of proteins that are susceptible to undergo glutathionylation depending on their sensitivity.

Desmin is the major component in intermediate filaments that plays a key role in maintaining structural and mechanical integrity of the sarcomere. From our proteomic analyses, we identified that desmin is undergoing glutathionylation under ischemic stress. Using adult and neonatal cardiomyocytes, we further investigate the effect of glutathionylation on myofibril integrity of desmin. We found that desmin lose its myofibril integrity upon oxidative stress in both adult and neonatal cardiomyocytes. Interestingly cysteine mutant of desmin recovers myofibril integrity in neonatal cardiomyocytes, suggesting that bulky glutathione modification at the rod domain may interfere with the desmin filament assembly. Desmin wild-type and mutant knock in cell lines can be generated using CRISPR-Cas9 gene editing technology. Using the developed cell lines further functional studies such as cell viability, myofibril integrity, and biochemical stability can be carried out under different ischemic stress conditions.

APPENDIX A – CHAPTER 2 SUPPORTING TABLE

Table A.2.1 - List of glutathionylated sarcomeric proteins with $R_{H/L}$ values

[a]Glutathionylated peptide – all cysteine numbers are from mouse

[b]NL – Light labeled peptides were not identified

Accession #	Name	Glutathionylated peptide[a]	$R_{H/L}$ (1:1)	$R_{H/L}$[b] (1:0)
ACTN1_MOUSE	actinin, alpha 1	MVSDINNAWGC$_{370}$*LEQAEK	0.95	55.6
		IC$_{480}$*DQWDNLGALTQK	0.85	24.0
		IDQLEC$_{690}$*DHQLIQEALIFDNK	0.85	28.1
ACTN4_MOUSE	actinin alpha 4	C$_{352}$*QLEINFNTLQTK	1.07	3.21
		IC$_{500}$*DQWDNLGSLTHSR	0.99	18.2
BAG3_MOUSE	BAG family molecular chaperone regulator 3	SQSPAASDC$_{185}$*SSSSSSASLPSSGR	0.64	12.8
		SGTPVHC$_{295}$*PSPIR	0.66	4.90
		VSSAPIPC$_{378}$*PSPSPAPSAVPSPPK	0.61	NL
CAPZB_MOUSE	capping protein (actin filament) muscle Z-line, beta	NLSDLIDLVPSLC$_{36}$*EDLLSSVDQPLK	1.33	13.2
		GC$_{147}$*WDSIHVVEVQEK	1.16	16.2
		DETVSDC$_{206}$*SPHIANIGR	0.67	29.0
CSRP3_MOUSE	cysteine and glycine-rich protein 3	TVYHAEEIQC$_{25}$*NGR	0.96	18.0
DESM_MOUSE	desmin	HQIQSYTC$_{332}$*EIDALKGTNDSLMR	0.89	30.5
DYST_MOUSE	dystonin	AC$_{5144}$*MQTFLK	0.93	NL
FLNA_MOUSE	filamin, alpha	C$_8$*GQSAAVASPGGSIDSR	0.72	4.89
		VQVQDNEGC$_{717}$*SVEATVK	1.04	99.0
		YTPC$_{441}$*GAGSYTIMVLFADQATPTSPIR	1.18	NL
		AHVAPC$_{1157}$*FDASK	0.75	22.6
		VANPSGNLTDTYVQDC$_{1312}$*GDGTYK	1.20	76.9
FLNC_MOUSE	filamin C, gamma	LYAQDADGC$_{713}$*PIDIK	0.87	33.7
		VC$_{1067}$*AYGPGLK	0.99	108.7
		VGVTEGC$_{1349}$*DPTR	0.81	19.2
		TPC$_{2680}$*EEVYVK	0.75	35.7
MYPC3_MOUSE	myosin binding protein C, cardiac	LTIDDVTPADEADYSFVPEGFAC$_{619}$*NLSAK	1.19	82.0
		LLC$_{715}$*ETEGR	0.67	49.5
MYL4_MOUSE	myosin, light polypeptide 4	ITYGQC$_{74}$*GDVLR	0.69	2.61
		MSEAEVEQLLSGQEADANGC$_{180}$*INYEAFVK	1.07	15.5
MLRA_MOUSE	myosin regulatory light chain 2, atrial	EAFSC$_{43}$*IDQNR	0.93	19.8

OBSL1_MOUSE	Obscurin-like protein 1	LEVEALPLQMC$_{1719}$*R	0.84	7.06
PDLI3_MOUSE	PDZ and LIM domain protein 3	AASYQLC$_{77}$*LK	1.10	46.2
PDLI5_MOUSE	PDZ and LIM domain protein 5	AC$_{73}$*TGSLNMTLQR	0.90	22.4
PYGM_MOUSE	muscle glycogen phosphorylase	IC$_{172}$*GGWQMEEADDWLR	0.81	156.3
RYR2_MOUSE	ryanodine receptor 2	C$_{2054}$*SSLQQLISETMVR	0.88	NL
SPTN1_MOUSE	spectrin alpha, non-erythrocytic 1	ALC$_{315}$*AEADR TYLLDGSC$_{2233}$*MVEESGTLESQLEATK	0.91 0.58	24.2 NL
CHIP_MOUSE	STIP1 homology and U-Box containing protein 1	AQQAC$_{200}$*IEAK	0.77	6.60
SYNE2_MOUSE	Nesprin-2	DSASETYC$_{328}$*NK TAAC$_{6148}$*PNSSEVLYTNAK	0.87 0.96	NL 13.7
TITIN_MOUSE	Titin	LSVTVTGC$_{3535}$*PKPK TSTEMSQEEAEGTLADLC$_{4250}$*PAVLK LDQAGEVLYQAC$_{13260}$*NAITTAILTVK FGC$_{17066}$*GPPVEIGPILAVDPLGPPTSPER GC$_{19461}$*EYVFR MVC$_{29497}$*SSVAR	0.84 0.99 0.86 1.41 1.05 0.94	20.6 15.7 8.64 NL 32.1 21.8

APPENDIX B – CHAPTER 3 SUPPORTING TABLES

Table B.3.1 - List of glutathionylated sarcomeric proteins

NL – Light labeled peptides were not found

Accession #	Protein Name	Peptide	E1 $R_{H/L}$	E2 $R_{H/L}$
P05064; P05063	Fructose-bisphosphate aldolase A;Fructose-bisphosphate aldolase C	CQYVTEK	0.85	0.56
P05064	Fructose-bisphosphate aldolase A	ALANSLACQGK	0.88	2.25
P09541; P09542	Myosin light chain 4;Myosin light chain 3	ITYGQCGDVLR	0.74	3.96
Q62261; P15508	Spectrin beta chain, non-erythrocytic 1;Spectrin beta chain, erythrocytic	IHCLENVDK	0.99	4.14
O70468	Myosin-binding protein C, cardiac-type	LLCETEGR	1.36	4.24
P16546	Spectrin alpha chain, non-erythrocytic 1	ALCAEADR	1.01	4.93
		GACAGSEDAVK	0.62	5.14
P63001; P60764	Ras-related C3 botulinum toxin substrate 1;Ras-related C3 botulinum toxin substrate 3	AVLCPPPVK	0.86	5.33
Q9WUD1	STIP1 homology and U box-containing protein 1	AQQACIEAK	1.46	5.67
Q9D8E6	60S ribosomal protein L4	SGQGAFGNMCR	1.24	6.17
Q8BTM8	Filamin-A	VQVQDNEGCSVEATVK	1.40	6.27
		CSGPGLSPGMVR	0.97	1.97
		AHVAPCFDASK	1.66	6.57
		VANPSGNLTDTYVQDCGDGTYK	1.13	7.21
P47757	F-actin-capping protein subunit beta	DETVSDCSPHIANIGR	0.92	7.17
Q8VHX6	Filamin-C	VCAYGPGLK	0.96	NL
		LYAQDADGCPIDIK	0.86	8.92
		VGVTEGCDPTR	0.52	6.52
Q60605	Myosin light polypeptide 6	CDFTEDQTAEFK	1.60	9.05
Q7TPR4	Alpha-actinin-1	MVSDINNAWGCLEQAEK	0.95	9.17
Q8VDD5	Myosin-9	LEEDQIIMEDQNCK	0.94	9.62
Q9JLV1	BAG family molecular chaperone regulator 3	SQSPAASDCSSSSSSASLPSSGR	0.83	9.66
O88342	WD repeat-containing protein 1	VCALGESK	0.70	10.8
Q60598	Src substrate cortactin	HCSQVDSVR	0.75	11.1

Q60598	Src substrate cortactin	CALGWDHQEK	0.81	19.0
P31001	Desmin	HQIQSYTCEIDALK	0.83	NL
Q99JY9	Actin-related protein 3	YSYVCPDLVK	0.76	NL
Q80X90	Filamin-B	VAVTEGCQPSR	2.02	NL

Table B.3.2 - List of glutathionylated proteins associated with mitochondria

NL – Light labeled peptides were not found

Accession #	Protein Name	Peptide	E1 $R_{H/L}$	E2 $R_{H/L}$
P05064; P05063	Fructose-bisphosphate aldolase A;Fructose-bisphosphate aldolase C	CQYVTEK	0.85	0.56
P05064	Fructose-bisphosphate aldolase A	ALANSLACQGK	0.88	2.25
Q02053; P31254	Ubiquitin-like modifier-activating enzyme 1;Ubiquitin-like modifier-activating enzyme 1 Y	SIPICTLK	0.90	2.26
P14824	Annexin A6	QEICQNYK	0.75	2.33
		GTVCAANDFNPDADAK	0.75	8.94
		ALLALCGGED	0.93	NL
Q9Z110	Delta-1-pyrroline-5-carboxylate synthase;Glutamate 5-kinase;Gamma-glutamyl phosphate reductase	GDECGLALGR	0.95	2.67
P14152	Malate dehydrogenase, cytoplasmic	VIVVGNPANTNCLTASK	0.85	2.73
Q9DCX2	ATP synthase subunit d, mitochondrial	SCAEFVSGSQLR	0.63	2.88
Q99KR7; Q9CR16; Q9ERU9	Peptidyl-prolyl cis-trans isomerase F, mitochondrial;Peptidyl-prolyl cis-trans isomerase D;E3 SUMO-protein ligase RanBP2	ALCTGEK	0.88	2.97
P06151; P00342; P16125	L-lactate dehydrogenase A chain;L-lactate dehydrogenase C chain;L-lactate dehydrogenase B chain	VIGSGCNLDSAR	0.80	3.00
P53702	Cytochrome c-type heme lyase	AYDYVECPVTGAR	0.57	3.10
Q8BTX9	Inactive hydroxysteroid dehydrogenase-like protein 1	EALSCQA	1.20	3.13
P30416	Peptidyl-prolyl cis-trans isomerase FKBP4;Peptidyl-prolyl cis-trans isomerase FKBP4, N-terminally processed	TQLAVCQQR	0.85	3.47
P08249	Malate dehydrogenase, mitochondrial	EGVVECSFVQSK	1.20	3.62
P62908	40S ribosomal protein S3	GCEVVVSGK	1.17	4.09
Q91VD9	NADH-ubiquinone oxidoreductase 75 kDa subunit, mitochondrial	AVTEGAQAVEEPSIC	1.13	4.94

Q9QUI0; Q62159	Transforming protein RhoA;Rho-related GTP-binding protein RhoC	LVIVGDGACGK	0.86	5.14
Q60930	Voltage-dependent anion-selective channel protein 2	SCSGVEFSTSGSSNTDTGK	0.83	5.55
		WCEYGLTFTEK	1.38	6.10
P51881	ADP/ATP translocase 2;ADP/ATP translocase 2, N-terminally processed	GLGDCLVK	0.51	5.73
Q9Z1Q9	Valine--tRNA ligase	ICLQPPPSSR	1.05	5.85
Q61035	Histidine--tRNA ligase, cytoplasmic	TNQPLSTC	0.86	5.98
P16858; Q64467	Glyceraldehyde-3-phosphate dehydrogenase;Glyceraldehyde-3-phosphate dehydrogenase, testis-specific	VPTPNVSVVDLTCR	0.74	6.15
P62908	40S ribosomal protein S3	GLCAIAQAESLR	0.61	6.16
P48962	ADP/ATP translocase 1	EFNGLGDCLTK	0.80	6.69
Q922Q8	Leucine-rich repeat-containing protein 59	ATVLDLSCNK	0.83	6.84
Q68FD5	Clathrin heavy chain 1	IHEGCEEPATHNALAK	0.67	6.85
		VIQCFAETGQVQK	0.62	NL
Q60931	Voltage-dependent anion-selective channel protein 3	VCNYGLTFTQK	0.65	7.14
P16858	Glyceraldehyde-3-phosphate dehydrogenase	AAICSGK	0.76	7.45
Q60597	2-oxoglutarate dehydrogenase, mitochondrial	AEQFYCGDTEGK	0.62	8.11
Q8C0I1	Alkyldihydroxyacetonephosphate synthase, peroxisomal	IVNLACK	0.94	9.61
P06151	L-lactate dehydrogenase A chain	DYCVTANSK	0.81	9.67
Q9QUH0	Glutaredoxin-1	AQEFVNCK	0.93	10.5
O08553	Dihydropyrimidinase-related protein 2	GLYDGPVCEVSVTPK	0.95	10.7
Q9CZB0	Succinate dehydrogenase cytochrome b560 subunit, mitochondrial	SLCLGPTLIYSAK	1.36	15.4
Q91ZA3	Propionyl-CoA carboxylase alpha chain, mitochondrial	MADEAVCVGPAPTSK	0.83	18.8
Q8K2B3	Succinate dehydrogenase [ubiquinone] flavoprotein subunit, mitochondrial	TLNEADCATVPPAIR	0.67	NL
Q99KI0	Aconitate hydratase, mitochondrial	VGLIGSCTNSSYEDMGR	0.81	NL
Q9Z1Q5	Chloride intracellular channel protein 1	EEFASTCPDDEEIELAYEQVAR	1.00	NL

Q9DCS3	Trans-2-enoyl-CoA reductase, mitochondrial	LALNCVGGK	0.73	NL
Q9QUR7	Peptidyl-prolyl cis-trans isomerase NIMA-interacting 1	SGEEDFESLASQFSDCSSAK	1.36	NL
Q9Z2I9	Succinyl-CoA ligase [ADP-forming] subunit beta, mitochondrial	ILACDDLDEAAK	0.94	NL
Q62351	Transferrin receptor protein 1	WNIDSSCK	1.48	NL

Table B.3.3 - List of glutathionylated proteins associated with cardiomyopathy

NL – Light labeled peptides were not found

Accession #	Protein Name	Peptide	E1 $R_{H/L}$	E2 $R_{H/L}$
P26039	Talin-1	CTQDLGNSTK	0.77	1.55
		AGALQCSPSDVYTK	1.12	5.36
Q8BTM8	Filamin-A	VQVQDNEGCSVEATVK	1.40	6.27
		CSGPGLSPGMVR	0.97	1.97
		AHVAPCFDASK	1.66	6.57
		VANPSGNLTDTYVQDCGDGTYK	1.13	7.21
P14824	Annexin A6	GTVCAANDFNPDADAK	0.75	8.94
		QEICQNYK	0.75	2.33
		ALLALCGGED	0.93	NL
P38647	Stress-70 protein, mitochondrial	TIAPCQK	1.06	2.42
O55143	Sarcoplasmic/endoplasmic reticulum calcium ATPase 2	ANACNSVIK	0.89	2.56
P97372	Proteasome activator complex subunit 2	AKPCGVR	1.15	4.21
		CGYLPGNEK	0.80	2.71
Q8CGC7	Bifunctional glutamate/proline--tRNA ligase;Glutamate--tRNA ligase;Proline--tRNA ligase	SCQFVAVR	0.94	2.79
		VACQGEVVR	0.84	2.87
Q99KR7; Q9CR16; Q9ERU9	Peptidyl-prolyl cis-trans isomerase F, mitochondrial;Peptidyl-prolyl cis-trans isomerase D;E3 SUMO-protein ligase RanBP2	ALCTGEK	0.88	2.97
P06151; P00342; P16125	L-lactate dehydrogenase A chain;L-lactate dehydrogenase C chain;L-lactate dehydrogenase B chain	VIGSGCNLDSAR	0.80	3.00
P17742	Peptidyl-prolyl cis-trans isomerase A;Peptidyl-prolyl cis-trans isomerase A, N-terminally processed	IIPGFMCQGGDFTR	0.98	4.72
		ITISDCGQL	0.95	3.03
Q09143	High affinity cationic amino acid transporter 1	TPDSNLDQCK	0.98	3.20
P17182	Alpha-enolase	VNQIGSVTESLQACK	0.84	3.35

Q6PHZ2	Calcium/calmodulin-dependent protein kinase type II subunit delta	ASTTTCTR	1.12	3.58
P09411	Phosphoglycerate kinase 1	FCLDNGAK	0.83	3.71
Q61990; P57722; P60335	Poly(rC)-binding protein 2;Poly(rC)-binding protein 3;Poly(rC)-binding protein 1	INISEGNCPER	0.71	3.90
Q6PDM2	Serine/arginine-rich splicing factor 1	EAGDVCYADVYR	0.58	3.90
P09541; P09542	Myosin light chain 4;Myosin light chain 3	ITYGQCGDVLR	0.74	3.96
P99024	Tubulin beta-5 chain	NMMAACDPR	0.71	4.48
		TAVCDIPPR	0.75	4.04
Q60876	Eukaryotic translation initiation factor 4E-binding protein 1	SAGSSCSQTPSR	1.09	4.22
O70468	Myosin-binding protein C, cardiac-type	LLCETEGR	1.36	4.24
P14211	Calreticulin	HEQNIDCGGGYVK	0.98	4.60
P48678	Prelamin-A/C;Lamin-A/C	AQNTWGCGSSLR	0.88	4.71
P10639	Thioredoxin	CMPTFQFYK	0.83	4.86
P16546	Spectrin alpha chain, non-erythrocytic 1	GACAGSEDAVK	0.62	5.14
		ALCAEADR	1.01	4.93
Q91VD9	NADH-ubiquinone oxidoreductase 75 kDa subunit, mitochondrial	AVTEGAQAVEEPSIC	1.13	4.94
Q9QUI0; Q62159	Transforming protein RhoA;Rho-related GTP-binding protein RhoC	LVIVGDGACGK	0.86	5.14
P00493	Hypoxanthine-guanine phosphoribosyltransferase	SYCNDQSTGDIK	0.79	5.15
P18760	Cofilin-1	AVLFCLSEDK	0.69	5.25
P29533	Vascular cell adhesion protein 1	QAQLQDAGIYECESK	0.93	5.29
P63001; P60764	Ras-related C3 botulinum toxin substrate 1;Ras-related C3 botulinum toxin substrate 3	AVLCPPPVK	0.86	5.33
Q60930	Voltage-dependent anion-selective channel protein 2	WCEYGLTFTEK	1.38	6.10
		SCSGVEFSTSGSSNTDTGK	0.83	5.55
Q9WUD1	STIP1 homology and U box-containing protein 1	AQQACIEAK	1.46	5.67

P51881	ADP/ATP translocase 2;ADP/ATP translocase 2, N-terminally processed	GLGDCLVK	0.51	5.73
P16858; Q64467	Glyceraldehyde-3-phosphate dehydrogenase;Glyceraldehyde-3-phosphate dehydrogenase, testis-specific	VPTPNVSVVDLTCR	0.74	6.15
P45376	Aldose reductase	HIDCAQVYQNEK	0.68	6.28
Q8BGQ7	Alanine--tRNA ligase, cytoplasmic	IQSLGDCK	1.28	6.50
Q8VHX6	Filamin-C	LYAQDADGCPIDIK	0.86	8.92
		VGVTEGCDPTR	0.52	6.52
		VCAYGPGLK	0.96	NL
P48962	ADP/ATP translocase 1	EFNGLGDCLTK	0.80	6.69
P16858	Glyceraldehyde-3-phosphate dehydrogenase	AAICSGK	0.76	7.45
Q01853	Transitional endoplasmic reticulum ATPase	LGDVISIQPCPDVK	0.81	7.46
P09411	Phosphoglycerate kinase 1	TGQATVASGIPAGWMGLDCGTESSK	0.82	7.52
Q61029	Lamina-associated polypeptide 2, isoforms beta/delta/epsilon/gamma	EMFPYEASTPTGISASCR	1.32	7.78
P60710	Actin, cytoplasmic 1;Actin, cytoplasmic 1, N-terminally processed	DDDIAALVVDNGSGMCK	1.24	8.13
P07356	Annexin A2	SVCHLQK	0.95	8.14
P58252	Elongation factor 2	EGALCEENMR	0.84	NL
		STLTDSLVCK	1.07	8.45
Q60605	Myosin light polypeptide 6	CDFTEDQTAEFK	1.60	9.05
Q7TPR4	Alpha-actinin-1	MVSDINNAWGCLEQAEK	0.95	9.17
Q8VDD5	Myosin-9	LEEDQIIMEDQNCK	0.94	9.62
Q9JLV1	BAG family molecular chaperone regulator 3	SQSPAASDCSSSSSSASLPSSGR	0.83	9.66
P06151	L-lactate dehydrogenase A chain	DYCVTANSK	0.81	9.67
Q9QUH0	Glutaredoxin-1	AQEFVNCK	0.93	10.5
Q9CZB0	Succinate dehydrogenase cytochrome b560 subunit, mitochondrial	SLCLGPTLIYSAK	1.36	15.4
Q8BJS4; Q9D666	SUN domain-containing protein 2;SUN domain-containing protein 1	CSETYETK	1.09	NL

Q8K2B3	Succinate dehydrogenase [ubiquinone] flavoprotein subunit, mitochondrial	TLNEADCATVPPAIR	0.67	NL
P31001	Desmin	HQIQSYTCEIDALK	0.83	NL
Q99KI0	Aconitate hydratase, mitochondrial	VGLIGSCTNSSYEDMGR	0.81	NL
Q91VH1	Adiponectin receptor protein 1	AEEDQACPVPQEEEEEVR	1.06	NL
Q6PHZ2; P11798	Calcium/calmodulin-dependent protein kinase type II subunit delta;Calcium/calmodulin-dependent protein kinase type II subunit alpha	QETVDCLK	0.52	NL
Q9ERZ4	Muscarinic acetylcholine receptor M2	GDACTPTSTTVELVGSSGQNGDEK	0.25	NL
Q80X90	Filamin-B	VAVTEGCQPSR	2.02	NL
P63017	Heat shock cognate 71 kDa protein	VCNPIITK	0.78	NL
P11438	Lysosome-associated membrane glycoprotein 1	CNTEEHIFVSK	0.74	NL
P70336	Rho-associated protein kinase 2	NCLLETAK	0.56	NL
Q9Z2I9	Succinyl-CoA ligase [ADP-forming] subunit beta, mitochondrial	ILACDDLDEAAK	0.94	NL
Q62351	Transferrin receptor protein 1	WNIDSSCK	1.48	NL
O70373	Xin actin-binding repeat-containing protein 1	ISGSTPCPPPSR	0.88	NL

Table B.3.4 - List of glutathionylated cysteines or neighboring residues (±1) with their mutations implicated in diseases

[a]Peptide – all cysteine numbers are from mouse

[b]Natural variants – mutations of cysteines or neighboring residues (±1) are found from UniProt database

[c]Disease Relevance - Diseases associated with indicated mutations found from UnitProt database[194] Diseases are listed with their phenotype-MIM number.[195]

* - mutations are predicted as 'probably damaging' in UniProt and PolyPhen-2 prediction tools.[196]

Stop - stop codon

X - frameshift

NL – Light labeled peptides were not identified

Gene Name	Protein Name	Peptide[a]	$R_{H/L}$ E1	$R_{H/L}$ E2	Natural Variant[b] X_{n-1}	Natural Variant[b] C_n	Y_{n-1}	Disease Relevance[c]
SOD1	Superoxide dismutase [Cu-Zn]	LAC$_{147}$GVIGIAQ	0.70	1.37	A→T/D	C→R	G→D/R	Amyotrophic lateral sclerosis 1 (ALS1) [#105400]
HINT1	Histidine triad nucleotide-binding protein 1	C$_{84}$AADLGLK	0.69	2.18		C→R	A→V*	Autosomal recessive axonal neuropathy with neuromyotonia (NMAN) [#137200]
PLOD3	Procollagen-lysine,2-oxoglutarate 5-dioxygenase 3	GVDYEGGGC$_{694}$R	0.91	3.45		C→X	R→C*	Bone fragility with contractures, arterial rupture, and deafness [#612394]
BAG3	BAG family molecular chaperone regulator 3	SQSPAASDC$_{185}$SSSSSSASLPSSGR	0.83	9.66		C→stop		Dilated cardiomyopathy [#613881], myofibrillar myopathy [#612954]
LMNA	Prelamin-A/C; Lamin-A/C	AQNTWGC$_{522}$GSSLR	0.88	4.71		C→R	G→R	Charcot-Marie-Tooth disease [#605588], dilated cardiomyopathy [#115200], congenital muscular dystrophy [#613205]
SPTAN1	Spectrin alpha chain, non-erythrocytic 1	ALC$_{315}$AEADR	1.01	4.93		C→R		Early infantile epileptic encephalopathy [#613477]
PLOD1	Procollagen-lysine,2-oxoglutarate 5-dioxygenase 1	VGEDYEGGGC$_{681}$R	0.73	3.56	G→V		R→W	Ehlers-Danlos syndrome, hydroxylysine-deficient [#225400]
SUN2	SUN domain-containing protein 2	C$_{577}$SETYETK	1.09	NL	R→stop	C→stop		Emery-Dreifuss muscular dystrophy [#310300]
MYH6	Myosin-6	LEDEC$_{949}$SELK	0.44	1.58	E→K	C→Y*	E→K	Familial hypertrophic cardiomyopathy 14 [#613251]
SDHA	Succinate dehydrogenase [ubiquinone] flavoprotein subunit	TLNEADC$_{654}$ATVPPAIR	0.67	NL		C→R/S/G		Mitochondrial complex II deficiency [#252011]
MYBPC3	Myosin-binding protein C, cardiac-type	LLC$_{715}$ETEGR	1.36	4.24	L→P	C→R		Hypertrophic cardiomyopathy [#115197]
HCCS	Cytochrome c-type heme lyase	AYDYVEC$_{70}$PVTGAR	0.57	3.10			P→T	Linear skin defects with multiple congenital anomalies 1 [#309801]
DES	Desmin	HQIQSYTC$_{332}$EIDALK	0.83	NL	T→I	C→R*	E→K	myofibrillar myopathy [#601419]
FLNC	Filamin-C	LYAQDADGC$_{713}$PIDIK	0.86	8.92	G→S*	C→W*		Hypertrophic cardiomyopathy [#617047], myofibrillar myopathy [609524]
PGK1	Phosphoglycerate kinase 1	TGQATVASGIPAGWM GLDC$_{316}$GTESSK	0.82	7.52	D→N	C→R		Phosphoglycerate kinase 1 deficiency [#300653]
PCCA	Propionyl-CoA carboxylase alpha chain, mitochondrial	MADEAVC$_{107}$VGPAPTSK	0.83	18.9	V→L	C→S*	C→X	Propionic acidemia [#606054]
SLC39A13	Zinc transporter ZIP13	SLGAAAAC$_{46}$R	0.68	0.62		C→Y*	R→C	Spondylocheirodysplasia, Ehlers-Danlos syndrome-like [#612350]
CSTB	Cystatin-B	MMC$_3$GAPSATMPATAE TQEVADQVK	1.46	7.09		C→W*	G→W/R	Unverricht-Lundborg syndrome [#254800]

APPENDIX C – COPYRIGHT PERMISSIONS

CCC RightsLink®

License Details

This Agreement between Maheeshi Yapa Abeywardana -- Maheeshi Yapa Abeywardana ("You") and Elsevier ("Elsevier") consists of your license details and the terms and conditions provided by Elsevier and Copyright Clearance Center.

Print Copy

License Number	5177190342241
License date	Oct 27, 2021
Licensed Content Publisher	Elsevier
Licensed Content Publication	Biochimica et Biophysica Acta (BBA) - Proteins and Proteomics
Licensed Content Title	Chemical-proteomic strategies to investigate cysteine posttranslational modifications
Licensed Content Author	Shalise M. Couvertier, Yani Zhou, Eranthie Weerapana
Licensed Content Date	Dec 1, 2014
Licensed Content Volume	1844
Licensed Content Issue	12
Licensed Content Pages	16
Type of Use	reuse in a thesis/dissertation
Portion	figures/tables/illustrations
Number of figures/tables/illustrations	2
Format	both print and electronic
Are you the author of this Elsevier article?	No
Will you be translating?	No
Title	Chemical Proteomic Identification and Functional Studies of Cardiac Protein Glutathionylation under Ischemic Stress
Institution name	Wayne State University
Expected presentation date	Nov 2021
Order reference number	12
Portions	Figure 1, Figure 3
Requestor Location	Maheeshi Yapa Abeywardana 5101 cass avenue DETROIT, MI 48202 United States Attn: Maheeshi Yapa Abeywardana
Publisher Tax ID	98-0397604
Total	**0.00 USD**

BACK

CCC RightsLink®

License Details

This Agreement between Maheeshi Yapa Abeywardana -- Maheeshi Yapa Abeywardana ("You") and Elsevier ("Elsevier") consists of your license details and the terms and conditions provided by Elsevier and Copyright Clearance Center.

Print   **Copy**

License Number	5177181246939
License date	Oct 27, 2021
Licensed Content Publisher	Elsevier
Licensed Content Publication	Trends in Cell Biology
Licensed Content Title	The Complex Interplay between Antioxidants and ROS in Cancer
Licensed Content Author	Isaac S. Harris,Gina M. DeNicola
Licensed Content Date	Jun 1, 2020
Licensed Content Volume	30
Licensed Content Issue	6
Licensed Content Pages	12
Type of Use	reuse in a thesis/dissertation
Portion	figures/tables/illustrations
Number of figures/tables/illustrations	1
Format	both print and electronic
Are you the author of this Elsevier article?	No
Will you be translating?	No
Title	Chemical Proteomic Identification and Functional Studies of Cardiac Protein Glutathionylation under Ischemic Stress
Institution name	Wayne State University
Expected presentation date	Nov 2021
Order reference number	124
Portions	Figure 2
Requestor Location	Maheeshi Yapa Abeywardana 5101 cass avenue
	DETROIT, MI 48202 United States Attn: Maheeshi Yapa Abeywardana
Publisher Tax ID	98-0397604
Total	**0.00 USD**

BACK

CCC | RightsLink®

My Orders > Orders > All Orders

License Details

This Agreement between Maheeshi Yapa Abeywardana -- Maheeshi Yapa Abeywardana ("You") and John Wiley and Sons ("John Wiley and Sons") consists of your license details and the terms and conditions provided by John Wiley and Sons and Copyright Clearance Center.

Print   Copy

License Number	5177180445747
License date	Oct 27, 2021
Licensed Content Publisher	John Wiley and Sons
Licensed Content Publication	FEBS Journal
Licensed Content Title	New roles for desmin in the maintenance of muscle homeostasis
Licensed Content Author	Shenhav Cohen, Harald Herrmann, Giulio Agnetti
Licensed Content Date	Apr 22, 2021
Licensed Content Volume	0
Licensed Content Issue	0
Licensed Content Pages	16
Type of Use	Dissertation/Thesis
Requestor type	University/Academic
Format	Print and electronic
Portion	Figure/table
Number of figures/tables	2
Will you be translating?	No
Title	Chemical Proteomic Identification and Functional Studies of Cardiac Protein Glutathionylation under Ischemic Stress
Institution name	Wayne State University
Expected presentation date	Nov 2021
Order reference number	123
Portions	Figure 1, Figure 2
Requestor Location	Maheeshi Yapa Abeywardana 5101 cass avenue
	DETROIT, MI 48202 United States Attn: Maheeshi Yapa Abeywardana
Publisher Tax ID	EU826007151
Total	**0.00 USD**

BACK

CCC **RightsLink**®

License Details

This Agreement between Maheeshi Yapa Abeywardana -- Maheeshi Yapa Abeywardana ("You") and John Wiley and Sons ("John Wiley and Sons") consists of your license details and the terms and conditions provided by John Wiley and Sons and Copyright Clearance Center.

Print   Copy

License Number	5177171474233
License date	Oct 27, 2021
Licensed Content Publisher	John Wiley and Sons
Licensed Content Publication	ChemBioChem
Licensed Content Title	Isotopically Labeled Clickable Glutathione to Quantify Protein S-Glutathionylation
Licensed Content Author	Young-Hoon Ahn, Bo Huang, Maheeshi Yapa Abeywardana, et al
Licensed Content Date	Oct 29, 2019
Licensed Content Volume	21
Licensed Content Issue	6
Licensed Content Pages	7
Type of Use	Dissertation/Thesis
Requestor type	Author of this Wiley article
Format	Print and electronic
Portion	Full article
Will you be translating?	No
Title	Chemical Proteomic Identification and Functional Studies of Cardiac Protein Glutathionylation under Ischemic Stress
Institution name	Wayne State University
Expected presentation date	Nov 2021
Order reference number	1234
Requestor Location	Maheeshi Yapa Abeywardana 5101 cass avenue DETROIT, MI 48202 United States Attn: Maheeshi Yapa Abeywardana
Publisher Tax ID	EU826007151
Total	**0.00 USD**

BACK

10/27/21, 1:36 PM   Rightslink® by Copyright Clearance Center

CCC
RightsLink®

🏠 Home   ❓ Help ⌄   📷 Live Chat   👤 Maheeshi Yapa Abeywardana ⌄

Proteomic Identification of Protein Glutathionylation in Cardiomyocytes

ACS Publications
Most Trusted. Most Cited. Most Read.

Author: Garrett C. VanHecke, Maheeshi Yapa Abeywardana, Young-Hoon Ahn

Publication: Journal of Proteome Research

Publisher: American Chemical Society

Date: Apr 1, 2019

Copyright © 2019, American Chemical Society

PERMISSION/LICENSE IS GRANTED FOR YOUR ORDER AT NO CHARGE

This type of permission/license, instead of the standard Terms and Conditions, is sent to you because no fee is being charged for your order. Please note the following:

- Permission is granted for your request in both print and electronic formats, and translations.
- If figures and/or tables were requested, they may be adapted or used in part.
- Please print this page for your records and send a copy of it to your publisher/graduate school.
- Appropriate credit for the requested material should be given as follows: "Reprinted (adapted) with permission from {COMPLETE REFERENCE CITATION}. Copyright {YEAR} American Chemical Society." Insert appropriate information in place of the capitalized words.
- One-time permission is granted only for the use specified in your RightsLink request. No additional uses are granted (such as derivative works or other editions). For any uses, please submit a new request.

If credit is given to another source for the material you requested from RightsLink, permission must be obtained from that source.

BACK   CLOSE WINDOW

CCC
RightsLink®

🏠 Home   ❓ Help ⌄   📞 Live Chat   👤 Maheeshi Yapa Abeywardana ⌄

Metabolic Synthesis of Clickable Glutathione for Chemoselective Detection of Glutathionylation

ACS Publications
Most Trusted. Most Cited. Most Read.

Author:
Kusal T. G. Samarasinghe, Dhanushka N. P. Munkanatta Godage, Garrett C. VanHecke, et al

Publication: Journal of the American Chemical Society

Publisher: American Chemical Society

Date: Aug 1, 2014

Copyright © 2014, American Chemical Society

BACK   CLOSE WINDOW

**CCC
RightsLink®**

Home   Help ∨   Live Chat   Sign in   Create Account

Identification and Quantification of Glutathionylated Cysteines under Ischemic Stress

ACS Publications
Most Trusted. Most Cited. Most Read.

Author:
Maheeshi Yapa Abeywardana, Kusal T. G. Samarasinghe, Dhanushka Munkanatta Godage, et al

Publication: Journal of Proteome Research

Publisher: American Chemical Society

Date: Sep 1, 2021

Copyright © 2021, American Chemical Society

PERMISSION/LICENSE IS GRANTED FOR YOUR ORDER AT NO CHARGE

This type of permission/license, instead of the standard Terms and Conditions, is sent to you because no fee is being charged for your order. Please note the following:

- Permission is granted for your request in both print and electronic formats, and translations.
- If figures and/or tables were requested, they may be adapted or used in part.
- Please print this page for your records and send a copy of it to your publisher/graduate school.
- Appropriate credit for the requested material should be given as follows: "Reprinted (adapted) with permission from {COMPLETE REFERENCE CITATION}. Copyright {YEAR} American Chemical Society." Insert appropriate information in place of the capitalized words.
- One-time permission is granted only for the use specified in your RightsLink request. No additional uses are granted (such as derivative works or other editions). For any uses, please submit a new request.

If credit is given to another source for the material you requested from RightsLink, permission must be obtained from that source.

BACK   CLOSE WINDOW

MDPI Open Access Information and Policy

All articles published by MDPI are made immediately available worldwide under an open access license. This means:

- everyone has free and unlimited access to the full-text of *all* articles published in MDPI journals;

- everyone is free to re-use the published material if proper accreditation/citation of the original publication is given;

- open access publication is supported by the authors' institutes or research funding agencies by payment of a comparatively low **Article Processing Charge (APC)** for accepted articles.

Permissions

No special permission is required to reuse all or part of article published by MDPI, including figures and tables. For articles published under an open access Creative Common CC BY license, any part of the article may be reused without permission provided that the original article is clearly cited. Reuse of an article does not imply endorsement by the authors or MDPI.

External Open Access Resources

Those who are new to the concept of open access might find the following websites or the *Open Access Explained!* video informative:

- **Wikipedia article on Open Access**

- Information Platform Open Access [in **English** , in **German**]

REFERENCES

1.	Di Minno, A.; Stornaiuolo, M.; Novellino, E., Molecular Scavengers, Oxidative Stress and Cardiovascular Disease. *J Clin Med* **2019,** *8* (11).

2.	Reverri, E. J.; Morrissey, B. M.; Cross, C. E.; Steinberg, F. M., Inflammation, oxidative stress, and cardiovascular disease risk factors in adults with cystic fibrosis. *Free Radic Biol Med* **2014,** *76*, 261-77.

3.	Csanyi, G.; Miller, F. J., Jr., Oxidative stress in cardiovascular disease. *Int J Mol Sci* **2014,** *15* (4), 6002-8.

4.	Fearon, I. M.; Faux, S. P., Oxidative stress and cardiovascular disease: novel tools give (free) radical insight. *J Mol Cell Cardiol* **2009,** *47* (3), 372-81.

5.	Pignatelli, P.; Menichelli, D.; Pastori, D.; Violi, F., Oxidative stress and cardiovascular disease: new insights. *Kardiol Pol* **2018,** *76* (4), 713-722.

6.	Parthasarathy, S.; Khan-Merchant, N.; Penumetcha, M.; Santanam, N., Oxidative stress in cardiovascular disease. *J Nucl Cardiol* **2001,** *8* (3), 379-89.

7.	Frostegård, J., Immunity, atherosclerosis and cardiovascular disease. *BMC medicine* **2013,** *11*, 117.

8.	Elahi, M. M.; Kong, Y. X.; Matata, B. M., Oxidative stress as a mediator of cardiovascular disease. *Oxid Med Cell Longev* **2009,** *2* (5), 259-69.

9.	Ceconi, C.; Boraso, A.; Cargnoni, A.; Ferrari, R., Oxidative stress in cardiovascular disease: myth or fact? *Arch Biochem Biophys* **2003,** *420* (2), 217-21.

10.	Inagi, R., Oxidative stress in cardiovascular disease: a new avenue toward future therapeutic approaches. *Recent Pat Cardiovasc Drug Discov* **2006,** *1* (2), 151-9.

11.   Selvaraju, V.; Joshi, M.; Suresh, S.; Sanchez, J. A.; Maulik, N.; Maulik, G., Diabetes, oxidative stress, molecular mechanism, and cardiovascular disease--an overview. *Toxicol Mech Methods* **2012,** *22* (5), 330-5.

12.   Strobel, N. A.; Fassett, R. G.; Marsh, S. A.; Coombes, J. S., Oxidative stress biomarkers as predictors of cardiovascular disease. *Int J Cardiol* **2011,** *147* (2), 191-201.

13.   Takano, H.; Zou, Y.; Hasegawa, H.; Akazawa, H.; Nagai, T.; Komuro, I., Oxidative stress-induced signal transduction pathways in cardiac myocytes: involvement of ROS in heart diseases. *Antioxid Redox Signal* **2003,** *5* (6), 789-94.

14.   Hamilton, C. A.; Miller, W. H.; Al-Benna, S.; Brosnan, M. J.; Drummond, R. D.; McBride, M. W.; Dominiczak, A. F., Strategies to reduce oxidative stress in cardiovascular disease. *Clin Sci (Lond)* **2004,** *106* (3), 219-34.

15.   Lakshmi, S. V.; Padmaja, G.; Kuppusamy, P.; Kutala, V. K., Oxidative stress in cardiovascular disease. *Indian J Biochem Biophys* **2009,** *46* (6), 421-40.

16.   Dusting, G. J.; Triggle, C., Are we over oxidized? Oxidative stress, cardiovascular disease, and the future of intervention studies with antioxidants. *Vasc Health Risk Manag* **2005,** *1* (2), 93-7.

17.   Popolo, A.; Autore, G.; Pinto, A.; Marzocco, S., Oxidative stress in patients with cardiovascular disease and chronic renal failure. *Free Radic Res* **2013,** *47* (5), 346-56.

18.   Burns, M.; Rizvi, S. H. M.; Tsukahara, Y.; Pimentel, D. R.; Luptak, I.; Hamburg, N. M.; Matsui, R.; Bachschmid, M. M., Role of Glutaredoxin-1 and Glutathionylation in Cardiovascular Diseases. *Int J Mol Sci* **2020,** *21* (18).

19.   Kayama, Y.; Raaz, U.; Jagger, A.; Adam, M.; Schellinger, I. N.; Sakamoto, M.; Suzuki, H.; Toyama, K.; Spin, J. M.; Tsao, P. S., Diabetic Cardiovascular Disease Induced by Oxidative Stress. *Int J Mol Sci* **2015,** *16* (10), 25234-63.

20.   Ray, P. D.; Huang, B. W.; Tsuji, Y., Reactive oxygen species (ROS) homeostasis and redox regulation in cellular signaling. *Cell Signal* **2012,** *24* (5), 981-90.

21.   Sachidanandam, K.; Fagan, S. C.; Ergul, A., Oxidative stress and cardiovascular disease: antioxidants and unresolved issues. *Cardiovasc Drug Rev* **2005,** *23* (2), 115-32.

22.   Prasad, K.; Dhar, I., Oxidative stress as a mechanism of added sugar-induced cardiovascular disease. *Int J Angiol* **2014,** *23* (4), 217-26.

23.   He, L.; He, T.; Farrar, S.; Ji, L.; Liu, T.; Ma, X., Antioxidants Maintain Cellular Redox Homeostasis by Elimination of Reactive Oxygen Species. *Cell Physiol Biochem* **2017,** *44* (2), 532-553.

24.   Chung, H. S.; Wang, S. B.; Venkatraman, V.; Murray, C. I.; Van Eyk, J. E., Cysteine oxidative posttranslational modifications: emerging regulation in the cardiovascular system. *Circ Res* **2013,** *112* (2), 382-92.

25.   Goswami, S. K.; Maulik, N.; Das, D. K., Ischemia-reperfusion and cardioprotection: a delicate balance between reactive oxygen species generation and redox homeostasis. *Ann Med* **2007,** *39* (4), 275-89.

26.   Wani, R.; Murray, B. W., Analysis of Cysteine Redox Post-Translational Modifications in Cell Biology and Drug Pharmacology. *Methods Mol Biol* **2017,** *1558*, 191-212.

27.   Giustarini, D.; Rossi, R.; Milzani, A.; Colombo, R.; Dalle-Donne, I., S-glutathionylation: from redox regulation of protein functions to human diseases. *J Cell Mol Med* **2004,** *8* (2), 201-12.

28.   Dalle-Donne, I.; Rossi, R.; Giustarini, D.; Colombo, R.; Milzani, A., S-glutathionylation in protein redox regulation. *Free Radic Biol Med* **2007,** *43* (6), 883-98.

29.   Bello-Klein, A.; Khaper, N.; Llesuy, S.; Vassallo, D. V.; Pantos, C., Oxidative stress and antioxidant strategies in cardiovascular disease. *Oxid Med Cell Longev* **2014,** *2014*, 678741.

30.   Bhardwaj, R.; Tandon, C.; Dhawan, D. K.; Kaur, T., Effect of endoplasmic reticulum stress inhibition on hyperoxaluria-induced oxidative stress: influence on cellular ROS sources. *World J Urol* **2017,** *35* (12), 1955-1965.

31.   Di Meo, S.; Reed, T. T.; Venditti, P.; Victor, V. M., Role of ROS and RNS Sources in Physiological and Pathological Conditions. *Oxid Med Cell Longev* **2016,** *2016*, 1245049.

32.   Lushchak, O. V.; Piroddi, M.; Galli, F.; Lushchak, V. I., Aconitase post-translational modification as a key in linkage between Krebs cycle, iron homeostasis, redox signaling, and metabolism of reactive oxygen species. *Redox Rep* **2014,** *19* (1), 8-15.

33.   Loschen, G.; Azzi, A.; Richter, C.; Flohé, L., Superoxide radicals as precursors of mitochondrial hydrogen peroxide. *FEBS letters* **1974,** *42* (1), 68-72.

34.   Turrens, J. F.; Boveris, A., Generation of superoxide anion by the NADH dehydrogenase of bovine heart mitochondria. *Biochemical Journal* **1980,** *191* (2), 421-427.

35.   Brand, M. D., The sites and topology of mitochondrial superoxide production. *Experimental gerontology* **2010,** *45* (7-8), 466-72.

36.   Lee, I. T.; Yang, C. M., Role of NADPH oxidase/ROS in pro-inflammatory mediators-induced airway and pulmonary diseases. *Biochem Pharmacol* **2012,** *84* (5), 581-90.

37.   Holmström, K. M.; Finkel, T., Cellular mechanisms and physiological consequences of redox-dependent signalling. *Nature reviews. Molecular cell biology* **2014,** *15* (6), 411-21.

38.   Munzel, T.; Gori, T.; Bruno, R. M.; Taddei, S., Is oxidative stress a therapeutic target in cardiovascular disease? *Eur Heart J* **2010,** *31* (22), 2741-8.

39.   Zhou, T.; Prather, E. R.; Garrison, D. E.; Zuo, L., Interplay between ROS and Antioxidants during Ischemia-Reperfusion Injuries in Cardiac and Skeletal Muscle. *Int J Mol Sci* **2018,** *19* (2).

40.   De Pascali, F.; Hemann, C.; Samons, K.; Chen, C. A.; Zweier, J. L., Hypoxia and reoxygenation induce endothelial nitric oxide synthase uncoupling in endothelial cells through tetrahydrobiopterin depletion and S-glutathionylation. *Biochemistry* **2014,** *53* (22), 3679-88.

41.   Budde, H.; Hassoun, R.; Tangos, M.; Zhazykbayeva, S.; Herwig, M.; Varatnitskaya, M.; Sieme, M.; Delalat, S.; Sultana, I.; Kolijn, D.; Gomori, K.; Jarkas, M.; Lodi, M.; Jaquet, K.; Kovacs, A.; Mannherz, H. G.; Sequeira, V.; Mugge, A.; Leichert, L. I.; Sossalla, S.; Hamdani, N., The Interplay between S-Glutathionylation and Phosphorylation of Cardiac Troponin I and Myosin Binding Protein C in End-Stage Human Failing Hearts. *Antioxidants (Basel)* **2021,** *10* (7).

42.   Konno, T.; Melo, E. P.; Chambers, J. E.; Avezov, E., Intracellular Sources of ROS/H2O2 in Health and Neurodegeneration: Spotlight on Endoplasmic Reticulum. *Cells* **2021,** *10* (2).

43.   Tew, K. D., Redox in redux: Emergent roles for glutathione S-transferase P (GSTP) in regulation of cell signaling and S-glutathionylation. *Biochem Pharmacol* **2007,** *73* (9), 1257-69.

44.   Drakulic, T.; Temple, M. D.; Guido, R.; Jarolim, S.; Breitenbach, M.; Attfield, P. V.; Dawes, I. W., Involvement of oxidative stress response genes in redox homeostasis, the level of reactive oxygen species, and ageing in Saccharomyces cerevisiae. *FEMS Yeast Res* **2005,** *5* (12), 1215-28.

45.   Carletti, B.; Passarelli, C.; Sparaco, M.; Tozzi, G.; Pastore, A.; Bertini, E.; Piemonte, F., Effect of protein glutathionylation on neuronal cytoskeleton: a potential link to neurodegeneration. *Neuroscience* **2011,** *192*, 285-94.

46.   Hu, Y.; Wang, T.; Liao, X.; Du, G.; Chen, J.; Xu, J., Anti-oxidative stress and beyond: multiple functions of the protein glutathionylation. *Protein Pept Lett* **2010,** *17* (10), 1234-44.

47.   Gu, L.; Robinson, R. A., Proteomic approaches to quantify cysteine reversible modifications in aging and neurodegenerative diseases. *Proteomics Clin Appl* **2016,** *10* (12), 1159-1177.

48.   Murray, C. I.; Van Eyk, J. E., Chasing cysteine oxidative modifications: proteomic tools for characterizing cysteine redox status. *Circ Cardiovasc Genet* **2012,** *5* (5), 591.

49.   Panieri, E.; Santoro, M. M., ROS homeostasis and metabolism: a dangerous liason in cancer cells. *Cell Death Dis* **2016,** *7* (6), e2253.

50.   Paulsen, C. E.; Carroll, K. S., Orchestrating redox signaling networks through regulatory cysteine switches. *ACS chemical biology* **2010,** *5* (1), 47-62.

51.   Majmudar, J. D.; Konopko, A. M.; Labby, K. J.; Tom, C. T.; Crellin, J. E.; Prakash, A.; Martin, B. R., Harnessing Redox Cross-Reactivity To Profile Distinct Cysteine Modifications. *J Am Chem Soc* **2016,** *138* (6), 1852-9.

52.   Couvertier, S. M.; Zhou, Y.; Weerapana, E., Chemical-proteomic strategies to investigate cysteine posttranslational modifications. *Biochim Biophys Acta* **2014,** *1844* (12), 2315-30.

53.   Shannon, D. A.; Weerapana, E., Orphan PTMs: Rare, yet functionally important modifications of cysteine. *Biopolymers* **2014,** *101* (2), 156-64.

54.   Harris, I. S.; DeNicola, G. M., The Complex Interplay between Antioxidants and ROS in Cancer. *Trends Cell Biol* **2020,** *30* (6), 440-451.

55.   Chia, S. B.; Elko, E. A.; Aboushousha, R.; Manuel, A. M.; van de Wetering, C.; Druso, J. E.; van der Velden, J.; Seward, D. J.; Anathy, V.; Irvin, C. G.; Lam, Y. W.; van der Vliet, A.; Janssen-

Heininger, Y. M. W., Dysregulation of the glutaredoxin/S-glutathionylation redox axis in lung diseases. *Am J Physiol Cell Physiol* **2020,** *318* (2), C304-C327.

56.   Almeida, A. S.; Vieira, H. L., Assessment of mitochondrial protein glutathionylation as signaling for CO pathway. *Methods Mol Biol* **2015,** *1264*, 343-50.

57.   Sun, C.; Shi, Z. Z.; Zhou, X.; Chen, L.; Zhao, X. M., Prediction of S-glutathionylation sites based on protein sequences. *PLoS One* **2013,** *8* (2), e55512.

58.   Su, D.; Gaffrey, M. J.; Guo, J.; Hatchell, K. E.; Chu, R. K.; Clauss, T. R.; Aldrich, J. T.; Wu, S.; Purvine, S.; Camp, D. G.; Smith, R. D.; Thrall, B. D.; Qian, W. J., Proteomic identification and quantification of S-glutathionylation in mouse macrophages using resin-assisted enrichment and isobaric labeling. *Free Radic Biol Med* **2014,** *67*, 460-70.

59.   Mohr, S.; Hallak, H.; de Boitte, A.; Lapetina, E. G.; Brune, B., Nitric oxide-induced S-glutathionylation and inactivation of glyceraldehyde-3-phosphate dehydrogenase. *J Biol Chem* **1999,** *274* (14), 9427-30.

60.   Mustafa Rizvi, S. H.; Shao, D.; Tsukahara, Y.; Pimentel, D. R.; Weisbrod, R. M.; Hamburg, N. M.; McComb, M. E.; Matsui, R.; Bachschmid, M. M., Oxidized GAPDH transfers S-glutathionylation to a nuclear protein Sirtuin-1 leading to apoptosis. *Free Radic Biol Med* **2021,** *174*, 73-83.

61.   Xiong, Y.; Uys, J. D.; Tew, K. D.; Townsend, D. M., S-glutathionylation: from molecular mechanisms to health outcomes. *Antioxid Redox Signal* **2011,** *15* (1), 233-70.

62.   Zhang, J.; Ye, Z. W.; Singh, S.; Townsend, D. M.; Tew, K. D., An evolving understanding of the S-glutathionylation cycle in pathways of redox regulation. *Free Radic Biol Med* **2018,** *120*, 204-216.

63.   Anathy, V.; Roberson, E. C.; Guala, A. S.; Godburn, K. E.; Budd, R. C.; Janssen-Heininger, Y. M., Redox-based regulation of apoptosis: S-glutathionylation as a regulatory mechanism to control cell death. *Antioxid Redox Signal* **2012,** *16* (6), 496-505.

64.   Cha, S. J.; Kim, H.; Choi, H. J.; Lee, S.; Kim, K., Protein Glutathionylation in the Pathogenesis of Neurodegenerative Diseases. *Oxid Med Cell Longev* **2017,** *2017*, 2818565.

65.   Shelton, M. D.; Mieyal, J. J., Regulation by reversible S-glutathionylation: molecular targets implicated in inflammatory diseases. *Mol Cells* **2008,** *25* (3), 332-46.

66.   Board, P. G.; Menon, D., Glutathione transferases, regulators of cellular metabolism and physiology. *Biochim Biophys Acta* **2013,** *1830* (5), 3267-88.

67.   Musaogullari, A.; Chai, Y. C., Redox Regulation by Protein S-Glutathionylation: From Molecular Mechanisms to Implications in Health and Disease. *Int J Mol Sci* **2020,** *21* (21).

68.   Wu, G.; Fang, Y. Z.; Yang, S.; Lupton, J. R.; Turner, N. D., Glutathione metabolism and its implications for health. *The Journal of nutrition* **2004,** *134* (3), 489-92.

69.   Anselmo, A. N.; Cobb, M. H., Protein kinase function and glutathionylation. *Biochem J* **2004,** *381* (Pt 3), e1-2.

70.   Cooper, A. J.; Pinto, J. T.; Callery, P. S., Reversible and irreversible protein glutathionylation: biological and clinical aspects. *Expert Opin Drug Metab Toxicol* **2011,** *7* (7), 891-910.

71.   Checconi, P.; Limongi, D.; Baldelli, S.; Ciriolo, M. R.; Nencioni, L.; Palamara, A. T., Role of Glutathionylation in Infection and Inflammation. *Nutrients* **2019,** *11* (8).

72.   Dominko, K.; Dikic, D., Glutathionylation: a regulatory role of glutathione in physiological processes. *Arh Hig Rada Toksikol* **2018,** *69* (1), 1-24.

73.   Dickinson, D. A.; Forman, H. J., Cellular glutathione and thiols metabolism. *Biochem Pharmacol* **2002,** *64* (5-6), 1019-26.

74.   Pimentel, D.; Haeussler, D. J.; Matsui, R.; Burgoyne, J. R.; Cohen, R. A.; Bachschmid, M. M., Regulation of cell physiology and pathology by protein S-glutathionylation: lessons learned from the cardiovascular system. *Antioxid Redox Signal* **2012,** *16* (6), 524-42.

75.   Townsend, D. M.; Lushchak, V. I.; Cooper, A. J., A comparison of reversible versus irreversible protein glutathionylation. *Adv Cancer Res* **2014,** *122*, 177-98.

76.   Galant, A.; Preuss, M. L.; Cameron, J. C.; Jez, J. M., Plant glutathione biosynthesis: diversity in biochemical regulation and reaction products. *Front Plant Sci* **2011,** *2*, 45.

77.   Chen, Y. R.; Chen, C. L.; Pfeiffer, D. R.; Zweier, J. L., Mitochondrial complex II in the post-ischemic heart: oxidative injury and the role of protein S-glutathionylation. *J Biol Chem* **2007,** *282* (45), 32640-54.

78.   Petrushanko, I. Y.; Yakushev, S.; Mitkevich, V. A.; Kamanina, Y. V.; Ziganshin, R. H.; Meng, X.; Anashkina, A. A.; Makhro, A.; Lopina, O. D.; Gassmann, M.; Makarov, A. A.; Bogdanova, A., S-glutathionylation of the Na,K-ATPase catalytic α subunit is a determinant of the enzyme redox sensitivity. *J Biol Chem* **2012,** *287* (38), 32195-205.

79.   Anashkina, A. A.; Poluektov, Y. M.; Dmitriev, V. A.; Kuznetsov, E. N.; Mitkevich, V. A.; Makarov, A. A.; Petrushanko, I. Y., A novel approach for predicting protein S-glutathionylation. *BMC Bioinformatics* **2020,** *21* (Suppl 11), 282.

80.   Petrushanko, I. Y.; Yakushev, S.; Mitkevich, V. A.; Kamanina, Y. V.; Ziganshin, R. H.; Meng, X.; Anashkina, A. A.; Makhro, A.; Lopina, O. D.; Gassmann, M.; Makarov, A. A.; Bogdanova, A., S-glutathionylation of the Na,K-ATPase catalytic alpha subunit is a determinant of the enzyme redox sensitivity. *J Biol Chem* **2012,** *287* (38), 32195-205.

81.   Gao, X. H.; Bedhomme, M.; Veyel, D.; Zaffagnini, M.; Lemaire, S. D., Methods for analysis of protein glutathionylation and their application to photosynthetic organisms. *Molecular plant* **2009,** *2* (2), 218-35.

82.   Butturini, E.; Boriero, D.; Carcereri de Prati, A.; Mariotto, S., Immunoprecipitation methods to identify S-glutathionylation in target proteins. *MethodsX* **2019,** *6*, 1992-1998.

83.   Li, Z.; Zhang, C.; Li, C.; Zhou, J.; Xu, X.; Peng, X.; Zhou, X., S-glutathionylation proteome profiling reveals a crucial role of a thioredoxin-like protein in interspecies competition and cariogenecity of Streptococcus mutans. *PLoS Pathog* **2020,** *16* (7), e1008774.

84.   Chou, C. C.; Chiang, B. Y.; Lin, J. C.; Pan, K. T.; Lin, C. H.; Khoo, K. H., Characteristic tandem mass spectral features under various collision chemistries for site-specific identification of protein S-glutathionylation. *J Am Soc Mass Spectrom* **2015,** *26* (1), 120-32.

85.   Samarasinghe, K. T.; Munkanatta Godage, D. N.; VanHecke, G. C.; Ahn, Y. H., Metabolic synthesis of clickable glutathione for chemoselective detection of glutathionylation. *J Am Chem Soc* **2014,** *136* (33), 11566-9.

86.   Kekulandara, D. N.; Samarasinghe, K. T.; Munkanatta Godage, D. N.; Ahn, Y. H., Clickable glutathione using tetrazine-alkene bioorthogonal chemistry for detecting protein glutathionylation. *Org Biomol Chem* **2016,** *14* (46), 10886-10893.

87.   Samarasinghe, K. T.; Munkanatta Godage, D. N.; Zhou, Y.; Ndombera, F. T.; Weerapana, E.; Ahn, Y. H., A clickable glutathione approach for identification of protein glutathionylation in response to glucose metabolism. *Mol Biosyst* **2016,** *12* (8), 2471-80.

88.   Claycomb, W. C.; Lanson, N. A., Jr.; Stallworth, B. S.; Egeland, D. B.; Delcarpio, J. B.; Bahinski, A.; Izzo, N. J., Jr., HL-1 cells: a cardiac muscle cell line that contracts and retains

phenotypic characteristics of the adult cardiomyocyte. *Proceedings of the National Academy of Sciences of the United States of America* **1998,** *95* (6), 2979-84.

89.   VanHecke, G. C.; Abeywardana, M. Y.; Ahn, Y. H., Proteomic Identification of Protein Glutathionylation in Cardiomyocytes. *J Proteome Res* **2019,** *18* (4), 1806-1818.

90.   Burgoyne, J. R.; Mongue-Din, H.; Eaton, P.; Shah, A. M., Redox signaling in cardiac physiology and pathology. *Circ Res* **2012,** *111* (8), 1091-106.

91.   Chen, Y. R.; Zweier, J. L., Cardiac mitochondria and reactive oxygen species generation. *Circ Res* **2014,** *114* (3), 524-37.

92.   Paulsen, C. E.; Carroll, K. S., Cysteine-mediated redox signaling: chemistry, biology, and tools for discovery. *Chemical reviews* **2013,** *113* (7), 4633-79.

93.   Adachi, T.; Weisbrod, R. M.; Pimentel, D. R.; Ying, J.; Sharov, V. S.; Schöneich, C.; Cohen, R. A., S-Glutathiolation by peroxynitrite activates SERCA during arterial relaxation by nitric oxide. *Nature medicine* **2004,** *10* (11), 1200-7.

94.   Alegre-Cebollada, J.; Kosuri, P.; Giganti, D.; Eckels, E.; Rivas-Pardo, J. A.; Hamdani, N.; Warren, C. M.; Solaro, R. J.; Linke, W. A.; Fernández, J. M., S-glutathionylation of cryptic cysteines enhances titin elasticity by blocking protein folding. *Cell* **2014,** *156* (6), 1235-1246.

95.   Chen, C. A.; Wang, T. Y.; Varadharaj, S.; Reyes, L. A.; Hemann, C.; Talukder, M. A.; Chen, Y. R.; Druhan, L. J.; Zweier, J. L., S-glutathionylation uncouples eNOS and regulates its cellular and vascular function. *Nature* **2010,** *468* (7327), 1115-8.

96.   Munkanatta Godage, D. N. P.; VanHecke, G. C.; Samarasinghe, K. T. G.; Feng, H. Z.; Hiske, M.; Holcomb, J.; Yang, Z.; Jin, J. P.; Chung, C. S.; Ahn, Y. H., SMYD2 glutathionylation contributes to degradation of sarcomeric proteins. *Nat Commun* **2018,** *9* (1), 4341.

97.   Bukowski, M. R.; Bucklin, C.; Picklo, M. J., Quantitation of protein S-glutathionylation by liquid chromatography-tandem mass spectrometry: correction for contaminating glutathione and glutathione disulfide. *Anal Biochem* **2015,** *469*, 54-64.

98.   Guo, J.; Gaffrey, M. J.; Su, D.; Liu, T.; Camp, D. G., 2nd; Smith, R. D.; Qian, W. J., Resin-assisted enrichment of thiols as a general strategy for proteomic profiling of cysteine-based reversible modifications. *Nature protocols* **2014,** *9* (1), 64-75.

99.   Aesif, S. W.; Janssen-Heininger, Y. M.; Reynaert, N. L., Protocols for the detection of s-glutathionylated and s-nitrosylated proteins in situ. *Methods Enzymol* **2010,** *474*, 289-96.

100.   Duan, J.; Gaffrey, M. J.; Qian, W. J., Quantitative proteomic characterization of redox-dependent post-translational modifications on protein cysteines. *Mol Biosyst* **2017,** *13* (5), 816-829.

101.   Lind, C.; Gerdes, R.; Hamnell, Y.; Schuppe-Koistinen, I.; von Löwenhielm, H. B.; Holmgren, A.; Cotgreave, I. A., Identification of S-glutathionylated cellular proteins during oxidative stress and constitutive metabolism by affinity purification and proteomic analysis. *Arch Biochem Biophys* **2002,** *406* (2), 229-40.

102.   Kramer, P. A.; Duan, J.; Gaffrey, M. J.; Shukla, A. K.; Wang, L.; Bammler, T. K.; Qian, W. J.; Marcinek, D. J., Fatiguing contractions increase protein S-glutathionylation occupancy in mouse skeletal muscle. *Redox Biol* **2018,** *17*, 367-376.

103.   MacLean, B.; Tomazela, D. M.; Shulman, N.; Chambers, M.; Finney, G. L.; Frewen, B.; Kern, R.; Tabb, D. L.; Liebler, D. C.; MacCoss, M. J., Skyline: an open source document editor for creating and analyzing targeted proteomics experiments. *Bioinformatics* **2010,** *26* (7), 966-968.

104.   Kiss, B.; Rohlich, P.; Kellermayer, M. S., Structure and elasticity of desmin protofibrils explored with scanning force microscopy. *J Mol Recognit* **2011,** *24* (6), 1095-104.

105.   Lacolley, P.; Challande, P.; Boumaza, S.; Cohuet, G.; Laurent, S.; Boutouyrie, P.; Grimaud, J. A.; Paulin, D.; Lamaziere, J. M.; Li, Z., Mechanical properties and structure of carotid arteries in mice lacking desmin. *Cardiovasc Res* **2001,** *51* (1), 178-87.

106.   Bar, H.; Strelkov, S. V.; Sjoberg, G.; Aebi, U.; Herrmann, H., The biology of desmin filaments: how do mutations affect their structure, assembly, and organisation? *J Struct Biol* **2004,** *148* (2), 137-52.

107.   Ribeiro Ede, A., Jr.; Pinotsis, N.; Ghisleni, A.; Salmazo, A.; Konarev, P. V.; Kostan, J.; Sjoblom, B.; Schreiner, C.; Polyansky, A. A.; Gkougkoulia, E. A.; Holt, M. R.; Aachmann, F. L.; Zagrovic, B.; Bordignon, E.; Pirker, K. F.; Svergun, D. I.; Gautel, M.; Djinovic-Carugo, K., The structure and regulation of human muscle alpha-actinin. *Cell* **2014,** *159* (6), 1447-60.

108.   Sjoblom, B.; Salmazo, A.; Djinovic-Carugo, K., Alpha-actinin structure and regulation. *Cell Mol Life Sci* **2008,** *65* (17), 2688-701.

109.   Borrego-Diaz, E.; Kerff, F.; Lee, S. H.; Ferron, F.; Li, Y.; Dominguez, R., Crystal structure of the actin-binding domain of alpha-actinin 1: evaluating two competing actin-binding models. *J Struct Biol* **2006,** *155* (2), 230-8.

110.   Yang, J.; Xu, X., alpha-Actinin2 is required for the lateral alignment of Z discs and ventricular chamber enlargement during zebrafish cardiogenesis. *FASEB J* **2012,** *26* (10), 4230-42.

111.   Bąchor, R.; Waliczek, M.; Stefanowicz, P.; Szewczuk, Z., Trends in the Design of New Isobaric Labeling Reagents for Quantitative Proteomics. *Molecules* **2019,** *24* (4).

112.   Beltran, C.; Pardo, R.; Bou-Teen, D.; Ruiz-Meana, M.; Villena, J. A.; Ferreira-Gonzalez, I.; Barba, I., Enhancing Glycolysis Protects against Ischemia-Reperfusion Injury by Reducing ROS Production. *Metabolites* **2020,** *10* (4).

113.   Bugger, H.; Pfeil, K., Mitochondrial ROS in myocardial ischemia reperfusion and remodeling. *Biochim Biophys Acta Mol Basis Dis* **2020,** *1866* (7), 165768.

114.   Kalogeris, T.; Baines, C. P.; Krenz, M.; Korthuis, R. J., Cell biology of ischemia/reperfusion injury. *International review of cell and molecular biology* **2012,** *298*, 229-317.

115.   Chen, W.; Li, D., Reactive Oxygen Species (ROS)-Responsive Nanomedicine for Solving Ischemia-Reperfusion Injury. *Front Chem* **2020,** *8*, 732.

116.   Giordano, F. J., Oxygen, oxidative stress, hypoxia, and heart failure. *The Journal of clinical investigation* **2005,** *115* (3), 500-8.

117.   Neubauer, S., The failing heart--an engine out of fuel. *The New England journal of medicine* **2007,** *356* (11), 1140-51.

118.   Hendrickson, S. C.; St Louis, J. D.; Lowe, J. E.; Abdel-aleem, S., Free fatty acid metabolism during myocardial ischemia and reperfusion. *Mol Cell Biochem* **1997,** *166* (1-2), 85-94.

119.   Granger, D. N.; Kvietys, P. R., Reperfusion injury and reactive oxygen species: The evolution of a concept. *Redox Biol* **2015,** *6*, 524-551.

120.   Depre, C.; Vatner, S. F., Cardioprotection in stunned and hibernating myocardium. *Heart failure reviews* **2007,** *12* (3-4), 307-17.

121.   Belke, D. D.; Larsen, T. S.; Lopaschuk, G. D.; Severson, D. L., Glucose and fatty acid metabolism in the isolated working mouse heart. *The American journal of physiology* **1999,** *277* (4), R1210-7.

122.   De Leiris, J.; Opie, L. H.; Lubbe, W. F., Effects of free fatty acid and enzyme release in experimental glucose on myocardial infarction. *Nature* **1975,** *253* (5494), 746-7.

123. Liu, Q.; Docherty, J. C.; Rendell, J. C.; Clanachan, A. S.; Lopaschuk, G. D., High levels of fatty acids delay the recovery of intracellular pH and cardiac efficiency in post-ischemic hearts by inhibiting glucose oxidation. *Journal of the American College of Cardiology* **2002,** *39* (4), 718-25.

124. Lopaschuk, G. D.; Collins-Nakai, R.; Olley, P. M.; Montague, T. J.; McNeil, G.; Gayle, M.; Penkoske, P.; Finegan, B. A., Plasma fatty acid levels in infants and adults after myocardial ischemia. *American heart journal* **1994,** *128* (1), 61-7.

125. Dalle-Donne, I.; Milzani, A.; Gagliano, N.; Colombo, R.; Giustarini, D.; Rossi, R., Molecular mechanisms and potential clinical significance of S-glutathionylation. *Antioxid Redox Signal* **2008,** *10* (3), 445-73.

126. Chen, F. C.; Ogut, O., Decline of contractility during ischemia-reperfusion injury: actin glutathionylation and its effect on allosteric interaction with tropomyosin. *Am J Physiol Cell Physiol* **2006,** *290* (3), C719-27.

127. Eaton, P.; Wright, N.; Hearse, D. J.; Shattock, M. J., Glyceraldehyde phosphate dehydrogenase oxidation during cardiac ischemia and reperfusion. *J Mol Cell Cardiol* **2002,** *34* (11), 1549-60.

128. VanHecke, G. C.; Yapa Abeywardana, M.; Huang, B.; Ahn, Y. H., Isotopically Labeled Clickable Glutathione to Quantify Protein S-Glutathionylation. *Chembiochem* **2020,** *21* (6), 853-859.

129. Cherkas, A.; Holota, S.; Mdzinarashvili, T.; Gabbianelli, R.; Zarkovic, N., Glucose as a Major Antioxidant: When, What for and Why It Fails? *Antioxidants (Basel)* **2020,** *9* (2).

130. Szklarczyk, D.; Morris, J. H.; Cook, H.; Kuhn, M.; Wyder, S.; Simonovic, M.; Santos, A.; Doncheva, N. T.; Roth, A.; Bork, P.; Jensen, L. J.; von Mering, C., The STRING database in 2017:

quality-controlled protein-protein association networks, made broadly accessible. *Nucleic acids research* **2017,** *45* (D1), D362-d368.

131.   Ong, S. B.; Samangouei, P.; Kalkhoran, S. B.; Hausenloy, D. J., The mitochondrial permeability transition pore and its role in myocardial ischemia reperfusion injury. *J Mol Cell Cardiol* **2015,** *78*, 23-34.

132.   Famiglietti, M. L.; Estreicher, A.; Gos, A.; Bolleman, J.; Géhant, S.; Breuza, L.; Bridge, A.; Poux, S.; Redaschi, N.; Bougueleret, L.; Xenarios, I., Genetic variations and diseases in UniProtKB/Swiss-Prot: the ins and outs of expert manual curation. *Human mutation* **2014,** *35* (8), 927-35.

133.   Clemen, C. S.; Herrmann, H.; Strelkov, S. V.; Schröder, R., Desminopathies: pathology and mechanisms. *Acta neuropathologica* **2013,** *125* (1), 47-75.

134.   Brodehl, A.; Gaertner-Rommel, A.; Milting, H., Molecular insights into cardiomyopathies associated with desmin (DES) mutations. *Biophysical reviews* **2018,** *10* (4), 983-1006.

135.   Inomata, Y.; Nagasaka, S.; Miyate, K.; Goto, Y.; Hino, C.; Toukairin, C.; Higashio, R.; Ishida, K.; Saino, T.; Hirose, M.; Tsumura, H.; Sanbe, A., Bcl-2-associated athanogene 3 (BAG3) is an enhancer of small heat shock protein turnover via activation of autophagy in the heart. *Biochem Biophys Res Commun* **2018,** *496* (4), 1141-1147.

136.   Basu, S.; Naha, A.; Veeraraghavan, B.; Ramaiah, S.; Anbarasu, A., In silico structure evaluation of BAG3 and elucidating its association with bacterial infections through protein-protein and host-pathogen interaction analysis. *J Cell Biochem* **2021**.

137.   Marzullo, L.; Turco, M. C.; De Marco, M., The multiple activities of BAG3 protein: Mechanisms. *Biochim Biophys Acta Gen Subj* **2020,** *1864* (8), 129628.

138.   Myers, V. D.; McClung, J. M.; Wang, J.; Tahrir, F. G.; Gupta, M. K.; Gordon, J.; Kontos, C. H.; Khalili, K.; Cheung, J. Y.; Feldman, A. M., The Multifunctional Protein BAG3: A Novel Therapeutic Target in Cardiovascular Disease. *JACC Basic Transl Sci* **2018,** *3* (1), 122-131.

139.   Hishiya, A.; Kitazawa, T.; Takayama, S., BAG3 and Hsc70 interact with actin capping protein CapZ to maintain myofibrillar integrity under mechanical stress. *Circ Res* **2010,** *107* (10), 1220-31.

140.   Selcen, D.; Muntoni, F.; Burton, B. K.; Pegoraro, E.; Sewry, C.; Bite, A. V.; Engel, A. G., Mutation in BAG3 causes severe dominant childhood muscular dystrophy. *Annals of neurology* **2009,** *65* (1), 83-9.

141.   Arimura, T.; Ishikawa, T.; Nunoda, S.; Kawai, S.; Kimura, A., Dilated cardiomyopathy-associated BAG3 mutations impair Z-disc assembly and enhance sensitivity to apoptosis in cardiomyocytes. *Human mutation* **2011,** *32* (12), 1481-91.

142.   Chen, Q.; Younus, M.; Thompson, J.; Hu, Y.; Hollander, J. M.; Lesnefsky, E. J., Intermediary metabolism and fatty acid oxidation: novel targets of electron transport chain-driven injury during ischemia and reperfusion. *Am J Physiol Heart Circ Physiol* **2018,** *314* (4), H787-H795.

143.   Igarashi, N.; Nozawa, T.; Fujii, N.; Kato, B.; Nonomura, M.; Matsuki, A.; Nakadate, T.; Igawa, A.; Asanoi, H.; Inoue, M.; Inoue, H., Evaluation of fatty acid metabolism in hearts after ischemia-reperfusion injury using a dual-isotope autoradiographic approach and tissue assay for metabolites of tracer. *J Nucl Med* **2005,** *46* (1), 160-4.

144.   Lopaschuk, G. D., Alterations in fatty acid oxidation during reperfusion of the heart after myocardial ischemia. *Am J Cardiol* **1997,** *80* (3A), 11A-16A.

145.   Perez-Sala, D.; Oeste, C. L.; Martinez, A. E.; Carrasco, M. J.; Garzon, B.; Canada, F. J., Vimentin filament organization and stress sensing depend on its single cysteine residue and zinc binding. *Nat Commun* **2015,** *6*, 7287.

146.   Kaus-Drobek, M.; Mucke, N.; Szczepanowski, R. H.; Wedig, T.; Czarnocki-Cieciura, M.; Polakowska, M.; Herrmann, H.; Wyslouch-Cieszynska, A.; Dadlez, M., Vimentin S-glutathionylation at Cys328 inhibits filament elongation and induces severing of mature filaments in vitro. *FEBS J* **2020,** *287* (24), 5304-5322.

147.   Stürner, E.; Behl, C., The Role of the Multifunctional BAG3 Protein in Cellular Protein Quality Control and in Disease. *Frontiers in molecular neuroscience* **2017,** *10*, 177.

148.   Ulrich, K.; Finkenzeller, C.; Merker, S.; Rojas, F.; Matthews, K.; Ruppert, T.; Krauth-Siegel, R. L., Stress-Induced Protein S-Glutathionylation and S-Trypanothionylation in African Trypanosomes-A Quantitative Redox Proteome and Thiol Analysis. *Antioxid Redox Signal* **2017,** *27* (9), 517-533.

149.   Forshaw, T. E.; Conway, M. E., Detection of S-Nitrosation and S-Glutathionylation of the Human Branched-Chain Aminotransferase Proteins. *Methods Mol Biol* **2019,** *1990*, 71-84.

150.   Duan, J.; Kodali, V. K.; Gaffrey, M. J.; Guo, J.; Chu, R. K.; Camp, D. G.; Smith, R. D.; Thrall, B. D.; Qian, W. J., Quantitative Profiling of Protein S-Glutathionylation Reveals Redox-Dependent Regulation of Macrophage Function during Nanoparticle-Induced Oxidative Stress. *ACS Nano* **2016,** *10* (1), 524-38.

151.   Gill, R. M.; O'Brien, M.; Young, A.; Gardiner, D.; Mailloux, R. J., Protein S-glutathionylation lowers superoxide/hydrogen peroxide release from skeletal muscle mitochondria through modification of complex I and inhibition of pyruvate uptake. *PLoS One* **2018,** *13* (2), e0192801.

152.   Yang, Y.; Jin, X.; Jiang, C., S-glutathionylation of ion channels: insights into the regulation of channel functions, thiol modification crosstalk, and mechanosensing. *Antioxid Redox Signal* **2014,** *20* (6), 937-51.

153.   Townsend, D. M., S-glutathionylation: indicator of cell stress and regulator of the unfolded protein response. *Mol Interv* **2007,** *7* (6), 313-24.

154.   Fratelli, M.; Demol, H.; Puype, M.; Casagrande, S.; Villa, P.; Eberini, I.; Vandekerckhove, J.; Gianazza, E.; Ghezzi, P., Identification of proteins undergoing glutathionylation in oxidatively stressed hepatocytes and hepatoma cells. *Proteomics* **2003,** *3* (7), 1154-61.

155.   Mieyal, J. J.; Chock, P. B., Posttranslational modification of cysteine in redox signaling and oxidative stress: Focus on s-glutathionylation. *Antioxid Redox Signal* **2012,** *16* (6), 471-5.

156.   Ito, H.; Iwabuchi, M.; Ogawa, K., The sugar-metabolic enzymes aldolase and triose-phosphate isomerase are targets of glutathionylation in Arabidopsis thaliana: detection using biotinylated glutathione. *Plant Cell Physiol* **2003,** *44* (7), 655-60.

157.   McGarry, D. J.; Chen, W.; Chakravarty, P.; Lamont, D. L.; Wolf, C. R.; Henderson, C. J., Proteome-wide identification and quantification of S-glutathionylation targets in mouse liver. *Biochem J* **2015,** *469* (1), 25-32.

158.   Zhao, X.; Ning, Q.; Ai, M.; Chai, H.; Yang, G., Identification of S-glutathionylation sites in species-specific proteins by incorporating five sequence-derived features into the general pseudo-amino acid composition. *J Theor Biol* **2016,** *398*, 96-102.

159.   Gianazza, E.; Eberini, I.; Ghezzi, P., Detection of protein glutathionylation. *Methods Mol Biol* **2009,** *519*, 397-415.

160. Hristova, M.; Veith, C.; Habibovic, A.; Lam, Y. W.; Deng, B.; Geiszt, M.; Janssen-Heininger, Y. M.; van der Vliet, A., Identification of DUOX1-dependent redox signaling through protein S-glutathionylation in airway epithelial cells. *Redox Biol* **2014,** *2*, 436-46.

161. Yapa Abeywardana, M.; Samarasinghe, K. T. G.; Munkanatta Godage, D.; Ahn, Y. H., Identification and Quantification of Glutathionylated Cysteines under Ischemic Stress. *J Proteome Res* **2021,** *20* (9), 4529-4542.

162. McMahon, D. K.; Anderson, P. A.; Nassar, R.; Bunting, J. B.; Saba, Z.; Oakeley, A. E.; Malouf, N. N., C2C12 cells: biophysical, biochemical, and immunocytochemical properties. *The American journal of physiology* **1994,** *266* (6 Pt 1), C1795-802.

163. Davis, M. A.; Ireton, R. C.; Reynolds, A. B., A core function for p120-catenin in cadherin turnover. *J Cell Biol* **2003,** *163* (3), 525-34.

164. Alharatani, R.; Ververi, A.; Beleza-Meireles, A.; Ji, W.; Mis, E.; Patterson, Q. T.; Griffin, J. N.; Bhujel, N.; Chang, C. A.; Dixit, A.; Konstantino, M.; Healy, C.; Hannan, S.; Neo, N.; Cash, A.; Li, D.; Bhoj, E.; Zackai, E. H.; Cleaver, R.; Baralle, D.; McEntagart, M.; Newbury-Ecob, R.; Scott, R.; Hurst, J. A.; Au, P. Y. B.; Hosey, M. T.; Khokha, M.; Marciano, D. K.; Lakhani, S. A.; Liu, K. J., Novel truncating mutations in CTNND1 cause a dominant craniofacial and cardiac syndrome. *Hum Mol Genet* **2020,** *29* (11), 1900-1921.

165. Keirsebilck, A.; Bonne, S.; Staes, K.; van Hengel, J.; Nollet, F.; Reynolds, A.; van Roy, F., Molecular cloning of the human p120ctn catenin gene (CTNND1): expression of multiple alternatively spliced isoforms. *Genomics* **1998,** *50* (2), 129-46.

166. Liu, D.; Zhang, H.; Cui, M.; Chen, C.; Feng, Y., Hsa-miR-425-5p promotes tumor growth and metastasis by activating the CTNND1-mediated beta-catenin pathway and EMT in colorectal cancer. *Cell Cycle* **2020,** *19* (15), 1917-1927.

167.   Liu, X.; Zhang, Y.; Wang, Y.; Bian, C.; Wang, F., Long non-coding RNA KCNQ1OT1 up-regulates CTNND1 by sponging miR-329-3p to induce the proliferation, migration, invasion, and inhibit apoptosis of colorectal cancer cells. *Cancer Cell Int* **2020,** *20*, 340.

168.   Tang, B.; Tang, F.; Wang, Z.; Qi, G.; Liang, X.; Li, B.; Yuan, S.; Liu, J.; Yu, S.; He, S., Overexpression of CTNND1 in hepatocellular carcinoma promotes carcinous characters through activation of Wnt/beta-catenin signaling. *J Exp Clin Cancer Res* **2016,** *35* (1), 82.

169.   Hu, G., p120-Catenin: a novel regulator of innate immunity and inflammation. *Critical reviews in immunology* **2012,** *32* (2), 127-38.

170.   Denes, L. T.; Riley, L. A.; Mijares, J. R.; Arboleda, J. D.; McKee, K.; Esser, K. A.; Wang, E. T., Culturing C2C12 myotubes on micromolded gelatin hydrogels accelerates myotube maturation. *Skeletal muscle* **2019,** *9* (1), 17.

171.   Winther, J. R.; Thorpe, C., Quantification of thiols and disulfides. *Biochim Biophys Acta* **2014,** *1840* (2), 838-46.

172.   Caccuri, A. M.; Antonini, G.; Allocati, N.; Di Ilio, C.; Innocenti, F.; De Maria, F.; Parker, M. W.; Masulli, M.; Polizio, F.; Federici, G.; Ricci, G., Properties and utility of the peculiar mixed disulfide in the bacterial glutathione transferase B1-1. *Biochemistry* **2002,** *41* (14), 4686-93.

173.   Marzuca-Nassr, G. N.; Vitzel, K. F.; Mancilla-Solorza, E.; Márquez, J. L., Sarcomere Structure: The Importance of Desmin Protein in Muscle Atrophy %J International Journal of Morphology. **2018,** *36*, 576-583.

174.   Agnetti, G.; Herrmann, H.; Cohen, S., New roles for desmin in the maintenance of muscle homeostasis. *FEBS J* **2021**.

175.   Singh, S. R.; Kadioglu, H.; Patel, K.; Carrier, L.; Agnetti, G., Is Desmin Propensity to Aggregate Part of its Protective Function? *Cells* **2020,** *9* (2).

176.   Mavroidis, M.; Athanasiadis, N. C.; Rigas, P.; Kostavasili, I.; Kloukina, I.; Te Rijdt, W. P.; Kavantzas, N.; Chaniotis, D.; van Tintelen, J. P.; Skaliora, I.; Davos, C. H., Desmin is essential for the structure and function of the sinoatrial node: implications for increased arrhythmogenesis. *Am J Physiol Heart Circ Physiol* **2020,** *319* (3), H557-H570.

177.   Paulin, D.; Li, Z., Desmin: a major intermediate filament protein essential for the structural integrity and function of muscle. *Exp Cell Res* **2004,** *301* (1), 1-7.

178.   Agbulut, O.; Li, Z.; Perie, S.; Ludosky, M. A.; Paulin, D.; Cartaud, J.; Butler-Browne, G., Lack of desmin results in abortive muscle regeneration and modifications in synaptic structure. *Cell Motil Cytoskeleton* **2001,** *49* (2), 51-66.

179.   Hol, E. M.; Capetanaki, Y., Type III Intermediate Filaments Desmin, Glial Fibrillary Acidic Protein (GFAP), Vimentin, and Peripherin. *Cold Spring Harbor perspectives in biology* **2017,** *9* (12).

180.   Capetanaki, Y., Desmin cytoskeleton in healthy and failing heart. *Heart failure reviews* **2000,** *5* (3), 203-20.

181.   Bova, M. P.; Yaron, O.; Huang, Q.; Ding, L.; Haley, D. A.; Stewart, P. L.; Horwitz, J., Mutation R120G in alphaB-crystallin, which is linked to a desmin-related myopathy, results in an irregular structure and defective chaperone-like function. *Proceedings of the National Academy of Sciences of the United States of America* **1999,** *96* (11), 6137-42.

182.   Capetanaki, Y.; Papathanasiou, S.; Diokmetzidou, A.; Vatsellas, G.; Tsikitis, M., Desmin related disease: a matter of cell survival failure. *Current opinion in cell biology* **2015,** *32*, 113-20.

183.   Fichna, J. P.; Karolczak, J.; Potulska-Chromik, A.; Miszta, P.; Berdynski, M.; Sikorska, A.; Filipek, S.; Redowicz, M. J.; Kaminska, A.; Zekanowski, C., Two desmin gene mutations associated with myofibrillar myopathies in Polish families. *PLoS One* **2014,** *9* (12), e115470.

184.   Lovering, R. M.; O'Neill, A.; Muriel, J. M.; Prosser, B. L.; Strong, J.; Bloch, R. J., Physiology, structure, and susceptibility to injury of skeletal muscle in mice lacking keratin 19-based and desmin-based intermediate filaments. *Am J Physiol Cell Physiol* **2011,** *300* (4), C803-13.

185.   Sharma, S.; Mucke, N.; Katus, H. A.; Herrmann, H.; Bar, H., Disease mutations in the "head" domain of the extra-sarcomeric protein desmin distinctly alter its assembly and network-forming properties. *J Mol Med (Berl)* **2009,** *87* (12), 1207-19.

186.   Bär, H.; Mücke, N.; Kostareva, A.; Sjöberg, G.; Aebi, U.; Herrmann, H., Severe muscle disease-causing desmin mutations interfere with in vitro filament assembly at distinct stages. *Proceedings of the National Academy of Sciences of the United States of America* **2005,** *102* (42), 15099-104.

187.   Dalakas, M. C.; Park, K. Y.; Semino-Mora, C.; Lee, H. S.; Sivakumar, K.; Goldfarb, L. G., Desmin myopathy, a skeletal myopathy with cardiomyopathy caused by mutations in the desmin gene. *The New England journal of medicine* **2000,** *342* (11), 770-80.

188.   van Groningen, J. J.; Bloemers, H. P.; Swart, G. W., Rat desmin gene structure and expression. *Biochim Biophys Acta* **1994,** *1217* (1), 107-9.

189.   Taylor, M. R.; Slavov, D.; Ku, L.; Di Lenarda, A.; Sinagra, G.; Carniel, E.; Haubold, K.; Boucek, M. M.; Ferguson, D.; Graw, S. L.; Zhu, X.; Cavanaugh, J.; Sucharov, C. C.; Long, C. S.; Bristow, M. R.; Lavori, P.; Mestroni, L., Prevalence of desmin mutations in dilated cardiomyopathy. *Circulation* **2007,** *115* (10), 1244-51.

190.   Goldfarb, L. G.; Vicart, P.; Goebel, H. H.; Dalakas, M. C., Desmin myopathy. *Brain : a journal of neurology* **2004,** *127* (Pt 4), 723-34.

191.   Even, C.; Abramovici, G.; Delort, F.; Rigato, A. F.; Bailleux, V.; de Sousa Moreira, A.; Vicart, P.; Rico, F.; Batonnet-Pichon, S.; Briki, F., Mutation in the Core Structure of Desmin Intermediate Filaments Affects Myoblast Elasticity. *Biophys J* **2017,** *113* (3), 627-636.

192.   Costa, M. L.; Escaleira, R.; Cataldo, A.; Oliveira, F.; Mermelstein, C. S., Desmin: molecular interactions and putative functions of the muscle intermediate filament protein. *Brazilian journal of medical and biological research = Revista brasileira de pesquisas medicas e biologicas* **2004,** *37* (12), 1819-30.

193.   Ackers-Johnson, M.; Li, P. Y.; Holmes, A. P.; O'Brien, S. M.; Pavlovic, D.; Foo, R. S., A Simplified, Langendorff-Free Method for Concomitant Isolation of Viable Cardiac Myocytes and Nonmyocytes From the Adult Mouse Heart. *Circ Res* **2016,** *119* (8), 909-20.

194.   Famiglietti, M. L.; Estreicher, A.; Gos, A.; Bolleman, J.; Gehant, S.; Breuza, L.; Bridge, A.; Poux, S.; Redaschi, N.; Bougueleret, L.; Xenarios, I.; UniProt, C., Genetic variations and diseases in UniProtKB/Swiss-Prot: the ins and outs of expert manual curation. *Hum Mutat* **2014,** *35* (8), 927-35.

195.   Hamosh, A.; Scott, A. F.; Amberger, J. S.; Bocchini, C. A.; McKusick, V. A., Online Mendelian Inheritance in Man (OMIM), a knowledgebase of human genes and genetic disorders. *Nucleic Acids Res* **2005,** *33* (Database issue), D514-7.

196.   Adzhubei, I. A.; Schmidt, S.; Peshkin, L.; Ramensky, V. E.; Gerasimova, A.; Bork, P.; Kondrashov, A. S.; Sunyaev, S. R., A method and server for predicting damaging missense mutations. *Nat Methods* **2010,** *7* (4), 248-249.

ABSTRACT

CHEMICAL PROTEOMIC IDENTIFICATION AND FUNCTIONAL STUDIES OF CARDIAC PROTEIN GLUTATHIONYLATION

by

MAHEESHI YAPA ABEYWARDANA

May 2022

Advisor: Prof. Young-Hoon Ahn

Major: Chemistry (Biochemistry)

Degree: Doctor of Philosophy

Elevated intracellular levels of reactive oxygen species (ROS) are associated with induction of oxidative stress. Increased levels of ROS participate in development of cardiovascular diseases by modifying proteins reversibly or irreversibly. Especially, the cysteine residues can undergo oxidative post-translational modifications such as glutathionylation. Glutathionylation is an important regulatory reversible thiol oxidation. Identification and quantification of glutathionylated proteins is important for the understanding of the molecular mechanisms behind initiation and progression of many diseases. Our lab previously developed a click chemistry-based method to detect and identify glutathionylation in cells by synthesizing clickable-glutathione.

We established a mass spectrometry-based strategy coupled with clickable glutathione in which two azido-Ala derivatives with isotopic mass difference were used to metabolically synthesize isotopically labelled clickable glutathione for identification and quantification of glutathionylated proteins. We applied this approach on HL-1

cardiomyocyte cells to identify and quantify 1398 glutathionylated peptides upon the addition of H_2O_2.

During ischemia and reperfusion, levels of ROS can be elevated causing oxidative modifications in cardiac proteins. By applying clickable glutathione approach on HL-1 cells under different metabolic alterations, we found that glucose is important for maintaining redox homeostasis, while fatty acid oxidation induces a high level of glutathionylation during reoxygenation. We applied our isotopically labeled clickable glutathione approach upon addition of fatty acids during reoxygenation, identifying and quantifying 248 glutathionylated proteins.

We developed a proteomic approach for the direct quantification of glutathionylated cysteines compared to the unmodified cysteines using a cysteine blocking clickable glutathione reagent (L-N_3-GS-SPy) that mimics the structure of clickable glutathione. We applied this quantification approach on C2C12 mouse skeletal muscle cell line and identified 1518 glutathionylated cysteines upon addition of H_2O_2.

Desmin is an intermediate filament that plays a key role in maintaining structural and mechanical integrity of sarcomere. From our proteomic analyses, we identified that desmin is undergoing glutathionylation under stress. Using rat cardiomyocytes, we investigate the effect of glutathionylation on myofibril integrity of desmin. We found that desmin lose its myofibril integrity upon oxidative stress. However, cysteine mutant of desmin recovers myofibril integrity, suggesting that glutathionylation may interfere with the desmin filament assembly.

AUTOBIOGRAPHICAL STATEMENT

MAHEESHI YAPA ABEYWARDANA

EDUCATION

Ph.D., Chemistry (Anticipated May 2022)

Department of Chemistry, Wayne State University, Detroit, MI, USA

Advisor: Prof. Young-Hoon Ahn

B.Sc., Chemistry (February 2013)

Institute of Chemistry Ceylon, Sri Lanka

Research Advisors: Dr. J. Goonaratne and Dr. S Sotheeswaran

AWARDS AND HONORS

- Thomas Rumble Fellowship, Department of Chemistry, Wayne State University, 2020 to 2021
- Paul and Carol C. Schaap Endowed Distinguished Graduate Award for Summer, 2020
- Competitive Graduate Research Assistantship, Graduate School, Wayne State University, 2019 to 2020
- Graduate School Citations for Excellence in Teaching, 2019

PUBLICATIONS

- **Yapa Abeywardana M**., Samarasinghe K.T.G., Munkanatta Godage D., Ahn Y.H. (2021) Identification and Quantification of Glutathionylated Cysteines under Ischemic Stress. Journal of proteome research. 20,4529- 4542 DOI: 10.1021/acs.jproteome.1c00473
- **Yapa Abeywardana M**., Ahn Y.H. (2020) Chemoproteomic Approach for Site-specific Identification of Protein S-Glutathionylation. Methods in Molecular Biology (Submitted)
- VanHecke G.¥, **Yapa Abeywardana M**.¥, Huang B., Ahn Y.H. (2020) Isotopically labelled Clickable Glutathione to Quantify Protein S-Glutathionylation. ChemBioChem. 21, 853-859 DOI: 10.1002/cbic.201900528 (¥Equal contribution)
- VanHecke G., **Yapa Abeywardana M**., Ahn Y.H. (2019) Proteomic identification of protein glutathionylation in cardiomyocytes. Journal of proteome research. 18, 1806-1818 DOI: 10.1021/acs.jproteome.8b00986